Landscape to regional scale patterns and drivers of forest insect disturbances: A remote sensing based study of western spruce budworm *Choristoneura occidentalis* in British Columbia, Canada

Dissertation

zur Erlangung des akademischen Grades
doctor rerum naturalium
(Dr. rer. nat.)

im Fach Geographie

eingereicht an der
Mathematisch-Naturwissenschaftlichen Fakultät
der Humboldt-Universität zu Berlin

von
Cornelius Senf, M.Sc.

Präsidentin der Humboldt-Universität zu Berlin
Prof. Dr. Sabine Kunst

Dekan der Mathematisch-Naturwissenschaftlichen Fakultät
Prof. Dr. Elmar Kulke

Gutachter:
Prof. Dr. Patrick Hostert
Prof. Dr. Joachim Hill
Prof. Dr. Birgit Kleinschmit

Eingereicht am: 12.07.2016
Tag der mündlichen Verteidigung: 21.09.2016

Acknowledgements

I would like to thank my supervisor Patrick Hostert for supporting me in developing my own ideas and projects, which greatly helped me in becoming an independent researcher. Also, I would like to thank Patrick for hosting me at the Geomatics Lab and providing such a great working environment and infrastructure. Second, I would like to thank my co-supervisor Mike Wulder, who always gave me constructive feedback within hours, introduced me to many interesting people and collaborators, took me on great bike rides, and supported me during my stays in Canada. Third I would like to thank Dirk Pflugmacher. It would have been impossible for me to finish this dissertation without his help. Moreover, Dirk taught me what research really is about. I am looking forward to further working together with you! Fourth, I would like to thank all my fellow PhD candidates, in particular Anika, Benjamin, B., Benjamin J., Christian, Florian, Laura, Maria, Marcel, and Philippe. I also like to thank the many post-docs/senior scientists at the Geomatics Lab, in particular Sebastian for his help, support, and excellent teaching skills. Also, I would like to thank Dagmar W. for all her help! Finally, I deeply thank my family for all their love and support during the good and during the not so good times of the past four years, as well as I thank Jana for her never ending love, support, togetherness, and early-morning discussions on statistics. I am looking forward to the next ten years!

Abstract

Insect disturbances play a key role for forest ecosystem dynamics by creating heterogeneous forest landscapes that are resilient to various changes, such as those caused by climate change. Insect disturbances are also important for the timber industry by reducing yields and wood quality during major outbreaks. Despite the ecological and economic importance of insect disturbances, the outbreak dynamics of defoliating insects of the coniferous forests of western North America – in particular by the western spruce budworm *Choristoneura occidentalis* – are yet poorly understood. This is partly caused by a lack of suitable methods for quantifying landscape to regional scale outbreak patterns. Remote sensing, which delivers a spatially and temporally explicit view on the Earth's surface properties, can help overcoming this challenge. Consequently, the overall goal of this dissertation was to increase the understanding of landscape to regional scale patterns and processes of insect defoliator disturbances in the coniferous forests of western North America with the help of Landsat remote sensing. Precisely, the research questions of my dissertation were: (1) How can Landsat remote sensing be used to map and quantify insect defoliator outbreaks? (2) What are the spatiotemporal patterns and processes of outbreaks of western spruce budworm in the coniferous forests of western North America? Using the current outbreak in British Columbia as example, I showed that Landsat time series can be used to map and quantify the spatial and temporal patterns of budworm infestation at the landscape and regional scale. In particular, I showed that the spectral patterns found for insect defoliation are significantly different from those found for other forest disturbances, such as harvest, fire, and bark beetle infestation. Using the Landsat-based maps, I developed a multi-level modeling framework to explain the spatial and temporal outbreak dynamics of western spruce budworm. The spatial and temporal outbreak dynamics of western spruce budworm were mainly driven by moth dispersal, host abundance at the landscape scale, by stand structure and species composition, and by regional-scale precipitation patterns. In addition, I found that those processes interacted within and across scales. While those results are in overall agreement with studies of historic outbreaks and other insect species, this study is the first to quantify those processes using spatially explicit data over a large extent and for the western spruce budworm. Concluding from my results, it is suggested that outbreak patterns of forest insect defoliation in the coniferous forests of western North America are governed by factors that go beyond stand level management. Forest management thus should consider those factors in their operational planning, as well as in their models of future forest change.

Zusammenfassung

Herbivore und xylophage Insekten spielen eine bedeutende Rolle im Erhalt von Waldökosystemen und stärken deren Resilienz gegenüber Umweltveränderungen wie etwa dem globalen Klimawandel. Insektenschäden haben auch eine ökonomische Bedeutung, da sie die Holzmenge und Holzqualität negativ beeinflussen. Obwohl die ökologische sowie ökonomische Bedeutung von Insekten bekannt ist, gibt es bisher wenig Forschung zu den Dynamiken von herbivoren Insekten in der nord-west amerikanischen Nadelholzzone, speziell durch die Art *Choristoneura occidentalis*. Der Mangel an Studien kann auf ein Fehlen von geeigneten Methoden zur Quantifizierung von Insektenausbrüchen auf der Landschafts- und Regionalskala zurückgeführt werden. Die Nutzung von Fernerkundung vermag diese Wissenslücke zu schließen. Das übergeordnete Ziel dieser Dissertation ist daher, anhand von Fernerkundung ein besseres Verständnis der raumzeitlichen Muster von Insektenausbrüchen in der nord-west amerikanischen Nadelholzzone zu erlangen. Die spezifischen Forschungsfragen der Dissertation sind: (1) Inwieweit kann Fernerkundung die Kartierung und Quantifizierung von Insektenausbrüchen, insbesondere durch Herbivoren, unterstützen? (2) Was sind die raumzeitlichen Muster und Prozesse von Ausbrüchen des *Choristoneura occidentalis* in der nord-west amerikanischen Nadelholzzone? Es konnte gezeigt werden, dass Fernerkundung, speziell mit der Landsat Sensorfamilie, ein geeigneter Weg ist um die raumzeitlichen Muster von Insektenausbrüchen zu rekonstruieren. Dabei ist besonders hervorzuheben, dass sich die spektral-temporalen Charakteristika von Insektenherbivorie deutlich von denen stärker ausgeprägter Störungen (Kahlschlag, Feuer, Borkenkäfer) abhoben. Anhand dieser Erkenntnis war es möglich, die raumzeitlichen Muster des letzten *Choristoneura occidentalis* Ausbruchs in Britisch Kolumbien, Kanada, zu rekonstruieren. Mit Hilfe eines multi-level Modellansatzes konnten die hauptsächlichen Triebkräfte hinter diesen raumzeitlichen Mustern erklärt werden. So zeigte sich, dass die Dynamiken hauptsächlich durch Ausbreitung adulter Motten, eine hohe Abundanz von Wirtsbäumen (*Pseudotsuga* spp.) in der Landschaft, regionale Niederschlagsmustern, sowie deren Interaktion erklärt werden konnten. Standfaktoren spielten eine untergeordnete Rolle. Diese Ergebnisse sind im Einklang mit Studien zu anderen Gattungen und Arten und mit historischen Studien, zeigen diese Prozesse aber erstmals für *Choristoneura occidentalis* sowie in einer räumlich expliziten Untersuchung. Aus den Ergebnissen kann geschlossen werden, dass Ausbrüche herbivorer Insekten in der nord-west amerikanischen Nadelholzzone durch Prozesse, welche über ein Management auf Standesebene hinausgehen, bestimmt werden. Ein nachhaltiges Waldmanagement sollte daher neben Standfaktoren auch Faktoren auf Landschafts- und Regionalebene berücksichtigen.

Contents

List of Figures

List of Tables

Chapter 1

Introduction

1.1 Forest ecosystems and disturbance dynamics

Forests cover approximately 40% of the Earth's ice-free land surface (Hansen et al., 2013). Forests harbor a large proportion of global biodiversity (Myers et al., 2000), they are the largest terrestrial sink of carbon (Pan et al., 2011), and they provide important services to humans such as food and timber supply (Food and of the United Nations, 2014). As such, forests are of global importance for humanity (Cardinale et al., 2012). A forest ecosystem includes all living organisms of a forest, reaching from the root system to the upper canopy (Waring and Running, 2007). All organisms within a forest ecosystem (plants, animals, and microorganisms) interact with each other and with their environment, in particular with the soil, atmosphere, and water systems (Kimmins, 2004). Those interactions are called ecosystem processes, which describe the fluxes of material and energy between varying pools within a forest ecosystem. Understanding those ecosystem processes is a crucial goal of many scientific disciplines, in particular of the field of ecosystem science (Turner, 2005; Wu and Hobbs, 2002).

Forest ecosystems and their underlying ecosystem processes range across spatial scales (Turner, 1989). The consideration of spatial scale is a fundamental concept in studying forest ecosystems. For example, on a global scale we might delineate a distinct forest ecosystem based on global scale processes such as global precipitation and temperature patterns (e.g., the boreal forest). However, we can 'zoom' into this ecosystem just to see that it is made up of an arrangement of smaller scale ecosystems, which are driven by regional scale processes such as the continentality of a region (e.g., deciduous versus evergreen taiga). Those regional scale processes again manifest into smaller scale processes, example given, the landscape scale distribution of precipitation – and thus tree species – along elevation gradients. Again, we can disassemble those landscape-scale processes into smaller processes operating at the stand scale (e.g., variation in hardwood composition due to variation in soil water content), the tree scale (e.g., varying diameter at breast height due to higher availability of light), and so on.

Forests ecosystems and ecosystem processes also range in time, meaning that they are dynamic systems and undergo a continuous change of state (Waring and Running, 2007). While leaves of deciduous trees change within one year, a stand is growing over decades, and the global forest ecosystems as we know them today have resembled over thousands of years. Forest ecosystem change is determined by two basic elements: disturbance and succession (Franklin et al., 2002). In ecology, disturbances are defined as (White and Pickett, 1985): "Any relatively discrete event that disrupts the structure of an ecosystem, community, or population, and changes resource availability of the physical environment." Thus, a forest disturbance represents an event that in some way disrupts the properties and characteristics of a

forest. Succession, in turn, describes the process of recovery and regeneration after disturbance. Natural forest disturbances include wildfires, floods, hurricanes, blowdowns, insect infestations, avalanches, among others. Those disturbances can be classified by their origin, being either biotic (e.g., insect infestation) or abiotic (e.g., fire), by their duration (e.g., a windstorms typically last one day while a volcanic eruption might last over months), and by their magnitude (e.g., a fire can be stand-replacing or just burn understory vegetation). Natural forest disturbances cause mortality among older or weakened trees, resulting in increased availability of light and nutrition to younger trees establishing in the understory (e.g., natural regeneration of pine *Pinus contorta* after mortality caused by bark beetles; Axelson et al., 2009), or giving room to pioneer species that are well-adapted to post-disturbance environments (e.g., post-fire establishment of aspen *Populus tremuloides*; Turner et al., 2003). If a landscape experiences disturbances of similar characteristics over a longer period, the landscape itself will be characterized by those disturbances. In this case, ecologists refer to the term disturbance regime, which is characterized by the spatial distribution, the frequency, the intensity, and other characteristics of disturbances occurring in this particular landscape (Turner, 2010). Disturbance regimes lead to distinct landscapes patterns, that is to a distinct spatial distribution of patches within the landscape. For example, frequent fires in the interior of North-West America have created a forest landscape dominated by seral or pioneering coniferous species with only some forests patches reaching old ages (Parker et al., 2006). The spatial distribution of patches determines the structure of a landscape, with structure being a product of landscape composition and configuration. Landscape composition describes the abundance of certain patches within the landscape (e.g., the amount of hardwoods within a watershed), whereas landscape configuration describes the spatial arrangement of patches (e.g., whether hardwoods are mixed with coniferous or if they occur in one large patch). Numerous studies have evaluated the impact of disturbances on landscape structure and, *vice versa*, the effects of landscape structure on disturbances. For example, it was found that insect disturbances can substantially change the fragmentation of forest landscapes (Coops et al., 2010), or that the amount of edges within a landscape increases the risk of blowdown during storms (Mitchell et al., 2001). Summing up, natural disturbances are integrated and important component of forest ecosystems, which help maintaining the important services that forests provide to humanity. However, human alterations can fundamentally change those systems.

Humans have altered forest ecosystems for centuries in order to obtain wood for construction, shelter, tool making, and fuel (Meyer and BL Turner, 1994). Alterations of forest ecosystems can either be in the form of converting forest land into non-forest land (e.g., conversion of forests to agricultural or urban areas), or

in the form of modifying the forests biogeophysical and biogeochemical properties. For example, fire suppression in lodgepole-pine dominated ecosystems has led to homogeneous landscapes of mature stands, which have substantially changed the underlying ecosystem processes. In particular, the high availability of mature pines – in conjunction with a series of mild winters – has led to widespread outbreak of mountain pine beetle in coniferous forests of Western North America (Negron and Popp, 2004). Hence, by changing one entity of the forest ecosystem – the spatial composition and configuration of mature lodgepole pine stands – the whole forest ecosystem has undergone substantial changes. Another example is the increase in blowdown disturbances in European forests due to changes in species composition (i.e., pure plantations of spruce *Picea* ssp Lindroth et al., 2009) or the increase in fires severity due to increased fuel in managed stands in the Rocky Mountains (Bigler et al., 2005). Moreover, human use of forests also can be seen as disturbance itself. For example, the harvest of forests substantially changes the structure of forest landscapes (Healey et al., 2008; Radeloff et al., 2000) and can thus result in a human-dominated disturbance regime (Noble and Dirzo, 1997). To encounter those shifts towards human-dominated disturbance regimes, management actions try to mimic natural disturbances (Long, 2009). However, those management techniques often oppose the simple goal of maximizing annual yields (Burton, 2010).

While management and use of forest ecosystems can be seen as direct modification of the ecosystems properties, humans also alter other systems that interact with the forest ecosystem, in particular the atmosphere, soil, and water systems (Trumbore et al., 2015). The most prominent and probably most dramatic alteration for forest ecosystems is climate change (Stocker, 2014). Climate change can shift the distribution of tree species and thus of forest ecosystems, on the one hand, and change disturbance dynamics and thus disturbance regimes, on the other (Dale et al., 2001b). Changing climate patterns, especially changing drought patterns, affect several disturbances agents (Allen et al., 2015). In particular, several studies found that fire frequency, severity, and extent can be expected to change under current climate change (Gauthier et al., 2015). Moreover, it was found that drought stress and drought-induced mortality have increased globally (Allen et al., 2010). Likewise, bark beetles migrated into areas previously thought to be unsuitable due to winter temperature restrictions (Bentz et al., 2010). Finally, blowdowns have increased with increasing frequency and severity of storms (Seidl et al., 2011). Those climate effects on disturbance dynamics are moreover often interrelated, adding to their complexity (Dale et al., 2001b).

All already ongoing or predicted changes in the context of global environmental change have substantial impacts on the services of forest ecosystems. Increasing the frequency, extent, and severity of forest fires has substantial impacts on human

life, property, and economy (Prestemon et al., 2006). Extensive forest mortality from insects, drought, and other stressors can impair the economic value of forests, water quality, cultural and spiritual values, and the recreational potential (Boyd et al., 2013; Weed et al., 2013). The importance of forests as global carbon sink may also be reduced by increasing forest disturbances (Kurz et al., 2008a,b). Finally, as regime shifts might overtake the adaptive capacity of species relying on particular disturbance regimes, human-induced alterations of forest ecosystems can impair the ecosystems biodiversity (Schulze et al., 2014). In consequence, there is a great need for understanding the complex processes and interactions of forest ecosystem and human activity, allowing the development of adequate management strategies that maintain the important services forests provide to humanity. While forest disturbance can result from a variety of agents, this dissertation focusses on insect disturbances, being among the most important agents of forest change in temperate and boreal forest ecosystems (Dale et al., 2001a).

1.2 Insect disturbances

Disturbances by native insects are natural and integrated processes of forest ecosystems around the globe. The forest insects commonly found in temperature and boreal forest regimes can be broadly group into xylophagous (wood-feeding, including bark, wood, and root) and folivorous (leaf-feeding) insects, among smaller groups of mucivores (fluid-feeders) (Table 1.1; Hicke et al., 2012). Wood-feeding insects of importance for temperate and boreal forests include several species of bark beetles, such as the mountain pine beetle *Dendroctonus ponderosae* in North America or the European spruce bark beetle *Ips typographus* in Europe. Bark beetles reproduce in the phloem tissues of live and dead trees and – through introduction of several fungal pathogens – clog the phloem, which limits the translocation of water and nutrients through the tree. Bark beetle infestation thus can be mortal for living trees. Leaf-feeding (defoliating) insects, such as of the genus *Choristoneura* in North America or the gypsy moth *Lymantria dispar* in Europe, feed on the needles or leaves of trees. As such, defoliators do not directly affect the trees water and nutrient cycles, though they impact the trees capacity for performing photosynthesis, which can lead to growth reduction, deformation, and tree mortality (Cooke et al., 2007).

Insect disturbances have several impacts on the forest ecosystem processes and services, in particular on the ecosystem biodiversity, the ecosystems biogeophysical and biogeochemical cycles, and the economic value of forest. From a biodiversity perspective, insect disturbances create a variety of biological legacies, including intact thickets of understory vegetation, large dead and alive overstory trees, logs and snags, and coarse wood debris, which all together provide valuable habitat for a va-

Table 1.1: Forest insect species that cause major disturbances in North America (adapted from (Hicke et al., 2012)

Insect type	Insect species	Host species	Origin	Major outbreaks
Bar beetles	Mountain pine beetle (*Dendroctonus ponderosae* Hopkins)	Pines of western North America (*Pinus*)	Native	1930s: 200,000 ha, Idaho, U.S.; 1970s to 1980s: 2 Mha, western U.S.; 2000s: 12 Mha, western Canada
	Spruce beetle (*Dendroctonus rufipennis* Kirby)	Spruces of western and northeastern North America (*Picea*)	Native	1990s: 1.5 Mha, Alaska, U.S.; Current: 112,000 in Alaska, U.S.
	Western balsam bark beetle (*Dryocoetes confusus* Swaine)	Subalpine fir (*Abies lasiocarpa* (Hook.) Nutt.)	Native	Ongoing: 216,000 ha, western U.S.
	Southern pine beetle (*Dendroctonus frontalis* Zimmermann)	Pines of the southern U.S. (*Pinus*)	Native	Mid-1980s: 10.5 Mha; Early 2000s: 5 Mha
	Conifer engraver species (*Ips* spp.)	Pines (*Pinus*) and spruces (*Picea*)	Native	2000s: 1.2 Mha, southwestern U.S
	Fir engraver beetle (*Scolytus ventralis* LeConte)	True firs (*Abies*)	Native	Ongoing: 20,000 ha, western U.S.
Defoliators	Eastern spruce budworm (*Choristoneura fumiferana* Clemens)	True firs (*Abies*) and spruces (*Picea*)	Native	1940s: 16 Mha, eastern Canada; 1970s to 1980s: 20 Mha, eastern Canada
	Western spruce budworm (*Choristoneura freemani* Razowski = *Choristoneura occidentalis* Freeman)	Douglas-fir (*Pseudotsuga menziesii* (Mirb.) Franco), true firs (*Abies*), and spruces (*Picea*)	Native	1980s: 5 Mha, western U.S.; Ongoing: 769,000 ha, western U.S. and 700,000 ha in western Canada
	Gypsy moth (*Lymantria dispar* Linnaeus)	Multiple tree species throughout north eastern U.S.	Invasive	Early 1980s: 5.3 Mha, north eastern U.S.; Ongoing: 60,000 ha, north eastern U.S.
	Forest tent caterpillar (*Malacosoma disstria* Hubner)	Broadleaf species in North America	Native	Early 2000s: 2.8 Mha in central U.S. and 14 Mha in Canada
Fluid feeders	Hemlock woolly adelgid (*Adelges tsugae* Annand)	Hemlock (*Tsuga*)	Invasive	Ongoing and expanding in 17 states in eastern U.S.
Wood borers	Emerald ash borer (*Agrilus planipennis* Fairmaire)	Ash (*Fraxinus*)	Invasive	Introduced in 2002 ongoing outbreak threatening species extirpations
Root feeders	Weevils (*Curculionidae* spp.)	Maple (*Acer*), birch (*Betula*)	Invasive	15% of fine root biomass of northern hardwood forests in upper Midwestern United States consumed annually

riety of cavity-nesting, shrub-nesting, and bark-drilling species (Saab et al., 2014). Moreover, insect disturbances can change forest successional pathways, transforming even-aged stands shaped by stand-replacing fires or harvest into more complex, multi-aged stands, which might positively influence landscape heterogeneity and biodiversity (Burton, 2010). As such, insect disturbances play a key role in maintaining biodiversity in forest ecosystems (Muller et al., 2008).

The changes caused by forest insects at the stand and landscape scale also impact biogeophysical and biogeochemical cycles and related ecosystem services (Edburg et al., 2012). Those impacts include changes in the water, carbon, and nutrient cycling, as well as impacts on the energy budget and micro-climate of forests. For example, insect disturbances can decrease the leave area of a forest, which in

turn is changing the forests transpiration, evaporation, and soil moisture content (Morehouse et al., 2008). Widespread infestation and mortality from insect disturbances can consequently impair important ecosystem services associated with water supply (Bearup et al., 2014). Likewise, insect infestation also changes the forests' carbon and nitrogen cycling through affecting the amount of live, dead, and decaying biomass (Hicke et al., 2012). Insect disturbances thus play a crucial role for the ecosystem services associated with carbon sequestration (Kurz et al., 2008a). In particular, insect infestation can shift forest resources from a net sink to a net source if experiencing widespread outbreaks of forest insects (Dymond et al., 2010; Kurz et al., 2008b).

Outbreaks of bark beetles and defoliators also have several negative economic consequences. The costs to manage and mitigate recent outbreaks of several bark beetle and defoliator species in the US have accumulate to over 1,500,000,000 US dollar annually, which is five times the costs of wildfire (Dale et al., 2001a). The wood volume lost due to forest insect infestation in Canada is close to that from harvest and greatly exceeded that from fire (Fleming, 2000). Insect disturbances are thus of economic importance for the timber industry and can have sensible impacts on local to regional economies (Burton, 2010). Salvage logging is a common management strategy to recover timber losses from insect infestation, which, however, has several negative effects on the biodiversity, functioning, and services of a forest ecosystem (Lindenmayer and Noss, 2006). Thus, a better understanding of insect disturbances is of great important for resource managers, which need to balance the multiple services forests provide.

Insect disturbances are dynamic, meaning that they vary throughout space and time. The majority of the forest insect species found in temperate and boreal forests show an eruptive behaviour, that is their population densities oscillate over time (Hicke et al., 2012, see Table 1.1 for a summary of the most recent major insect outbreaks in North America). The question whether an insect population reaches outbreak levels depends on many factors at varying spatial scales (Raffa et al., 2008). In particular, several thresholds need to be passed in order to develop landscape to regional scale outbreaks (Fig. 1.1). Between outbreaks, the insects are present at low population densities in the so-called endemic state. During this endemic state, insects will only sporadically infest single trees or tree groups throughout their host range (host entry threshold; Fig. 1.1). The actual selection of trees for attack is determined by tree scale traits and physiological factors (Negron and Popp, 2004), by previous infestation, drought, or diseases that weaken the trees defensive system (Allen et al., 2015), and by insect behaviour, that is which tree is chosen for oviposition (Progar et al., 2014). After selecting a tree, insect individuals will successfully reproduce (reproduction threshold; Fig. 1.1), depending on tree physiology and

traits (e.g., phenology; Nealis and Regniere, 2014), the density of local populations (Nealis et al., 2009), and climate conditions (Nealis, 2012). If reproduction rates exceed mortality rates (i.e. from starvation and predation), the local population will increase in size, successfully infesting trees in the near surrounding (Robertson et al., 2007). At this point, the incipient epidemic state is entered, resulting in infestations of larger, spatially auto-correlated patches (Aukema et al., 2006). Whether insects successfully infest larger patches depends on several factors. This includes the availability and quality of hosts within close proximity (i.e., stand-scale characteristics; Klutsch et al., 2009), the density of the insect population, and several external controls, in particular if and how the stand is managed, example given by application of pesticides. Once those stand scale thresholds have been passed, infestation patches will increase in size and coalesce to form larger patches of infestation (landscape scale outbreak threshold; Fig. 1.1) and the outbreak enters the epidemic state. However, not the entire landscape will be infested, resulting in a mosaic of infested and un-infested patches, where spatial distribution is determined by insect dispersal (Anderson and Sturtevant, 2011), availability, quality, and heterogeneity/connectivity of the habitat at the landscape scale (Seidl et al., 2015; Simard et al., 2012), as well as on (topographic) barriers (Robertson et al., 2009). Under normal conditions, epidemic populations collapse at some point in time, either triggered by climate conditions or by decline in food resources (Flower et al., 2014; Wulder et al., 2006a), leading to the collapse of the outbreak. However, if climate conditions stay favourable and if – at the landscape scale – hosts are abundant and connected, landscape scale outbreaks can collapse into a regional scale outbreak (regional scale outbreak threshold; Fig. 1.1). To form a regional scale outbreak, there must be several synchronous eruptions of landscape scale outbreaks, which often is a result of synchronization of climate conditions (Flower et al., 2014; Haynes et al., 2013; Seidl et al., 2015) and long-term insect dispersal (Anderson and Sturtevant, 2011; Haynes et al., 2013). Thus, understanding – and subsequently predicting – insect outbreak dynamics requires consideration of factors across several magnitudes of scales (Seidl et al., 2011; Sturtevant et al., 2015). In particular, the thresholds associated with the transition from a stand to landscape scale, and from a landscape to regional scale outbreak must be well understood in order to develop management strategies that efficiently reduce the risk of outbreaks with significant ecological and economic impacts (Raffa et al., 2008).

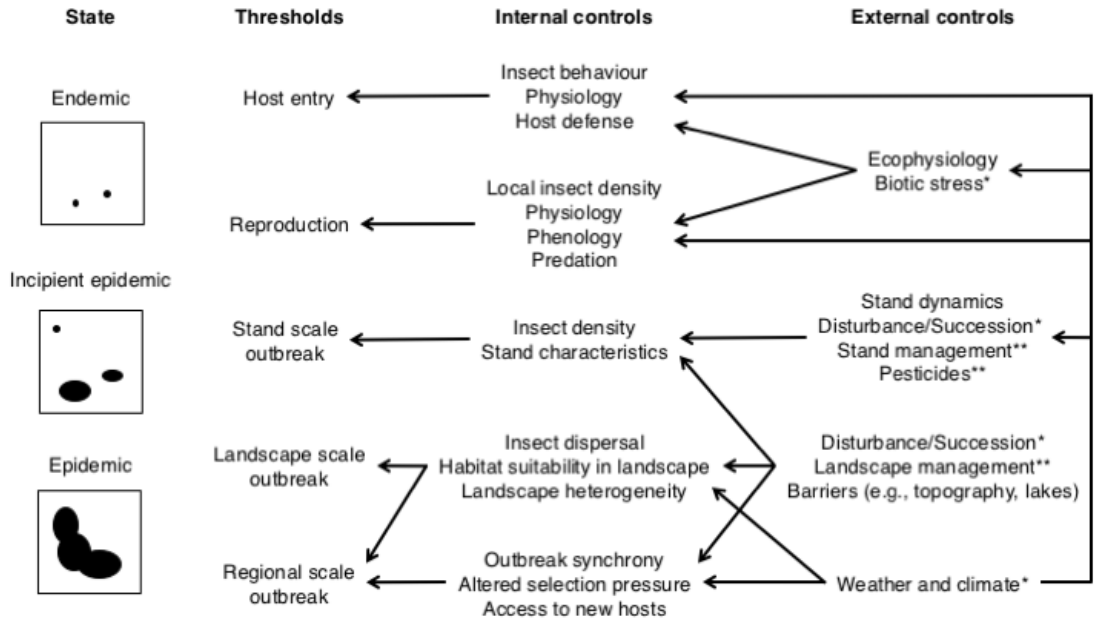

Figure 1.1: Schematic representation of thresholds that need to be passed to form a landscape to regional scale insect outbreak, including internal and external controls of thresholds. Internal and external controls interact across scales. One asterisk (*) indicates indirect anthropogenic influence on external control. Two asterisks (**) indicate direct anthropogenic influence on external controls. The figure is adapted from Raffa et al. (2008).

1.3 Budworm disturbances in the coniferous forests of western North America

Even though insect infestation is a global phenomenon that is found throughout all biomes, this dissertation focusses on temperate coniferous forests, in particular on Douglas-fir (*Pseudotsuga* spp.) dominated forest of western North America. Douglas-fir is one of the most important and valuable timber trees and it has been a major component of the forests of western North America (Franklin et al., 1981). The latitudinal range of Douglas-fir is among the greatest of any conifer of North America. It is endemic between 19° and 55° north (Fig. 1.2b). From the coast of British Columbia and Vancouver Island, Canada, the habitat extends south along the Pacific Coast Ranges of the U.S. for about 2,200 km, representing the range of the coastal variety, *menziesii*. From the interior of British Columbia, an even larger habitat stretches along the Rocky Mountains into the mountains of central Mexico, covering a distance of nearly 4,500 km and comprising the range of the other variety, *glauca* or blue Douglas-fir.

A representative of the interior Douglas-fir forests of western North America is the Interior Douglas-fir Forest (IDF) zone of British Columbia (Hope et al., 1991,

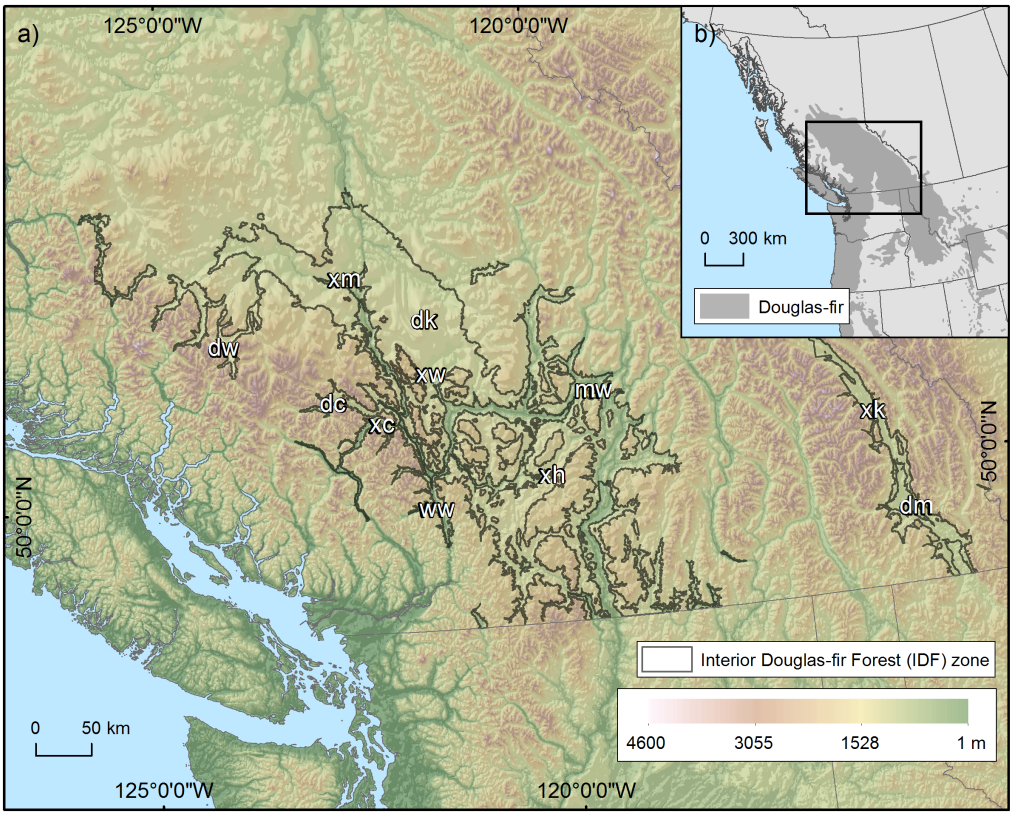

Figure 1.2: The main map (a) shows the Interior Douglas-fir Forest zone (IDF), which is the study region of the dissertation. The IDF is located in British Columbia, Canada, and represents the northern end of the Douglas-fir habitat (b). The abbreviations in the main map indicate the biogeoclimatic subzones of the IDF (please see Table 1.2 for further information).

Fig. 1.2a). The IDF zone is located in the interior plateau and mountains of British Columbia (between 49° and 53° North) and set between the Coastal Mountains to the west, the Cascade Mountains to the south, and the Rocky Mountains to the east. The topography of the IDF is composed of gently rolling hills and large valleys (i.e., along the Columbia, Fraser, and Thompson rivers), with elevations ranging between 600 and 1,450 m. The IDF has a continental climate characterized by warm and dry summers, a fairly long growing season, and cold winters. The main factors controlling the climate are the Coastal and Cascade Mountains, resulting in substantial shadowing effects to the prevailing easterly flowing air. The mean annual temperature is 1.6 to 9.5 °C, with 2 to 5 months of average temperatures below 0 °C, and 3 to 5 months of average temperatures above 10 °C. The mean annual precipitation ranges from 300 to 750 mm, except in the wettest areas where precipitation exceeds 1,000 mm, and up to 50% of the precipitation falls as snow during winter (all values from Hope et al., 1991). Substantial growing season moisture deficits are common in the region (Overpeck and Udall, 2010) and night frosts can occur at any time. The IDF is furthermore subdivided into seven biogeoclimatic

subzones (Pojar et al., 1987, Table 1.2 and Fig. 1.2a), which characterize the IDF's local climatic variants according to their relative temperature and moisture regime. While the IDF is generally considered dry (subzone *dw*, *dm*, *dk*, and *dc*), the valleys are usually extreme dry (subzone *xm*, *xw*, *xc*, *xh*, and *xk*). Moist to wet climates are found only in the Coastal Mountains and in the Rocky Mountains (subzone *ww* and *mw*). The southern dry valleys are warm to hot (subzones *xw* and *xh*), while the northern dry valleys are more mild to cold (subzones *xm* and *dk*). Very cool regions are only found in the Coastal Mountains (subzones *dc* and *xc*).

Table 1.2: Biogeoclimatic subzones of the Interior Douglas-fir Forest zone with main climate characteristics and relative distribution.

Subzone	Description	Mean temperature in °C	Mean precipitation in mm (as snow in %)	Percent of IDF (%)
xc	very dry cool	2.5	557 (44)	10
xk	very dry cold	2.5	579 (45)	7
xm	very dry mild	4.5	429 (30)	3
xw	very dry warm	5.5	370 (25)	2
xh	very dry hot	6.6	404 (24)	15
dc	dry cool	2.6	822 (50)	6
dk	dry cold	3.7	497 (35)	30
dm	dry mild	3.7	691 (41)	11
dw	dry warm	4	573 (34)	4
mw	moist warm	5	788 (37)	11
ww	wet warm	7.2	870 (25)	1

The vegetation of the IDF is characterized by stands of mature blue Douglas-fir (*Pseudotsuga menziesii* (Mirb.) Franco) at elevations between 900 and 1,200 m, mixed stands of blue Douglas-fir and ponderosa pine (*Pinus ponderosa* Douglas ex C. Lawson) at elevations between 600 and 900 m, as well as mixed stands of blue Douglas-fir and lodgepole pine (*Pinus contorta* Douglas ex Loudon) at elevations between 1,200 and 1,450 m. Pure Douglas-fir stands often have an open canopy, due to common ground fires in the past that favoured survival of mature trees with thick bark. The low elevation valleys are largely non-treed and covered by bunchgrass or by open stands of ponderosa pine. Trembling aspen and paper birch are also widely abundant as seral species or along wetter areas. The IDF borders the Montane Spruce zone at higher elevations, which is characterized by extensive seral stands of lodgepole pine. To the north, the IDF transitions into the Sub-Boreal Pine and Spruce and the Sub-Boreal Spruce zone. The Sub-Boreal Pine zone is dominated by extensive seral stands of lodgepole pine, whereas the Sub-Boreal Spruce zone is dominated by white spruce (*Picea glauca* (Moench) Voss) and Engelmann spruce (*Picea engelmannii* Parry ex. Engelmann).

The IDF experienced a complex disturbance history with low intensity ground fires and insect defoliation, in particular by the western spruce budworm (*Choristoneura freemani* Razowski = *Choristoneura occidentalis* Free.[1]) (Alfaro et al.,

[1]Note that the binomial name for western spruce budworm has changed from *Choristoneura occidentalis* Freeman to *Choristoneura freemani* Razowski during the writing of the thesis.

2014; Axelson et al., 2015). Western spruce budworm is a defoliator native to western North America, with populations being found from New Mexico to British Columbia (Nealis, 2008). The primary host of western spruce budworm is Douglas-fir and true fir, but trees from other families, such as spruce, hemlock and pine might be affected if growing on site (Maclauchlan et al., 2006). Western spruce budworms complete one life cycle from egg to adult moth within 12 months. Moths emerge from pupa cases between July and August. After maturation, females deposit approximately 150 eggs on the underside of host tree needles. Larvae hatch from the eggs after 10 days and spin hibernacula for overwintering under bark scales or in and among lichens. In May to June, depending on climatic variations, larvae leave their hibernacula and start mining on one-year old needles or closed buds. As soon as shoots flush, they start mining the new foliage until completely consumed. Larvae become fully grown in July, on average 30 to 40 days after leaving their overwintering sites, and pupate for about 10 days on or near their last feeding site.

Western spruce budworm populations normally occur at low levels, but populations periodically increase to outbreak levels (Cooke et al., 2007). Outbreaks of western spruce budworm can lead to widespread defoliation from a few to up to 25 years (Campbell et al., 2006; Campbell, 1993). Common damages from western spruce budworm outbreaks are growth defects, reduced lumber quality, and tree mortality (Alfaro et al., 1982, 1985; Shepherd, 1994). Growth defects negatively affect wood supply by reducing timber volume (MacLean et al., 2001), with long-term losses exceeding 50% of the potential stand volume (Alfaro and Maclauchlan, 1992). Tree mortality, which occurs after several consecutive years of defoliation and often in conjunction with secondary bark beetle (Hummel and Agee, 2003; Shepherd, 1994), alters the age-class distribution and species composition of forest stands, having significant influences on the stands successional pathway (Hadley and Veblen, 1993). Western spruce budworm thus is a significant disturbance agent of the Douglas-fir forests of western North America (Hicke et al., 2012; Meigs et al., 2015).

Despite a large body of research investigating spatiotemporal outbreak dynamics of bark beetle species (Seidl et al., 2015; Simard et al., 2012) and defoliators of broadleaved and coniferous forests of eastern and boreal North America (Bouchard and Auger, 2013; Foster et al., 2013b), surprisingly little is known about the dynamics of defoliators of the coniferous forests of western North America (i.e., western spruce budworm). In particular, there is little information beyond that of laboratory or field experiments (e.g., Nealis, 2012; Nealis et al., 2009), involving only single individuals and few selected trees. While much process understanding results from those controlled experiments, we have seen earlier that landscape to regional scale outbreaks – as observed during the past decades (Hicke et al., 2012; Meigs et al., 2015) – are governed by processes across multiple scales. Fully understanding

outbreaks of western spruce budworm thus requires a more holistic, multi-scale view on insect disturbance patterns and processes. A reason for the lack of studies on landscape to regional scale patterns and processes of defoliator outbreaks in western North America might be the lack of adequate data for tackling such questions. One approach to fill this gap is the use of remote sensing data, which delivers spatially and temporally consistent information on the Earth's surface.

1.4 Remote sensing in ecosystem science

Remote sensing has a long history in the mapping and monitoring of ecosystems and ecosystem processes. While very early studies of ecosystem properties using remote sensing were primarily based on airborne data (Campbell and Wynne, 2011), the launch of the first Multispectral Scanner System (MSS) on board Landsat 1 (formerly Earth Resources Technology Satellite) in 1972 opened a new era of space-born remote sensing. With MSS, a consistent set of medium-resolution (60 m), multi-spectral (four bands) image data that covered large spatial extents (185 km by 185 km) was available to the scientific community. In particular, researchers were – for the first time ever – able to systematically monitor the biogeophysical and biogeochemical conditions of ecosystems across the Earth (Pecora, 1967). That way, Landsat MSS delivered a great set of maps, including land cover maps (Nelson et al., 1987) and forest cover and type maps (Jarvis, 1994), that were well suited for tackling research questions going beyond the plot and stand scale.

Following MSS, there has been an intensive development of new satellite sensors, which cover all regions of the electromagnetic spectrum as well as a range of spatial and temporal resolutions. In particular, the Thematic Mapper (TM) onboard Landsat 4 (1982 – 1993) and Landsat 5 (1984 – 2012) had an improved spatial resolution of 30 m and six multi-spectral bands plus one thermal band at 120 m spatial resolution. Beginning with Landsat 6 (1993) and followed by Landsat 7 (1999 – ongoing), the sensor instruments were again improved to the Enhanced Thematic Mapper (ETM; Landsat 6) and the Enhanced Thematic Mapper Plus (ETM+; Landsat 7). While Landsat 6 never reached its orbit, the ETM+ instrument onboard Landsat 7 had an additional 15 m resolution panchromatic band and the thermal bands spatial resolution was improved to 60 m. However, in 2003 the ETM+ Scan Line Corrector (SLC) failed, resulting in a substantial loss of valid observations per image. In 2013, Landsat 8 was launched with two new instruments onboard: The Operational Land Imager (OLI) and the Thermal Infrared Sensor (TIRS). OLI has one additional spectral band in the blue wavelength region, as well as an additional cirrus band for cloud detections. TIRS has two thermal infrared bands at 100 m spatial resolution. Besides Landsat, there exists a wide range of alternative multi-spectral, medium-

resolution sensors (Belward and Skøien, 2015; Wulder et al., 2008). However, most of those sensors are part of governmental programs and have restricted or costly data access. The newest development in terms of multi-spectral sensors is Sentinel-2, which was developed by the European Space Agency (ESA) and launched in June 2015. Sentinel-2 has similar spectral characteristics like OLI, though a higher spatial (10 m in visible and 20 m in near- and shortwave-infrared bands) and temporal (up to five days) resolution.

To meet the needs of other scientific communities, that is the climate, oceanographic, and cryospheric science communities, a new set of sensors was launched in 1999 and 2000, respectively, named the MODerate-resolution Imaging Spectroradiometer (MODIS) sensor onboard the Terra and Aqua satellites. MODIS was planned as successor of Advanced Very High Resolution Radiometer (AVHRR) series of satellites. MODIS is sensing the Earth's surface every 1 to 2 days with a spatial resolution of 500 to 1,000 m covering a swath width of 2,330 km at 36 spectral bands. MODIS was developed to improve the understanding of global dynamics and processes occurring on the land, in the oceans, and in the lower atmosphere, especially through its high temporal resolution that allowed for tracking intra-annual variation in photosynthetic activity (Zhang et al., 2003). The ready-to-use structure of its data products made MODIS the first choice for ecosystem modelers. In particular, MODIS delivered regular interval (8 or 16 days) composites of standard vegetation indices and bidirectional reflectance distribution function corrected surface reflectance products that were accompanied by easy-to-use quality products. Moreover, MODIS delivered annual products such as land cover maps (Garcia-Mora et al., 2012) or phenological metrics (Jonsson and Eklundh, 2002). Researchers relying on remote sensing data as input to ecosystem models (e.g., carbon models; Potter et al., 2007) could thus use a standardized product at minimum processing costs and that is available on a very regular basis.

Besides Landsat and MODIS, remote sensing scientists working in the field of ecosystem science often made use of space- and air-borne high-resolution and very-high-resolution multi- and hyper-spectral sensors, as well as active sensors, in particular Light Detection And Ranging (LiDAR). High- and very-high-resolution sensors ($<$10 and $<$1 m spatial resolution, respectively; e.g., RadpidEye or IKONOS) provide detailed information on vegetation structure and single trees, though their applicability is limited by their often small spatial extents and high acquisition costs (Wulder et al., 2004). Nonetheless, they can provide important and rapid information to managers on processes in specific regions of interest (Falkowski et al., 2009; White, 2012). Space-borne high-resolution data can also help in generating reference data for up-scaling of field data to medium and coarse resolution satellite data (Meddens et al., 2011, 2013). Hyperspectral sensors provide a spectrally more

detailed picture of the Earth's surface characteristics than multi-spectral sensors and the high spectral resolution offers great opportunity for mapping ecological processes that go beyond the general characterization of vegetation structure, example given the leaf chemistry of plants (Smith et al., 2003) or vegetation communities (Underwood et al., 2003). LiDAR – an active laser sensor – delivers spatially high resolution information on the height, vertical structure, and coverage of vegetation, which can be used to estimate various structural parameters (Bolton et al., 2013). In particular, LiDAR is the 'gold standard' for mapping vegetation biomass (Pflugmacher et al., 2014), an ecosystem property of great interest to many scientists and managers.

The three types of sensors introduced in the previous paragraphs – high, medium, and low spatial resolution sensors with multi- to hyper-spectral resolution – have particular weaknesses and strength when it comes to mapping and monitoring ecosystem properties and processes. In particular, there is a trade-off between spatial resolution (the spatial grain of ecological analysis) and the temporal resolution (the effective temporal frequency of an observation; Fig. 1.3a). Very-high- and high-resolution sensors allow for a detailed spatial analysis of single trees or plants. However, those images often come from air-borne sensors or commercial satellite programs that have a very low repeat cycle and high acquisition costs, respectively. With data from the Landsat satellite series, the spatial grain of analysis decreases to 30 m and the repeat cycle increases to potentially 8 days (combining Landsat 5 and 7 or 7 and 8). However, most regions have not been continuously imaged every 16 days, because Landsat data acquisition follows the Long-term Data Acquisition Plan (LTAP), which gives priority to scenes over the continental US (Arvidson et al., 2006). Further considering cloud cover and Landsat 7's failed scan-line corrector, the effective temporal resolution is often much greater than 16 days (Ju and Roy, 2008). With MODIS, the spatial grain of analysis again decreases to 500 to 1,000 m, but there is potential daily imagery, though due to clouds the effective repeat cycle is 8 to 16 days, depending on the MODIS product.

Depending on the application, one or the other sensor might be a better choice (Fig. 1.3b). For example, agricultural processes cover very short time spans (rapid green-up in spring and harvest in summer), requiring a much higher temporal frequency than studies of drought processes, which often last over several years. Hence, a weakly MODIS time series might be necessary for delivering detailed intra-annual information on crop phenology (Sakamoto et al., 2005), but an annually spaced Landsat time series might be enough information for tracking vegetation changed caused by droughts (Assal et al., 2016). While the temporal resolution required for crop and drought monitoring is relatively well defined, the required spatial resolution depends on the system of interest. In particular, MODIS might be well suited

for mapping large fields in intensively used areas (Ozdogan, 2010), though might fail in areas of generally more fragmented and complex landscapes (Senf et al., 2015). Some other processes are less restricted in temporal resolution than in spatial grain. Harvest patches, for example, have often a very consistent size of a few hectares (in the US and Canada), making it hard to detect them with MODIS (Jin and Sader, 2005), and using very high-resolution imagery is costly to acquire over large spatial extents (Wulder et al., 2008). The temporal resolution required for mapping harvest depends on the study goals and can range from a few time steps (Kuemmerle et al., 2009) to annual (Griffiths et al., 2012). Thus, the choice of satellite data for studying ecosystems largely depends on the ecosystem and its ecosystem processes. Nonetheless, there are several sensors that are used more often than others. In the following, I will focus on the Landsat series of satellites, being the by far most important set of satellites for ecosystem science (Cohen and Goward, 2004; Kennedy et al., 2014).

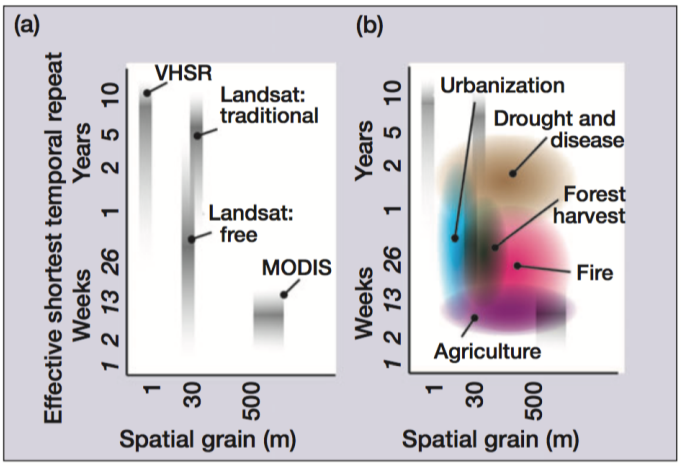

Figure 1.3: Trade-off between spatial and temporal resolution and associated sensors (a) and applications/processes (b). The figure is taken from Kennedy et al. (2014).

The Landsat series of satellites are particularly useful for ecosystem science and monitoring, mainly due to their spatial and temporal resolution and due to their outstanding long time series of more than 40 years (Cohen and Goward, 2004; Wulder et al., 2008). While past approaches incorporating Landsat often relied on single images that had to be purchased at approximately 600 US-Dollars per image (Wulder et al., 2012), a new data policy in 2008 has substantially changed the way Landsat data – and earth observation data in general – are used in ecosystem science and monitoring. In essence, the United States Geological Survey (USGS) decided upon an open data policy, which made all new and archived Landsat data held by the USGS freely available through the Earth Resources Observation and Science (EROS) Center (Wulder et al., 2012). However, much of the data from Landsat 1 through Landsat 5 has not been collected from the USGS, but from international cooperator

nations or regional groupings of nations such as the ESA. That way, many images collected outside the US were not affected by the USGS open data policy, still hampering the use of Landsat data for long-term ecological monitoring outside the U.S. (Senf et al., 2015). To fill this data gap, the Landsat international cooperator nations decided upon a Landsat Global Archive Consolidation (LGAC), which aimed at integrating all globally distributed Landsat archives into a single, freely and easily accessible, centralized global archive housed at EROS (Wulder et al., [in press]).

The great amount of freely available data has triggered the development of new methods for mass data processing, in particular standardized ways for radiometric and atmospheric correction, cloud masking, topographic correction, and geometric corrections (Hostert et al., 2015). Atmospheric correction is a key requirement for time series analysis (Kennedy et al., 2007) and many approaches have been developed in the past (for a detailed review see Banskota et al., 2014). Shortly prior to the opening of the Landsat archive, a notable advancement in atmospheric correction was made by the Landsat Ecosystem Disturbance Adaptive Processing System (LEDAPS) software (Masek et al., 2006), which employs an absolute atmospheric correction procedure called the Second Simulation of the Satellite Signal in the Solar Spectrum (S6) code by Vermote et al. (1997). The advantage of LEDAPS is that the program estimates per-pixel aerosol optical thickness (AOT) using the Dense Dark vegetation method developed by Kaufman et al. (1997), and that the program automatically retrieves additional ancillary data (i.e., water vapour and surface pressure, digital topography maps, ozone concentration) from various sources (Masek et al., 2006). The LEDAPS approach can be applied to Landsat TM and ETM+ data (Claverie et al., 2015) and the USGS has thus adopted LEDAPS as operational correction algorithm for their Surface Reflectance High Level Data Products. For Landsat 8, a new atmospheric correction algorithm was developed (Vermote et al., [in press]), which shows little differences to the surface reflectance obtained from Landsat 7 (Roy et al., [in press]). In terms of cloud masking, Zhu and Woodcock (2012) developed the Fmask algorithm, which was later translated into CFmask (a faster version implemented in the programming language C) and adopted as operational cloud screening algorithm for the Landsat Surface Reflectance High Level Data Products. While LEDAPS and CFmask have allowed for easy integration of large amounts of Landsat data from various sensors (White and Wulder, 2014), there is still room for improvement of existing methods (Frantz et al., 2016, 2015).

The frequent availability of cloud-free imagery has also triggered new developments in ecosystem related Landsat analysis (Kennedy et al., 2014). With nearly annual time series of Landsat data, new methods such for detecting abrupt forest disturbances caused by harvest and fire were developed (Griffiths et al., 2012; Huang et al., 2010; Schroeder et al., 2011), leading to continental scale analyses of forest

disturbances (Masek et al., 2013, 2008). The frequent availability of images in the open USGS archive has not only increased the temporal depth of analysis, but has also ended the per scene analysis of single Landsat images (Hansen and Loveland, 2012). By using compositing techniques – that is the selection of best pixels to create a pseudo-image of cloud-free observations over large extents (Griffiths et al., 2013) – a new series of studies was triggered that mapped stand-replacing forest disturbances over very large areas such as the Canadian boreal forests (Hermosilla et al., 2015b), the Russian boreal forests (Potapov et al., 2011), the Carpathians (Griffiths et al., 2014), and globally (Hansen et al., 2013). However, many forest disturbances are not necessarily stand-replacing, requiring a more sensitive mapping approach that allows for detecting gradual disturbances associated with forest health decline (Cohen et al., 2016; Meigs et al., 2011; Vogelmann et al., 2009). Consequently, there has been a recent development of algorithms that can simultaneously detect abrupt and gradual disturbances in Landsat time series (Hermosilla et al., 2015a; Kennedy et al., 2012, 2010; Moisen et al., [in press]). In detail, those algorithms fit a simple, piecewise linear function to each pixels spectral trajectory, representing the spectral-temporal characteristics of the pixel (i.e., the magnitude, duration, and rate of spectral change). Using those spectral-temporal characteristics allowed for separating varying disturbance agents (Kennedy et al., 2015) and for translating disturbances mapped from Landsat into units applicable to forest management, example given, into dead tree basal area (Bright et al., 2014; Meigs et al., 2011) or (changes in) forest biomass (Pflugmacher et al., 2012, 2014). That way, using Landsat time series allows for characterizing forest disturbances at a spatial, temporal, and thematic level necessary for understating and monitoring forest ecosystem changes. Nonetheless, there are still challenges associated with the detection and mapping of insect disturbances (Coops et al., 2006a), in particular if considering varying insect agents such as bark beetles and defoliators.

1.5 Research questions and objectives

The overall goal of this dissertation is to increase the understanding of landscape to regional scale patterns and processes of insect defoliator disturbances in the coniferous forests of western North America with the help of Landsat time series analysis. In order to develop a methodological set that can be utilized for achieving this goal, the first research question of the dissertation is:

Research Question I: How can Landsat remote sensing be used to map and quantify insect defoliator outbreaks?

While much progress in the mapping of forest disturbances was made in the last decade, the spatially and temporally consistent mapping of insect disturbances is still challenging. In particular, it is not well understood if and how disturbances from varying insect agents can be separated. Consequently, the objectives belonging to Research Question 1 are:

Objective 1: Characterize the spectral-temporal characteristics of insect disturbances using annual Landsat time series..

Objective 2: Test how well defoliator disturbances can be distinguished from other disturbance agents, that is bark beetle infestation, harvest, and fire.

Using a Landsat based approach likely allows for the reconstruction and analysis of historic insect defoliator outbreaks, which in turn allows for generating novel insights into the complex dynamics of insect outbreaks. To better understand the patterns and processes of defoliator disturbances in coniferous forests of western North America, the second research question of the dissertation is:

Research Question II: What are the spatiotemporal patterns and processes of outbreaks of western spruce budworm in the coniferous forests of western North America?

Answering the second research question requires an improved understanding of the spatiotemporal patterns of western spruce budworm at ecologically relevant spatial and temporal resolutions. Using the IDF zone of British Columbia as an example, the second objective of the dissertation consequently is:

Objective 3: Utilize the Landsat time series approach developed under Research Question 1 to quantify the spatiotemporal patterns of western spruce budworm infestation during its recent outbreak in British Columbia, Canada.

An improved understanding and mapping of the spatiotemporal outbreak pattern of western spruce budworm allows for the analysis of underlying drivers at the landscape and regional scale. As discussed above, regional scale outbreak dynamics are hypothesized to be driven by climate synchrony, while landscape scale patterns are hypothesized to be driven by stand to landscape scale factors. To test those hypotheses for the western spruce budworm in British Columbia, the dissertations third and fourth objectives are:

Objective 4: Assess and analyze potential drivers of regional scale western spruce budworm infestation patterns, in particular the regional scale weather variability patterns related to outbreak initiation.

Objective 5: Assess and analyze potential drivers of landscape scale western spruce budworm infestation patterns, in particular if and how factors across multiple scales can explain observed spatiotemporal patterns of western spruce budworm infestation.

This thesis is structured into three main research chapters following this introduction. Each chapter consists of one stand-alone manuscript published or submitted for publication to a peer-reviewed international journal. In particular, Research Question I is covered by Chapter II (published in *Remote Sensing of Environment*), whereas Research Question II is covered by Chapter III (in review with the *Canadian Journal of Remote Sensing*) and by Chapter IV (submitted to *Landscape Ecology*). The dissertation is synthesized in Chapter V.

Chapter 2

Characterizing spectral-temporal patterns of defoliator and bark beetle disturbances using Landsat time series

Cornelius Senf, Dirk Pflugmacher, Michael A. Wulder, and Patrick Hostert
Remote Sensing of Environment, 2015, Volume 170, Pages 166-177

DOI: 10.1016/j.rse.2015.09.019
Submitted on 12. March 2015; Revised on 11. September 2015; Accepted on 23. September 2015

Abstract

Defoliators and bark beetles are natural disturbance agents in many forest ecosystems around the world. Mapping the spatial and temporal patterns of insect disturbance dynamics can help in understanding their impacts on forest ecosystem resilience and functioning, and in developing adaptive management strategies. In recent years, much progress has been made in landscape-level analyses of insect-induced disturbances using remotely sensed data. However, many studies have focused on single insect agents or aggregated different insect agents into a single group. In this study, we characterized the temporal-spectral patterns associated with bark beetle and defoliator disturbances using Landsat time series between 1990 and 2013, with the objective to test if the two insect disturbances can be separated with Landsat data. We analyzed a recent outbreak of mountain pine beetle (*Dendroctonus ponderosae* Hopkins) and western spruce budworm (*Choristoneura freemani* Razowski) in British Columbia, Canada. To characterize the disturbance and recovery trends associated with insect disturbances we used the LandTrendr segmentation algorithm. We fitted LandTrendr spectral trajectories to annual normalized burn ratio (NBR) and Tasseled Cap (TC) time series, from which we then extracted a set of disturbance metrics. With these disturbance metrics, two random forest models were trained to a) distinguish insect disturbances from harvest and fire disturbances; and to b) attribute the insect disturbances to the most likely agent, i.e. mountain pine beetle or western spruce budworm. Insect disturbances were successfully mapped with an overall accuracy of 76.8%, and agents were successfully attributed with overall accuracies ranging from 75.3% to 88.0%, depending on whether only pure host-stands or mixed stands with both insect hosts were considered. In the case of mixed host stands, nearly 45% of the western spruce budworm disturbances were falsely attributed to mountain pine beetle. Spectral metrics describing disturbance magnitude were more important for distinguishing the two insect agents than the disturbance duration. Spectral changes associated with western spruce budworm disturbances had generally lower magnitudes than mountain pine beetle disturbances. Moreover, disturbances by western spruce budworm were more strongly associated with changes in TC greenness, whereas disturbances by mountain pine beetle were more strongly associated with changes in TC brightness and wetness. The results reflect the ephemeral nature of defoliators versus the tree mortality impacts of bark beetles in our study area. This study demonstrates the potential of Landsat time series for mapping bark beetle and defoliator disturbances at the agent level and highlights the need for distinguishing between the two insect agents to adequately capture their impacts on ecosystem processes.

2.1 Introduction

Insect disturbances play an important role in forest ecosystem dynamics by renewing old and susceptible forests, recycling nutrients, and providing food for wildlife (Parker et al., 2006). There is increasing evidence that human actions through management and climate change have altered the interactions between insects and forests, resulting in more widespread insect outbreaks (Raffa et al., 2008; Schoennagel et al., 2004; Swetnam and Lynch, 1993). Using climate change projections, current research indicates that outbreaks will become more frequent in the future (Logan et al., 2003; Volney and Fleming, 2000; Woods et al., 2010), which will have significant consequences for the future carbon balance of forests (Hicke et al., 2012; Kurz et al., 2008a,b).

Monitoring insect outbreaks with remote sensing data systematically over space and time can help with understanding landscape-scale causes and consequences of insect disturbances. Two of the most prevalent insect agents causing widespread tree damage and mortality are bark beetles and defoliators. Since impacts of defoliators and bark beetles on ecosystem function and structure are different (Hicke et al., 2012), distinguishing between insect agents is important to adapt forest management strategies and to improve ecosystem process models. However, studies mapping insect disturbances over large areas usually group defoliators and bark beetles into a single disturbance category (Huang et al., 2010; Kennedy et al., 2012; Masek et al., 2013).

In coniferous forests of North America, the most important bark beetle is the mountain pine beetle (*Dendroctonus ponderosae* Hopkins). Mountain pine beetles reproduce in the phloem below the bark and introduce a fungus, which clogs the phloem and limits the translocation of water and nutrients through the tree. By using pheromones, the beetles usually follow a cooperative behaviour strategy (mass attack) to help overcome the defensive system of trees. Attacks by mountain pine beetle are not noticeable in the first year of infestation (green-attack stage) but typically lead to complete discoloration (red-attack stage) in the second year and complete defoliation (grey-attack stage) in the third year (Wulder et al., 2006a). However, the progression of infestation by mountain pine beetle can vary by region, site, and species (Wulder et al., 2006a).

In comparison to bark beetles, defoliating insects cause mild to moderate disturbances (Cooke et al., 2007). The most prominent defoliators in coniferous forests of North America are in the genus *Choristoneura* (spruce budworm), including the eastern spruce budworm (*C. fumiferana* Clemems), the jack pine budworm (*C. pinus pinus* Freeman), the western spruce budworm (*C. freemani* Razowski), the 2-year-cycle spruce budworm (*C. biennis* Free.), and the coastal spruce budworm (*C. orae* Free.) (Nealis, 2008). From those, the western spruce budworm is most important

for western North America (Hicke et al., 2012). Western spruce budworm larvae feed primarily on current-year foliage, which can lead to chlorosis, crown dieback, and tree death; particularly when insect populations are high over several years and in cases of secondary infestation by bark beetles (Alfaro et al., 1985, 1982; Shepherd, 1994). Nonetheless, if defoliation rates are low, most trees typically will experience little damage and recover within several years (Campbell et al., 2006; Shepherd, 1994). Western spruce budworm outbreaks return every 30 years on average, though the intensity of outbreaks can vary significantly (Alfaro et al., 2014; Axelson et al., 2015).

Previous studies have shown that Landsat's spectral bands can be used to discriminate healthy forests from insect disturbed forests. Also, with a 30 m spatial resolution, Landsat operates at a scale that is informative for ecological research and management decisions (Cohen and Goward, 2004; Wulder et al., 2008). Early studies utilizing Landsat for insect disturbance mapping in coniferous forests typically used spectral information from one or two images, including the Tasseled Cap components (Franklin et al., 1995; Skakun et al., 2003), spectral bands (Franklin et al., 2003), spectral mixture analysis (Radeloff et al., 1999), and vegetation indices based on near-infrared and shortwave-infrared reflectance (Franklin et al., 2008). However, approaches based on single years and binary maps are somewhat restricted in characterizing the complex ecological dynamics of insect outbreaks. Thus, a more comprehensive mapping approach is needed, utilizing as many points in time as possible and characterizing the disturbance magnitude and duration (Gillanders et al., 2008; Kennedy et al., 2014).

Following the opening of the United States Geological Survey (USGS) Landsat archive and the related increase in capacity to produce time series (Wulder et al., 2012), annual Landsat time series were successfully used in a number of studies to capture insect-infestation. While implemented just prior to the opening of the USGS archive, Goodwin et al. (2008) used annual Landsat time series to capture infestation by mountain pine beetle in British Columbia. In this study, spectral trajectories displayed little to no change in the first year of infestation, but a decreasing trend in subsequent years. Similar spectral and temporal trends were found for mountain pine beetle in Montana (Assal et al., 2014), in Colorado (Meddens and Hicke, 2014), and in Oregon (Meigs et al., 2011). The changes in Landsat spectral trajectories were linked to tree mortality (Meigs et al., 2011; Pflugmacher et al., 2012), which enabled a landscape-scale assessment of mountain pine beetle impacts (Bright et al., 2014; Meigs et al., 2015). Defoliator disturbances were also associated with gradual changes in the spectral signal (Meigs et al., 2011; Vogelmann et al., 2009, 2012), but spectral trajectories were highly variable. Changes during defoliation were explained by decreasing vigor, top-kill, and increasing mortality resulting from

consecutive defoliation events, though many trajectories also showed quick spectral recovery after disturbance. Thus, recent studies suggest that Landsat time series can be utilized to characterize the complex spatial and temporal dynamics of insect outbreaks, but spectral trajectories vary considerable among insect agents, regions, and outbreak intensities. To better understand the ecological dynamics of insect disturbances, a better understanding of the spectral-temporal trajectories of individual insect agents is needed, enabling a more detailed mapping of insect disturbances – that is by distinguishing between bark beetle and defoliator disturbances.

Here, our goal was to determine the capacity of spectral-temporal trajectories from annual Landsat time series to map defoliator and bark beetle disturbance dynamics in southern-interior British Columbia, Canada. Our specific objectives were to:

1. Test how well bark beetle and defoliator disturbances can be distinguished with Landsat time series.

2. Characterize the spectral-temporal trajectories of bark beetle and defoliator disturbances with respect to severity, duration, and spectral recovery.

3. Map the spatial and temporal pattern of mountain pine beetle and western spruce budworm disturbances.

2.2 Study site

Our study site is located in the interior of British Columbia, Canada, occupying an area of approximately 149,700 km^2. The outer extent of the study site (hereafter referred to as Interior) is delineated by eight Landsat footprints (WRS-2 path/row: 45/25, 45/26, 46/24, 46/25, 46/26, 47/24, 47/25, 48/24; Fig. 2.1). In British Columbia, a province-wide biogeoclimatic classification system has been established that describes the natural ecozones based on climatic and vegetation characteristics (Pojar et al., 1987). The Interior is dominated by the Interior Douglas-fir Forest zone (Hope et al., 1991). The Interior Douglas-fir Forest zone is characterized by mature Douglas-fir (*Pseudotsuga menziesii* (Mirb.) Franco) stands at mid-elevations (900 – 1,200m), mixed stands of Douglas-fir and ponderosa pine (*Pinus ponderosa* Douglas ex C. Lawson) at lower elevations (600 – 900m), and mixed stands of Douglas-fir and lodgepole pine (*Pinus contorta* Douglas) at higher elevations (1,200 – 1,450). The Interior Douglas-fir Forest borders the Montane Spruce zone at higher elevations, which is actually a transition zone to the Engelmann Spruce and Subalpine Fir zone. In the Interior, the Montane Spruce zone is characterized by extensive seral stands of lodgepole pine. At lower elevations, the Interior Douglas-fir Forest borders the Ponderosa Pine zone, which is dominated by open stands of ponderosa

pine. In the northern part of the study site, the Interior Douglas-fir Forest borders the Sub-Boreal Pine and Spruce zone. The Sub-Boreal Pine and Spruce zone is dominated by lodgepole pine. The very low elevation areas are part of the largely non-treed bunchgrass zone.

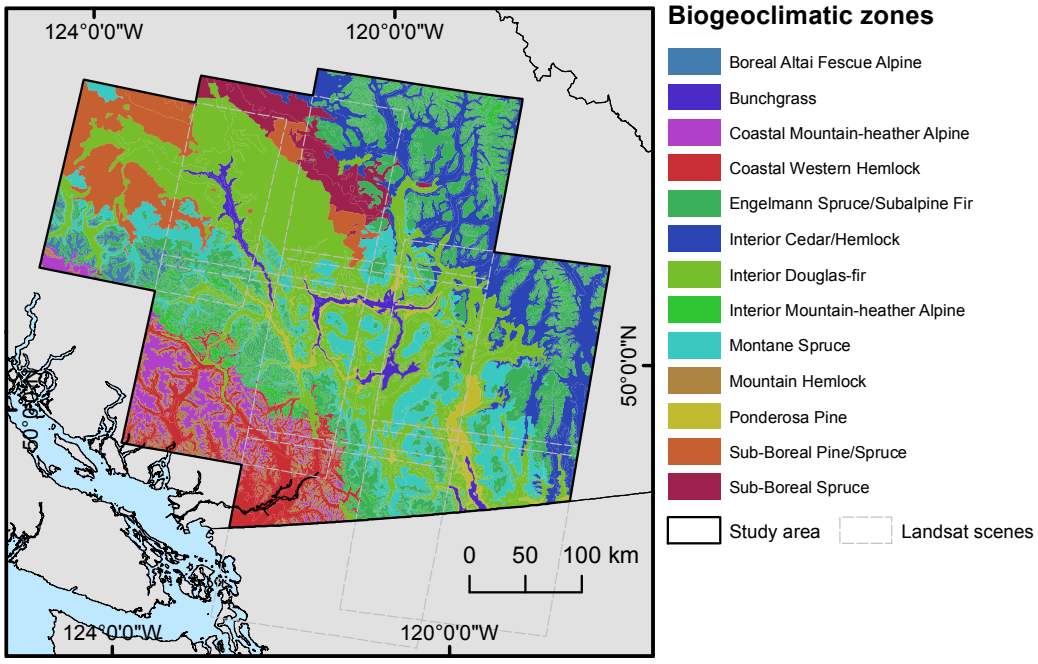

Figure 2.1: Study area in British Columbia. The main map shows the major biogeoclimatic zones (BEC zones) in the study area.

The Interior and in particular the Interior Douglas-fir Forest have experienced a complex history of fire and insect disturbances (Campbell et al., 2006; Maclauchlan et al., 2006). There are records of western spruce budworm outbreaks over the past 400 years, although outbreak frequency has increased markedly during the past century (Campbell et al., 2006). The most recent outbreak from 1999 to 2012 affected the whole IDF and peaked in 2007 at approximately one million hectares of defoliated trees. It was the largest outbreak in recorded history (Westfall and Ebata, 2012). In British Columbia, western spruce budworm mainly feeds on Douglas-fir and true fir, though other species such as hemlock, Engelmann spruce, larch, and pine might occasionally be attacked if growing on site (Maclauchlan et al., 2006). Mountain pine beetle is also active in the Interior. The most recent outbreak occurred between 2002 and 2012 and led to high mortality rates in ponderosa and lodgepole pine stands (Westfall and Ebata, 2012). Even though mountain pine beetle can feed on any pine species, lodgepole-pine is considered its primary host in British Columbia (Wulder et al., 2006a).

2.3 Data and methods

2.3.1 Landsat data and LandTrendr disturbance mapping

We used the LandTrendr segmentation approach (Kennedy et al., 2010) to map and characterize disturbances between 1990 and 2013. To achieve this, we followed three main steps: 1) create annual time series of cloud-free, anniversary-date observations; 2) fit time series trajectories for each pixel; and 3) derive a set of metrics from each trajectory to describe the disturbance and recovery characteristics of each pixel. We processed all Landsat footprints individually in their original UTM projection (WGS84) and then mosaicked the final disturbance metrics for the whole study site in the BC Albers Equal Area (NAD83) projection. For mosaicking, we used Voronoi polygons as edge lines between neighbouring scenes (Kennedy et al., 2012). Areas that were non-forest in 1990 were masked out using a binary forest cover map created from supervised classification.

To minimize the effect of phenology and data gaps caused by atmospheric interference, LandTrendr builds annual anniversary-date, best observation composites using all cloud-free observations from each scene and overlapping scenes within a pre-defined seasonal window (Kennedy et al., 2010). We downloaded all available Landsat Thematic Mapper (TM) and Enhanced Thematic Mapper Plus (ETM+) scenes from the US Geological Survey (USGS) archive and used the LEDAPS algorithm (Masek et al., 2006) to produce surface reflectance images for the 23-year time period. For building the best observation composites, we defined the seasonal window as ±30 days around July 15th. Clouds, cloud shadows, and snow were detected and masked out using the Fmask algorithm (Zhu and Woodcock, 2012).

Once a consistent annual time series is created, the LandTrendr algorithm fits spectral trajectories to the time series by dividing it into a series of connected linear segments following two main steps: First, the start and end of each segment is determined by estimating the years of change using a spectral index of choice (segmentation process). Second, the spectral index values at vertices are estimated (fitting process), yielding a trajectory of interconnected segments that characterize the disturbance history for each pixel (Fig. 2.2). The segment breakpoints are called vertices. In this study, we used the Normalized Burn Ratio (NBR) (Key and Benson 2006) to derive the segmentation and then applied the fitting to NBR and the first three Tasseled Cap (TC) components (Crist, 1985). NBR has previously been demonstrated to be sensitive to insect disturbances in North America (e.g., De Beurs and Townsend, 2008; Meigs et al., 2011; Townsend et al., 2012) and has been used with LandTrendr in other studies (Kennedy et al., 2010, 2012; Meigs et al., 2011). However, NBR is only a single spectral index based on two bands, whereas the TC components are multi-dimensional indices derived from the multispectral

data space. The TC components are sensitive to green vegetation abundance and vigor (greenness), canopy structure and moisture (wetness), and background soil signal (brightness) (Cohen and Goward, 2004) and have been used in many studies mapping insect infestation (e.g., Coops et al., 2006b; Skakun et al., 2003; Wulder et al., 2006b).

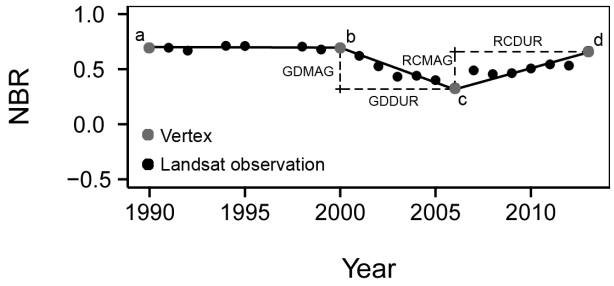

Figure 2.2: Exemplified LandTrendr segmentation and spectral trajectory fitted to an NBR time series. Grey dots (a-d) indicate vertices. Disturbance and recovery metrics derived from the trajectory are shown.

Finally, we derived a set of metrics describing the spectral-temporal characteristics of the trajectory fitted to NBR and TC trajectories, closely following Meigs et al. (2011) and Pflugmacher et al. (2014). For each pixel's trajectory, we first identified the greatest disturbance segment, defined as the segment with the greatest negative change in NBR. From the greatest disturbance segment, we calculated the change magnitude (GDMAG; Fig. 2.2), segment duration (GDDUR; Fig. 2.2), and recorded the onset of disturbance, defined as the first year of the greatest disturbance segment. Similarly, we calculated recovery magnitude (RCMAG; Fig. 2.2) and duration (RCDUR; Fig. 2.2) from the spectral recovery segment following the greatest disturbance segment. To facilitate interpretation, the NBR change magnitudes of disturbance and recovery were converted to percent change relative to the spectral value of the pre-disturbance condition (start vertex of each segment).

2.3.2 Mapping approach

We followed a two-phase classification approach to map spatial and temporal patterns of mountain pine beetle and western spruce budworm disturbances (Goodwin et al., 2008; Meigs et al., 2015): First, we classified the LandTrendr disturbance and recovery metrics into harvest and fire disturbances, insect disturbances, and undisturbed areas. We refer to this classification phase as disturbance classification. Second, we assigned all pixels identified as insect disturbances in the first classification phase a likelihood of being disturbed by either mountain pine beetle or western spruce budworm (in the following referred to as insect agent attribution).

Phase one: disturbance classification

In the first classification phase, we used the LandTrendr disturbance metrics to classify forest changes into 1) insect disturbances, 2) harvest and fire disturbances, and 3) undisturbed forest. Clear-cut harvest and fires behave differently in spectral and temporal space than insect disturbances, which makes them distinguishable with Landsat time series (Goodwin et al., 2008; Kennedy et al., 2012; Meigs et al., 2015). While insect disturbance can lead to complete stand mortality, spectral change magnitudes associated with harvest and fire disturbances are usually significantly higher (Goodwin et al., 2008; Hais et al., 2009), and of shorter duration (Meigs et al., 2015). As reference data, we randomly selected and labeled 800 pixels closely following the approach by Cohen et al. (2010), Kennedy et al. (2012), Pflugmacher et al. (2012) and Meigs et al. (2015).

For identifying and labeling disturbances in the reference pixels, we used Landsat image chips, Landsat spectral trajectory plots, high-resolution imagery, the provincial aerial overview survey (AOS) database (Wulder et al., 2009), the provincial Vegetation Resource Inventory (VRI) database (Leckie and Gillis, 1995), and the Canadian National Fire Database. The AOS collects polygon-level data on insect agent and disturbance severity during aerial overflights. The AOS (Fig. 2.7) is currently the most comprehensive database on insect disturbances at the landscape level (Meddens et al., 2012), but it is not a precise spatial product as it has several positional and attribution limitations, and it is subject to a certain observer bias, such as off-nadir viewing, variations in lighting conditions, and interpreter experience and fatigue, among others (Wulder et al., 2006a). To reduce uncertainties in the AOS data, we omitted polygons with the severity class 'trace', indicating only single infested trees within a stand (Wulder et al., 2009). Moreover, we only included insect disturbed pixels within mountain pine beetle and western spruce budworm host-tree stands according to the VRI. Stands in the VRI are delineated using very-high-resolution imagery, and species composition is assigned using photo interpretation (Leckie and Gillis, 1995). Species composition information includes the six leading species including their relative abundance. In total, 358 pixels were undisturbed, 145 were disturbed by harvest or fire, and 267 pixels were disturbed by insects (either mountain pine beetle or western spruce budworm). A small proportion (30 pixels) could not clearly be assigned to one of the three categories, and those were excluded from further analyses. In Figure 2.3 we present examples of all three disturbances classes.

Using the reference pixels, we trained a random forest classification model (Breiman, 2001) provided in the *randomForest* package (Liaw and Wiener, 2002) of the statistical software R. The random forest model was validated using the out-of-bag confusion matrix (Breiman, 2001), from which we estimated overall, users, and pro-

ducers accuracies, as well as errors of omission and commission.

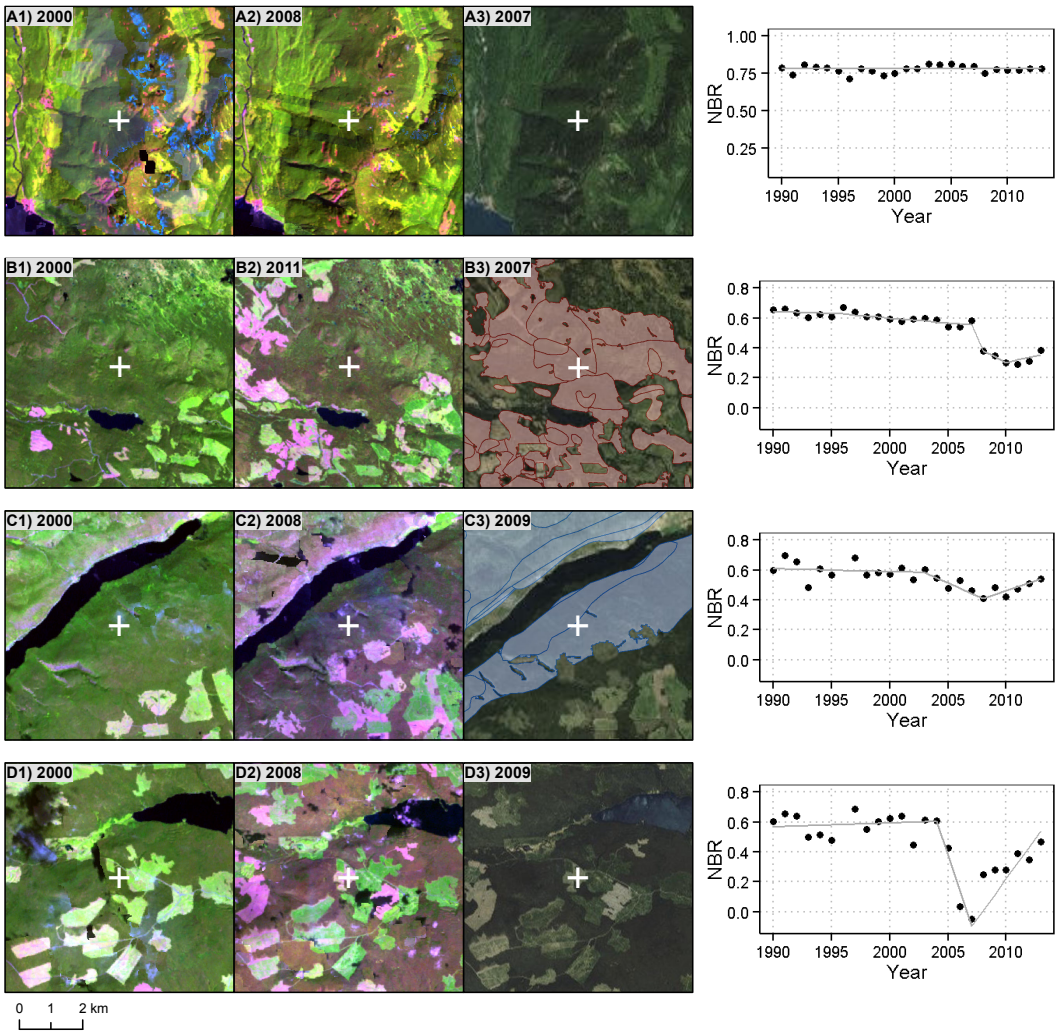

Figure 2.3: Four examples of Landsat spectral trajectories (black dots) and LandTrendr fitted trajectories (grey lines) with corresponding Landsat image chips (columns one and two; R/G/B=Landsat band 4/5/3) and very high-resolution imagery (column three). For mountain pine beetle and western spruce budworm disturbances (rows B and C) the AOS polygons also are shown.

Phase two: insect agent attribution

Following the disturbance mapping in phase one (Section 2.3.2), we estimated for each insect-disturbed pixel the probability of being disturbed by mountain pine beetle or western spruce budworm, respectively. Continuous probabilities of class presence offer greater flexibility in interpreting map predictions than discrete classes, i.e., by choosing more conservative or relaxed estimates of the total area disturbed (Wulder et al., 2006b). For this purpose, we calibrated a second random forest model with a second reference dataset based on the AOS and the VRI database. We selected all insect disturbance pixels covered by either a mountain pine beetle

or a western spruce budworm AOS polygon, again omitting the *trace* class. Some areas (16% of all pixels) were covered by mountain pine beetle and western spruce budworm polygons, and we omitted those pixels from the reference set to avoid confusion between both insects. For model training, we further narrowed down the selection to those pixels identified as pure mountain pine beetle or western spruce budworm host-stands in the VRI (i.e. 100% Douglas-fir or 100% lodgepole pine), reducing unrelated spectral variability in the reference data (Franklin et al., 2003). From this selection, we randomly drew 10,000 pixels for training of a random forests model as described in Section 2.3.2; and sampled 10,000 pixels for validating the model in pure stands. Moreover, we sampled a second reference set of 10,000 pixels, covering pure and mixed stands. Using two reference sets – that is one sampled in pure host stands and one sampled independently of host-configuration – allowed us to assess the effects of mixed stands on attribution accuracy.

Using the trained random forest model, we predicted the probability of mountain pine beetle and western spruce budworm disturbances for all insect disturbances pixels. In random forest, the probability of class membership is estimated from the proportion of tree votes obtained by a class.

2.4 Results

2.4.1 Classification of disturbances and insect agents

The disturbance classification yielded an overall accuracy of 76.8% (Table 2.1), with the highest users and producers accuracies in the harvest/fire disturbance class (80.9% and 84.8%, respectively), slightly lower users and producers accuracies for the undisturbed class (78.8% and 83.2%, respectively), and moderate accuracies for the insect disturbance class (70.8% and 63.7%, respectively). Class confusion was highest between insect disturbances and undisturbed areas. In total, 34±9% of the forested area was disturbed by insects and 20±9% were disturbed by harvest or fire. Most of the forested area in the study area (46±6%) was stable over the study period. The classification map (Fig. 2.4) was used to mask out undisturbed areas and harvest/fire disturbances in the following results.

The binary classification of mountain pine beetle and western spruce budworm disturbances (using a probability threshold of $p = 0.5$) achieved an overall accuracy of 88.0% in pure host-stands (Table 2.2), indicating that the two insects can be reliably distinguished using disturbance and recovery metrics derived from Landsat time series. Nonetheless, the overall accuracy dropped to 75.3% when mixed stands were considered (Table 2.3), suggesting that the attribution of insect agents is more difficult in stands composed of different host tree species. For pure stands

Table 2.1: Validation of the first classification phase (disturbance classification), which distinguishes undisturbed areas, insect disturbances, and clear-cut harvest and fire disturbances. The confusion matrix is derived from the out-of-bag sample of the random forest model.

		Reference					
	Class	Undisturbed	Insect	Harvest and Fire	Total	Users accuracy [%]	Error of commission [%]
Map	Undisturbed	298	74	6	378	78.8	21.2
	Insect	54	170	16	240	70.8	29.2
	Harvest and Fire	6	23	123	152	80.9	19.1
	Total	358	267	145			
	Producers accuracy [%]	83.2	63.7	84.8		Overall accuracy [%]	
	Error of omission [%]	16.8	36.3	15.2		76.8	

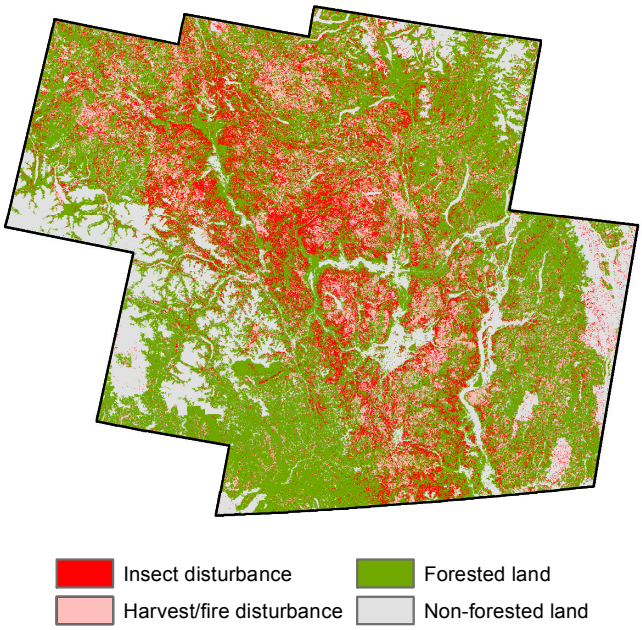

Figure 2.4: Map derived in the disturbance classification phase showing undisturbed areas, harvest/fire disturbances, and insect disturbances. A binary map of the insect disturbances is later used to mask out undisturbed areas and areas disturbed by harvest/fire (Fig. 2.7).

(Table 2.2), the producers and users accuracies were well balanced between both insects, whereas the users accuracy for mountain pine beetle disturbances was substantially lower (55.9%) for the mixed stands, which means that mountain pine beetle infected areas were overestimated in those stands.

2.4.2 Spectral-temporal characteristics of mountain pine beetle and western spruce budworm disturbances

Some differences between mountain pine beetle and western spruce budworm disturbances were apparent when comparing the disturbance and recovery metrics

Table 2.2: Validation of the first classification phase (disturbance classification), which distinguishes undisturbed areas, insect disturbances, and clear-cut harvest and fire disturbances. The confusion matrix is derived from the out-of-bag sample of the random forest model.

		Reference				
	Agent	WSBW	MPB	Total	Users accuracy [%]	Error of commission [%]
Map	WSBW	4996	563	5559	89.9	10.1
	MPB	636	3805	4441	85.7	14.3
	Total	5632	4368			
	Producers accuracy [%]	88.7	87.1		Overall accuracy [%]	
	Error of omission [%]	11.3	12.9		88	

Table 2.3: Validation of the first classification phase (disturbance classification), which distinguishes undisturbed areas, insect disturbances, and clear-cut harvest and fire disturbances. The confusion matrix is derived from the out-of-bag sample of the random forest model.

		Reference				
	Agent	WSBW	MPB	Total	Users accuracy [%]	Error of commission [%]
Map	WSBW	4970	450	5420	91.7	8.3
	MPB	2021	2559	4580	55.9	44.1
	Total	6991	3009			
	Producers accuracy [%]	71.1	85		Overall accuracy [%]	
	Error of omission [%]	28.9	15		75.3	

(Fig. 2.5). Disturbance magnitudes in NBR for mountain pine beetle were on average 20% higher than for western spruce budworm. For mountain pine beetle 50% of the disturbances had a disturbance magnitude higher than 40%, whereas for western spruce budworm this was only the case for 30% of the disturbances. The TC components showed more distinct differences between mountain pine beetle and western spruce budworm disturbances magnitudes (Fig. 2.6). Western spruce budworm disturbances showed a 30% higher decline in greenness than mountain pine beetle disturbances; whereas mountain pine beetle disturbances showed a three times higher decline in brightness than western spruce budworm. Moreover, mountain pine beetle disturbances showed a slightly higher increase in wetness during disturbance than western spruce budworm. This finding suggests that the TC components are of particular importance for separating between defoliator and bark beetle disturbances.

Differences in disturbance duration were not as distinct, though some general patterns could be observed (Fig. 2.5): For mountain pine beetle, 50% of the disturbances were very short (two years or less), 20% of the disturbances were between three and five years in duration, and 30% of the disturbances persisted longer than 5 years. In comparison, western spruce budworm disturbances were only slightly longer on average (five years compared to four years for mountain pine beetle), though the proportion of long-duration (>5 years) disturbances was higher (40%). Only 20% of the western spruce budworm disturbances were between three and five

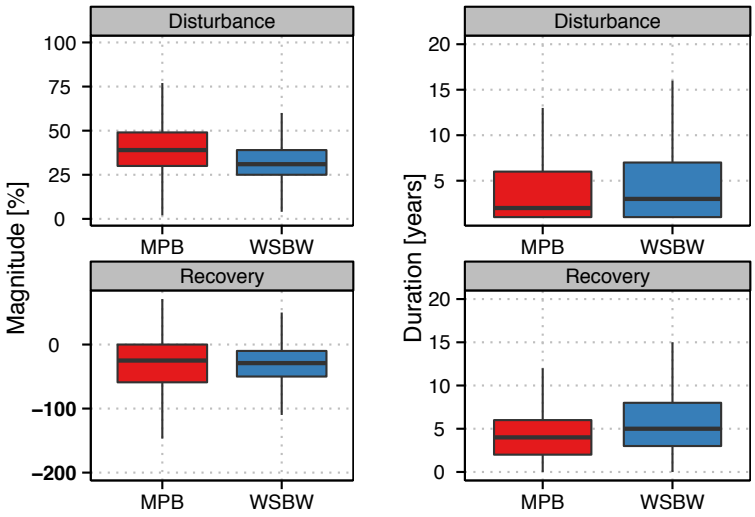

Figure 2.5: Boxplots of the disturbance and recovery metrics for the NBR stratified by insect agent. Disturbance and recovery magnitude from NBR are expressed in percent.

years, and the remaining 40% were two years or shorter.

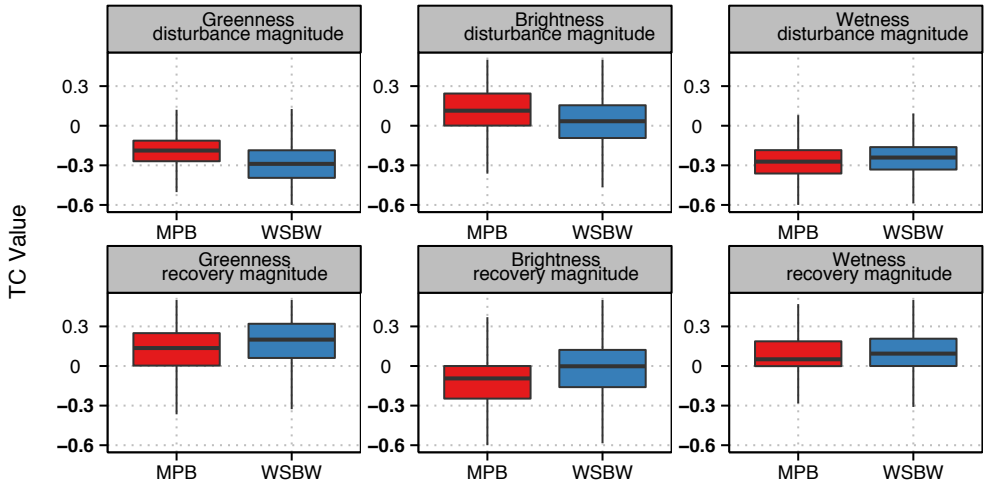

Figure 2.6: Boxplots of the disturbance and recovery metrics for the TC components stratified by insect agent. Change magnitudes from TC components are expressed as absolute change in greenness, brightness, and wetness, respectively.

Differences in NBR recovery magnitude (Fig. 2.5) were not as distinct as differences for disturbances, with mountain pine beetle experiencing a slightly higher variation in recovery magnitude. For recovery duration, however, western spruce budworm disturbances resulted in longer recovery durations compared to those following mountain pine beetle disturbances. For the TC recovery magnitudes (Fig. 2.6), western spruce budworm and mountain pine beetle disturbed stands tended to com-

pletely recover in TC greenness. For spectral recovery in wetness, both insects had lower spectral recovery values than the changes in wetness during disturbance. Recovery in brightness was close to the changes during disturbance for mountain pine beetle and close to zero for western spruce budworm.

2.4.3 Spatial and temporal pattern of mountain pine beetle and western spruce budworm disturbances

The maps of mountain pine beetle and western spruce budworm disturbance probability (Fig. 2.7) resembled the disturbance patterns of the aerial overview survey quite well, although the spatial detail is much higher. Some differences can be found for mountain pine beetle in the northwestern part of the study area, though this area has also been subject to intensive salvage logging and fire (Fig. 2.4). High probabilities of mountain pine beetle disturbances are concentrated in the lodgepole pine dominated area in the northeastern part of the study site (Sub-boreal Pine and Spruce zone and Sub-boreal Spruce zone), and in the higher elevation regions of the Montane Spruce zone. High probabilities of western spruce budworm disturbances are concentrated in lower-elevation parts of the Douglas-fir dominated areas (Interior Douglas-fir zone) and in the low area bunchgrass zones.

The temporal dynamics of the western spruce budworm and mountain pine beetle outbreak show distinct differences between both agents (Fig. 2.8). For our study area, the mountain pine beetle outbreak began in 2000, peaked in 2007, and decreased afterwards. The current western spruce budworm outbreak also started in 2000 and peaked in 2003. After 2003, infestations by western spruce budworm steadily declined until 2010. Comparing the Landsat based estimates to the temporal profiles of the AOS maps, substantial differences can be observed. The AOS-based area estimates are higher than the Landsat-based estimates, especially for mountain pine beetle. Nevertheless, the temporal patterns of the Landsat based estimates resemble the AOS based trajectories quite well.

2.5 Discussion

2.5.1 Mapping mountain pine beetle and western spruce budworm disturbances

Mapping approach

Our results confirm that insect disturbances can be distinguished reliably from undisturbed areas and more intense disturbances such as clear-cut harvest and fire

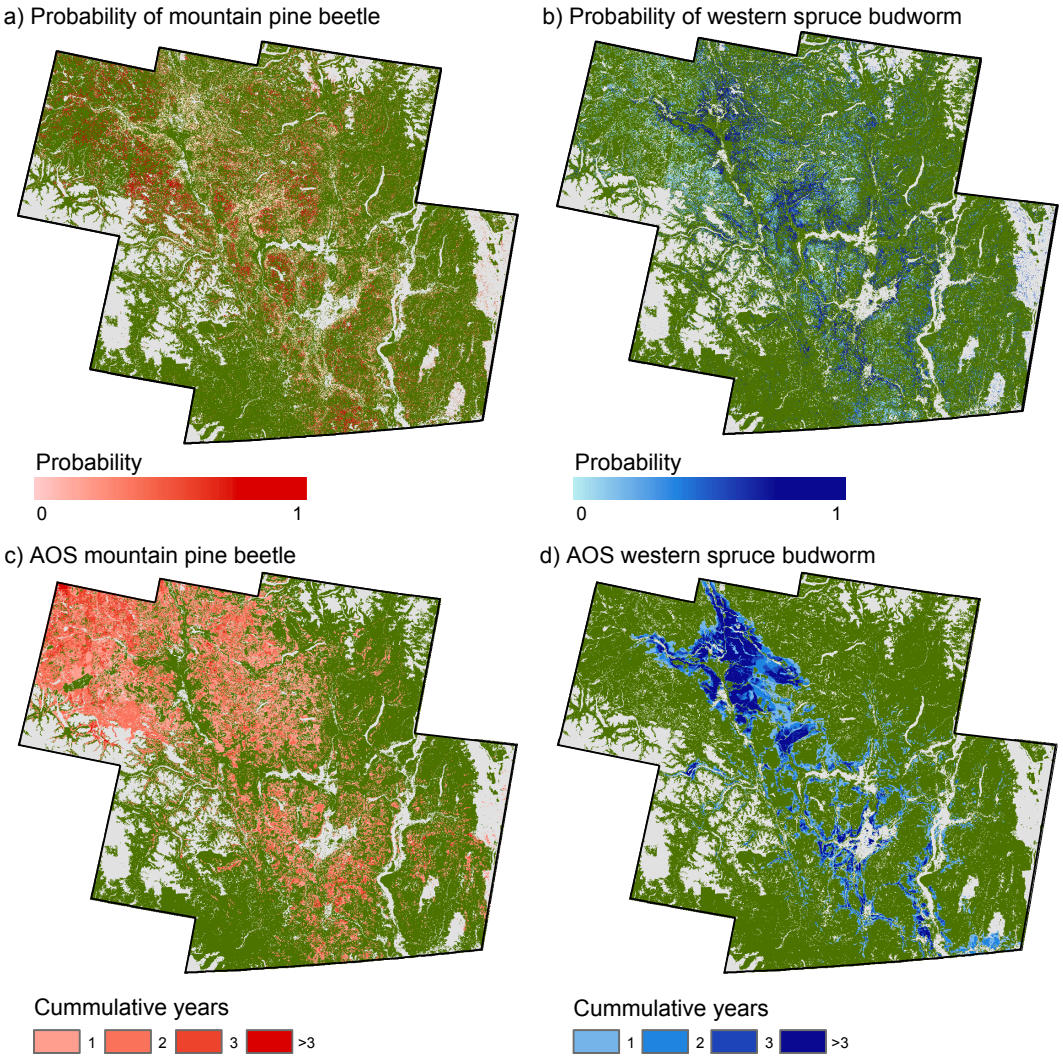

Figure 2.7: Mapped probability of (a) mountain pine beetle and (b) western spruce budworm disturbances in comparison to the Aerial Overview Survey (AOS) maps (c and d).

(Goodwin et al., 2008; Kennedy et al., 2012; Meigs et al., 2015), though insect disturbances might be confused with undisturbed areas once disturbance magnitudes are low. This issue was previously reported by other studies (Coops et al., 2006a; Kennedy et al., 2012) and results from the fact that slight disturbances are easily confused with spectral changes caused by residual clouds or phenological differences in the source image stack. Since this confusion results in a higher error of omission for insect disturbances, our resulting insect disturbance map is a more conservative estimation of the total area affected.

We presented evidence that defoliator and bark beetle disturbances can be separated in pure host-stands using spectral and temporal disturbance metrics derived from Landsat time series. However, once mixed stands were considered, there was a high likelihood (44.1%; Table 2.3) of mountain pine beetle disturbances being

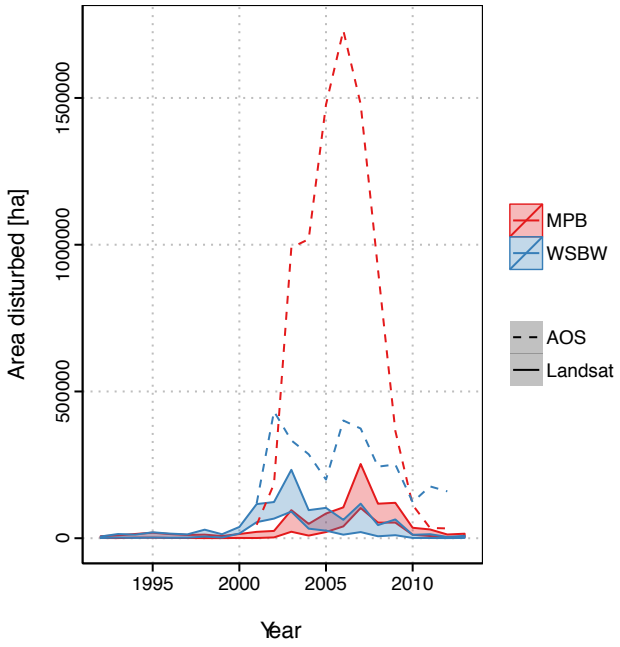

Figure 2.8: Temporal dynamics of the western spruce budworm and mountain pine beetle outbreak as estimated from Landsat and the Aerial Overview Survey (AOS) maps. Shown is the area (in hectares) disturbed by one of each insect over time. Landsat estimates are based on different thresholds used for classifying the probability output into presence/absence maps of mountain pine beetle and western spruce budworm. The upper bound represents all stands with a probability greater 0.5 and the lower bound represents all stands with a probability of greater 0.8.

falsely attributed. These errors were predominately located at the border between the Douglas-fir and the lodgepole pine dominated zones, where stands mixed between host- and non-host-trees are common. In those stands, western spruce budworm is the predominant agent of disturbance, but the spectral-temporal signal can be mixed between western spruce budworm and single pines attacked by mountain pine beetle. It is moreover possible that errors in the AOS database are more prevalent in those mixed stands, where different agents are hard to separate visually. Our mixed reference data set might thus include some false labels caused from erroneous attribution the AOS data. Using the VRI information, which is spatially explicit, can help identify stands that are more likely to be classified falsely.

In contrast to the methodological approach suggested by Meigs et al. (2015), which combines LandTrendr with AOS maps using a simple overlay analysis, we used the AOS data to train a model assigning a likelihood of insect agent to each disturbance pixel identified by LandTrendr. Our approach thus allows also attributing agents to insect disturbances outside of AOS polygons. By restricting the training process to those polygons coinciding with host-trees of each insect agent (Franklin et al., 2003), we moreover avoid false attribution by spatially erroneous AOS poly-

gons (i.e. mountain pine beetle AOS polygons in pure Douglas-fir forests).

Spatial and temporal pattern of western spruce budworm and mountain pine beetle disturbances

Our maps show the spatial and temporal patterns of the current outbreaks of mountain pine beetle and western spruce budworm in southern British Columbia, and they spatially expand the maps developed by Meigs et al. (2015) for the USA Pacific Northwest. The spatial patterns of mountain pine beetle and western spruce budworm probability resembled the BEC zones (Fig. 2.1) and thus the availability of host trees in our study area. Distinct differences in the probability were found for the northern zones (Sub-boreal Pine/Spruce zone) and for the higher elevation zones (Mountain Spruce zone) of the study area, where lodgepole pine is the leading species, and climatic conditions are considered to be less favorable for western spruce budworm. Highest probabilities of western spruce budworm disturbances were found in the lower elevation, hot and dry regions of the Interior Douglas-fir Forest zone, where western spruce budworm is known to be most active (Maclauchlan et al., 2006). In zones mixed between hosts of both insects, however, probabilities of either mountain pine beetle or western spruce budworm were generally lower, indicating that both insects might be present. In those areas, the attribution of one specific agent is thus hampered.

The mountain pine beetle outbreak in our study area started in 2000 and peaked in 2007, whereas the province-wide peak was in 2005 (Meddens et al., 2012). Since our study area is located south of the major lodgepole pine areas of British Columbia, the lag to the provincial trends is not unexpected. The western spruce budworm outbreak peaked earlier than mountain pine beetle. There is evidence that drought can influence western spruce beetle population dynamics and trigger outbreaks (Flower et al., 2014; Hicke et al., 2012), and the drought years 2000-2004 (Schwalm et al., 2012) might be one of the causes for the current outbreak.

Using probability maps instead of discrete class labels allowed for a flexible interpretation of results (Wulder et al., 2006b). Depending on the application, one can chose more conservative or relaxed thresholds, targeting management actions more precisely. Alternatively, it is possible to select the probability threshold based on a selection criteria such as maximized overall accuracy, kappa, or using receiver-operating characteristics (ROC) analysis (Manel et al., 2001).

Even though temporal patterns and trends of mountain pine beetle and western spruce budworm disturbances resembled each other in the Landsat and AOS maps (Fig. 2.8), we found substantial differences in the actual infestation area estimates (Fig. 2.7 and 2.8). Those differences were not unexpected and have been reported previously (Meigs et al., 2015), and emerge from the positional issues and the nature

of the manual attribution of AOS maps. AOS maps are manually prepared with infestation boundaries often generalized and including areas with non-infested trees or non-vegetated areas. While the Landsat-based estimates might underestimate trace insect disturbances (i.e., single infested trees), the large differences between the Landsat-and AOS based estimates reinforce that area estimates derived from AOS maps must be interpreted with caution (Wulder et al., 2006a).

2.5.2 Spectral-temporal characteristics of mountain pine beetle and western spruce budworm disturbances

Disturbance magnitude

Spectral change magnitudes were important predictors for distinguishing mountain pine beetle and western spruce budworm disturbances, which is not surprising as it directly relates to the biology and disturbance ecology of the two insects, particularly with respect to disturbance severity and contagiousness. Mountain pine beetle disturbances commonly lead to complete defoliation and mortality within a few years (Wulder et al., 2006a), explaining the high spectral change magnitudes associated with mountain pine beetle disturbances. Moreover, mountain pine beetle disturbances commonly occur in aggregated patches (Coops et al., 2010), which facilitates the detection with 30 m Landsat pixels (Meddens et al., 2013; Skakun et al., 2003). Infestation patterns by western spruce budworm are often diffuse (Cooke et al., 2007) and result in lower mortality rates, especially if feeding periods are short as in our case (Shepherd, 1994). Nonetheless, trees will show partial symptoms such as chlorosis, deformation, or top-kill (Campbell et al., 2006; Maclauchlan et al., 2006), which also influence the spectral disturbance magnitude. Looking at the VRI database, the rate of dead standing trees (percent of dead trees in relation to dead and alive trees per stand) in Douglas-fir stands affected by western spruce budworm was 15.4% (SD = 4.8%) compared to 44.9% (SD = 28.2%) for lodgepole pine stands affected by mountain pine beetle. Hence, the differences in disturbance magnitude between mountain pine beetle and western spruce budworm disturbances evident in in this study can be explained by the different impacts both insects have on tree mortality.

Even though we found expected differences in disturbance magnitude, we also observed an overlap between both insect agents (Fig. 2.5). Healthy trees present in mixed stands, which dampen the disturbance signal, might cause low disturbance severities for mountain pine beetle (Skakun et al., 2003). High disturbance severities for western spruce budworm might be the result of western spruce budworm co-occurring with secondary bark beetle (Hummel and Agee 2003) or drought (Flower et al., 2014). Hence, even though disturbance magnitude was of importance

for distinguishing between bark beetle and defoliator disturbances, there is high variability, which complicates the mapping in heterogeneous landscapes where hosts of both insects are present. In our study area, approximately 7% of the lodgepole pine and Douglas-fir stands were comprised a mixture of both host species (i.e., either lodgepole pine or Douglas-fir made up > 10% secondary species composition).

The disturbance metrics obtained from the TC components showed a more nuanced picture of the differences between both insect agents than the disturbance metrics obtained from the NBR. The NBR only captured the overall differences in tree mortality, whereas the changes in TC can be attributes to the different impacts both insects have on the tree canopy. The changes in wetness associated with mountain pine beetle can be attributed to the complete defoliation and thus change of the tree canopy caused by mountain pine beetle, which is corroborated by several other studies (Coops et al., 2009; Franklin et al., 2003; Hais et al., 2009; Skakun et al., 2003; Wulder et al., 2006b). The three times higher changes in brightness for mountain pine beetle disturbances can be attributed to higher bark, branch, and soil reflectance in completely defoliated stands (Hais et al., 2009). As a confounding factor, stands experiencing change at the canopy level can also exhibit stronger understory reflectance (Radeloff et al., 1999). In fact, Hais et al. (2009) found that increasing understory reflectance can increase TC greenness during bark beetle disturbance, which, however, was not the case in our study.

The higher changes in TC greenness associated with western spruce budworm defoliation found in this study might be an indication of the ephemeral changes in foliage, with low impacts on the overall canopy structure of a tree. This result is in agreement with a western spruce budworm outbreak in Oregon (Franklin1995) and with Gypsy Moth (*Lymantria dispar* Lin.) defoliation in northern Wisconsin (Thayn, 2013). Both studies showed that TC greenness was more important for predicting defoliation than wetness and brightness. A study of the jack pine budworm in Wisconsin (Radeloff et al., 1999) moreover found that changes in green needle fraction, obtained from spectral mixture analysis, had the highest correlation to populations of jack pine budworm.

Disturbance duration

The disturbance duration also showed differences between mountain pine beetle and western spruce budworm, with mountain pine beetle exhibiting mostly short-duration disturbances and western spruce budworm mostly medium- to long-duration disturbances. Mountain pine beetle infestations often follow a three-year scheme (i.e., green-, red-, and grey-attack stage; Goodwin et al., 2008; Wulder et al., 2006b), which is reflected in the high proportion of short-duration disturbances (two years or less) for mountain pine beetle found in this study. For western spruce budworm, the

majority of the disturbances were longer than two years, which reflects the common feeding periods of two to five years in our study area (Shepherd, 1994), though we also observed disturbances longer five years. Even though western spruce budworm disturbances tended to be longer than mountain pine beetle disturbances, duration observed in this study were still shorter than durations reported in a study from Oregon (Meigs et al., 2011). They found more distinct differences in disturbance duration between mountain pine beetle and western spruce budworm and chose a threshold of six years to visually separate both insect agents. For our study, this separation based solely on disturbance duration was not possible, suggesting that a combination of severity and duration metrics achieves best results in separating different insect agents.

Spectral recovery

The spectral recovery signals for western spruce budworm disturbances were generally longer than those for mountain pine beetle infestations. The recovery magnitudes for western spruce budworm disturbances were close the disturbance magnitudes, emphasizing the ephemeral nature of insect defoliation, with often complete regeneration of foliage in the years following the disturbance (Campbell et al., 2006; Cooke et al., 2007). However, understory vegetation also can contribute to the recovery signal by benefiting from the increased light availability in stand experiencing defoliation (Lynch and Moorcroft, 2008). The spectrally faster recovery of lodgepole pine stands may be an indication of such understory tree and shrub vegetation, which capitalizes on increased availability of water, sunlight, and nutrients in mountain pine beetle affected stands. This interpretation is also supported by the rapid changes in brightness following infestation, indicating that soil signals, which are present immediately after infestation, are rapidly covered by understory tree and shrub vegetation.

2.5.3 Transferability to other regions and uncertainties in the analysis

While this study shows that spectral and temporal patterns of insect disturbances are useful for distinguishing different insect agents, a review of the literature indicates that such patterns can vary by region and outbreak, which means that classification models and logics derived in our study may not be directly transferable to another region. For example, the western spruce budworm outbreak in our study was relatively short and mild, which is typical for this insect (Cooke et al., 2007). However, western spruce budworm impacts can also be more severe if the defoliation lasts over several years or co-occurs with secondary bark beetles. For

example, Meigs et al. (2015) found that mountain pine beetle and western spruce budworm generally had equal impacts on tree mortality, which is in contrast to our findings. Differences might result from the relatively light impacts of the current western spruce budworm outbreak compared to past outbreaks in British Columbia (Axelson et al., 2015; Lynch and Moorcroft, 2008) and from differences in regional climate, land use history, and management. For a more severe outbreak, the disturbance magnitudes of mountain pine beetle and western spruce budworm might be less important for distinguishing both insect agents than the disturbance duration (as in Meigs et al. (2011)).

The datasets used in this study have particular strength and weaknesses, introducing uncertainties that need to be considered while transferring methods derived in this study to other regions. First of all, our initial disturbance classification is based on photo-interpretation (i.e. interpretation of Landsat spectral trajectories, image chips, and high-resolution data; Fig 2.3), which might be prone to errors. Visually detecting high intensity disturbances such as harvest and fire is relatively easy to achieve, given their significant impact on the Landsat spectral trajectory (Fig 2.3). Photo-interpretation has thus been used frequently for labeling reference pixels of such disturbances (Cohen et al., 2010; Kennedy et al., 2012). However, visually detecting transient disturbances, i.e. as caused by light insect disturbances, can be more challenging. We used additional auxiliary data to guide interpretation of insect disturbances, which helped to separate true disturbances from spectral change caused from natural variance in the source stack, i.e. atmospheric noise, residual clouds, phenological differences, or spatial mis-registration.

A second source of uncertainty in the data arises from the AOS maps. Even though the AOS maps are the most comprehensive database on insect disturbances at the landscape level, they are not a precise spatial product. Spatial inaccuracy of the AOS polygons can result from numerous causes, including off-nadir viewing, variations in lighting conditions, and interpreter experience and fatigue, among others (Wulder et al., 2006a). For example, we identified stands where mountain pine beetle was detected even though no host-trees were present according to the VRI database. To account for this potential error in model training, we reduced the selection of training pixels to those pixels where the AOS maps coincided with the respective host tree (Franklin et al., 2003). For validating the model in pure and mixed stands (Table 2.3), however, we did not apply this filtering step, allowing for a more realistic representation of the landscape (i.e., by including pure and mixed stands). The second validation sample might thus include labeling errors resulting from the AOS dataset. Further research should consider alternative training/validation approaches based on ground-surveys, though for large spatial extents (as in the case of our study), those approaches can be very expensive and

time-consuming (Cohen et al., 2010).

2.6 Conclusion

In this study we characterized bark beetle and defoliator disturbances in southern-interior British Columbia, Canada, using a well-established Landsat-based time series segmentation approach. From our results, we conclude that Landsat can be utilized to distinguish between bark beetle and defoliation disturbances in our study region, using specific spectral-temporal features. In making the distinction between agents of insect disturbance the magnitude of disturbance was found to be of highest importance. Bark beetle disturbances led primarily to changes in wetness and brightness (i.e., changes in the tree structure such as complete needle loss). Defoliation disturbances were of lower magnitude and linked to changes in greenness (i.e., changes in the trees' foliage). The resulting maps and estimates offer a combined and detailed picture of the mountain pine beetle and western spruce budworm outbreaks in our study region through quantifying both the temporal and spatial dynamics. These otherwise unavailable spatially explicit and quality assured maps can help inform science and management information needs as well as offering new opportunities for addressing increasingly refined forest reporting objectives.

Acknowledgements

We thank Prof. Robert Kennedy, of Oregon State University, for making LandTrendr freely available (http://landtrendr.forestry.oregonstate.edu/) and we thank three anonymous reviewers for their very helpful comments.

Chapter 3

Using Landsat to assess the relationship between spatiotemporal patterns of western spruce budworm infestations and regional-scale weather variability

Cornelius Senf, Michael A. Wulder, Elizabeth M. Campbell, and Patrick Hostert
Canadian Journal of Remote Sensing, in review[1]

Submitted on 16. February 2016; Revised on 19. May 2016

[1]A revised version of this chapter was meanwhile accepted for publication: Senf, C., Wulder, M. A., Campbell, E. and Hostert P. (2016) Using Landsat to assess the relationship between spatiotemporal patterns of western spruce budworm outbreaks and regional-scale weather variability. Canadian Journal of Remote Sensing. DOI: 10.1080/07038992.2016.1220828

Abstract

Western spruce budworm is a native defoliator of coniferous forests of western North America. Past research has shown that climate is a principal driver of budworm outbreaks, though the underlying relationships are yet not fully understood. We utilized Landsat time series to investigate the relationships between spatiotemporal patterns of budworm infestations and weather variability. Landsat-based maps of budworm infestations from 1995 to 2013 were produced and used to describe spatiotemporal patterns of the most recent outbreak in British Columbia. Superposed epoch analysis and regression analysis were used to explore relationships between spatiotemporal outbreak patterns and annual temperature and precipitation anomalies. We found that initiation of outbreaks was preceded by autumn precipitation deficits that were 12% lower than the long-term average and co-occurred with lower summer precipitation of up to 20% below the long-term average. Spring temperatures shortly before outbreak initiation were by 0.7°C lower than normal, while winter temperatures during outbreaks were above average by 0.5°C. We conclude that the most recent outbreak of western spruce budworm in British Columbia co-occurred with distinct weather pattern that might have supported budworm population development. Furthermore, our results demonstrate the usefulness of Landsat for assessing landscape- to regional-scale drivers of insect disturbances.

3.1 Introduction

Western spruce budworm (*Choristoneura freemani* Razowski = *C. occidentalis* Freeman) is a native defoliator that feeds primarily on Douglas-fir (*Pseudotsuga menziesii* (Mirb.) Franco) and true firs (*Abies* spp.) throughout western North America (Nealis, 2008). Defoliation by the western spruce budworm is generally seen as an ephemeral disturbance and important for maintaining ecosystem heterogeneity and functioning (Hadley and Veblen, 1993; Cooke et al., 2007). Prolonged periods of defoliation, however, can lead to significant reductions in tree growth, crown dieback, and tree mortality that also reduce timber quality and quantity (Alfaro et al., 1985, 1982). Large trees stressed by budworm defoliation also are susceptible to secondary bark beetle infestations that typically kill their hosts (Alfaro et al., 1982; Shepherd, 1994; Campbell et al., 2006).

Localized western spruce budworm outbreaks tend to occur synchronously over large geographic regions. The synchrony and dynamics of budworm outbreaks are driven by multiple factors, including dispersal of adult moths (Anderson and Sturtevant, 2011; Cooke et al., 2007), synchrony in annual weather patterns over large spatial scales (i.e., the Moran effect; Moran, 1953), and land use activities, such as fire suppression and logging that have increased the extent of stands densely stocked with budworm hosts homogenizing forest landscapes (Flower et al., 2014; Swetnam and Lynch, 1993). While studies regarding the effects of land use on patterns of western spruce budworm outbreak have produced similar results, the effects of climate variability on outbreak dynamics remain inconclusive. Dendrochronology studies in British Columbia have shown that outbreaks coincide with periods of drought (Campbell et al., 2006; Thomson et al., 1984; Campbell et al., 2005). However, other tree-ring studies in New Mexico and Colorado showed that outbreaks follow wetter than average years (Swetnam and Lynch, 1993; Ryerson et al., 2003). These contradictory findings suggest regional differences in the effects of climate on western spruce budworm outbreak dynamics. Further analyses, over a range of temporal and spatial scales, are necessary to better understand how the dynamics of budworm outbreaks are related to climate, particularly given the increasing importance of global climate change.

Archival records indicate that several western spruce budworm outbreaks have occurred in Douglas-fir forests of southern British Columbia. Tree-ring studies report that western spruce budworm outbreaks of varying duration and intensity recurred about every 30 years over the last four centuries (Axelson et al., 2015; Alfaro et al., 2014). Aerial overview survey maps indicate that the most recent outbreak of western spruce budworm in British Columbia started in about 2000 and defoliated a cumulative maximum area of 847,138 hectares in 2007 (Westfall and Ebata, 2012). Both sources of data on outbreak history, dendrochronological archives and

aerial surveys, have limitations for assessing landscape- to regional-scale disturbance dynamics (Bright et al., 2014; Meddens and Hicke, 2014; Meigs et al., 2015). The spatial extent of dendrochronological data is typically limited and aerial survey data are limited by spatial errors in mapping the area and cause of defoliation (Wulder et al., 2009). Current research suggests that annual Landsat time series could be utilized to map the spatiotemporal patterns of insect disturbances (Senf et al., 2015; Meigs et al., 2011), thus delivering further insights and evidence at spatial and temporal scales currently not covered by studies based on tree rings and aerial surveys. By using Landsat time series, researchers and managers can for the first time assess the landscape- to regional-scale drivers underlying insect outbreaks, such as the effects of regional-scale weather variability on outbreak dynamics.

Our objective was to identify the precipitation and temperature patterns related to western spruce budworm disturbance dynamics during its most recent outbreak in British Columbia, Canada. We utilize a Landsat-based approach that allows for an accurate representation of spatiotemporal outbreak patterns over larger spatial extents than are practical to implement with dendrochronology field studies, and with higher spatial precision than is achievable with aerial surveys. Thus, our study extends past dendrochronological research and increases the ecological resolution of research based on aerial surveys showing the effect of climate variability on historic western spruce budworm outbreaks in this and other regions.

3.2 Data and methods

3.2.1 Study area

Our study area is located in south-central British Columbia, Canada, and delineated by the Interior Douglas-fir (IDF) biogeoclimatic zone (Hope et al., 1991) plus a 10 km buffer (Fig. 3.1). The southern part of the study area is characterized by mountainous terrain, which flattens out towards the more northern regions. The regional climate is characterized as relatively hot and dry, putting the IDF biogeoclimatic zone among the driest areas in Canada (Hope et al., 1991). The mean annual precipitation is 254.5 mm and the mean annual temperature is 7.8 C (data from the weather station in Merritt, BC), with a July mean temperature of 18.8C and a January mean temperature of -3°C. Towards the northern part of the study area (central interior), the precipitation increases to 307.6 mm, and the mean annual temperature drops to 4.5°C (data from the weather station in Williams Lake, BC), also with lower July and January means, 16.0°C and -6.7°C, respectively[2]. Moreover, a temperature gradient occurs with elevation; valleys of the southern interior

[2]All values obtained from: `https://climate.weather.gc.ca`

are dry and hot with precipitation increasing and temperatures decreasing in higher elevation forests.

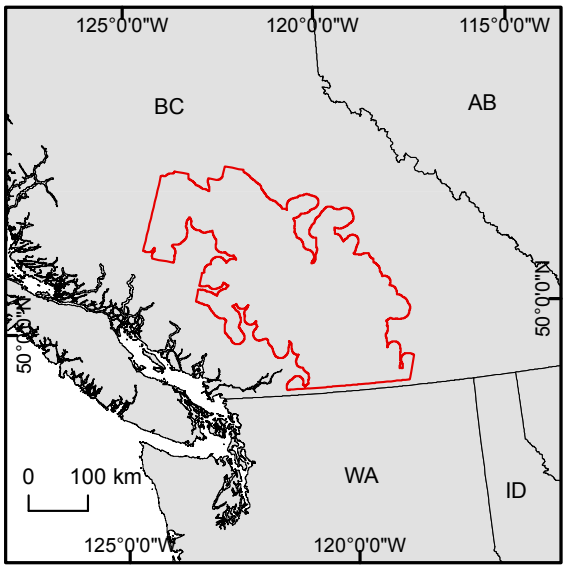

Figure 3.1: Location of the study area (red), which is delineated by a 10 km buffer around the Interior Douglas-fir Forest (IDF) biogeoclimatic zone. The study area is covered by approximately eight Landsat scenes.

Douglas-fir, which is most prone to western spruce budworm defoliation in British Columbia (Senf2015, Maclauchlan, Brooks, and Hodge 2006), is the dominant species of the IDF zone. Stands of nearly pure Douglas-fir occur between 900 and 1200m, while mixed stands of Douglas-fir and ponderosa pine (*Pinus ponderosa* Douglas ex C. Lawson) occur between 600 and 900 m, and mixed stands of Douglas-fir and lodgepole pine (*Pinus contorta* Douglas) occur between 1200 and 1450 m.

3.2.2 Landsat-based map of western spruce budworm infestations

We used maps depicting the annual probability of western spruce budworm infestation generated from a Landsat-based time series analyses in a previous study (Senf et al., 2015). Those maps represent the most recent outbreak of western spruce budworm in British Columbia (1995 – 2013). The mapping methods are described by Senf et al. (2015), but we provide salient details here. In essence, the western spruce budworm infestation probability maps are based on a set of spectral-temporal metrics derived from a time series segmentation algorithm (LandTrendr; Kennedy et al., 2010) that captures spectral-temporal changes at the pixel scale. Those spectral-temporal changes were used in conjunction with a classification model to separate western spruce budworm infestation from more severe disturbances caused by harvest, fire, and bark beetle infestation. This present study utilized those probability

maps to produce binary maps of localized western spruce budworm infestations occurrences in our study area. To do so, we reclassified the continuous surface of infestation probability into binary maps of western spruce budworm infestation presence and absence by choosing a probability threshold greater than 50%. To reduce the chance of false positives (i.e., falsely attributing disturbance caused by Douglas-fir tussock moth or Douglas-fir beetle to western spruce budworm), we followed the approach suggested by Meigs et al. (2015) and overlaid the infestation patches with aerial survey polygons of western spruce budworm defoliation. We thereby increased the likelihood of correctly attributing western spruce budworm infestations to vegetation changes detected by the Landsat time series while avoiding false positives generated by aerial survey mapping errors. To assess potential uncertainties in the resulting maps, we compared the infestation initiation date recorded by Landsat to the first year in which western spruce budworm was recorded in the aerial survey. It is important to note that once Landsat can detect western spruce budworm infestation, continuous defoliation normally persists for several consecutive years. In our study area, the average duration of an outbreak was approximately four years, though long outbreak periods of up to 15 years also occurred (Senf et al., 2015).

3.2.3 Historical climate data

We used ClimateWNA v5.1 (Wang et al., 2012) to calculate seasonal precipitation and temperature time series. To reduce the amount and redundancy of data in our analysis, we calculated climate time series for 1,000 randomly sampled Landsat pixel locations in areas disturbed by spruce budworm. Precipitation and temperature were expressed as total seasonal precipitation (mm) and seasonal average temperature (°C), respectively. The seasons cover winter (Dec – Feb), spring (Mar – May), summer (Jun – Aug), and autumn (Sep – Nov) precipitation and temperature. These periods roughly correspond to important stages in budworm life history events, with larvae emerging and establishing feeding sites in late April and May, larval feeding through to adult emergence and egg-laying occurring during the summer, and larval over-wintering from September through March of the following year (Nealis, 2008). We also calculated 30-year (1981 – 2010) normals of seasonal temperature precipitation for each sampled pixel.

3.2.4 Superposed Epoch Analysis

We used Superposed Epoch Analysis (SEA) to explore the relationship between annual precipitation and temperature anomalies and the year western spruce budworm infestation was initiated according to our Landsat analysis. The principal idea of SEA is to compose time series values (i.e., precipitation and temperature) in tempo-

ral relation (i.e., years) to key events (i.e., infestation initiation). By composing the values, that is, by calculating the arithmetic mean, random signals such as cyclic events or noise not related to the key event should ideally average out, highlighting the true signal related to the key events. SEA has been used to detect the effects of volcanic eruptions on temperature time series (Gennaretti et al., 2014) as well as to assess the effect of droughts on insect outbreaks reconstructed from dendrochronological time series (Flower et al., 2014). Our approach to SEA does not compose weather variables of several outbreaks within one time series, but rather 1,000 time series of localized infestations within one outbreak period (1995 – 2012) over our entire study area. Hence, we rely on a space-for-time approach to detect spatial patterns of infestation initiation related to spatial variation in s weather patterns over the study area.

To perform the SEA, we ordered all seasonal climate time series on a 21-year time window centered on the infestation initiation year recorded in the Landsat analysis. Hence, for each season, we derived precipitation and temperature values for ten years preceding infestation initiation, the initiation year, and for ten years following infestation initiation. We then calculated the arithmetic mean from all seasonal values within each year in relation to infestation initiation. This composited the temperature and precipitation values into mean anomalies for each of the ten years prior to, and following, the initiation of a localized outbreak. For ease of interpretation, we transposed the composited anomaly into absolute changes in precipitation and temperature compared to long-term normals (1980 – 2010).

To evaluate the significance of the precipitation and temperature anomalies, we applied a parametric bootstrap to calculate confidence intervals at the 99% level for the composed values. To account for multiple comparisons, we further applied a Bonferroni-correction to the confidence intervals. We regarded precipitation or temperature anomalies as significant anomalies if the Bonferroni-corrected 99% confidence intervals of the composed value did not overlap with zero.

3.2.5 Regression analysis

To identify the most influential precipitation and temperature variables on regional western spruce budworm outbreak dynamics, we used regression analysis describing relationships between annual infestation rates and seasonal precipitation and temperature averages across all sampled pixels for each year (1995 – 2012; n = 18). Annual infestation rates were calculated by dividing the total area infested in one year (x_t) by the total area infested in all years ($IR_t = x_t/\Sigma x_t$)). A similar approach was used to assess regional-scale climate drivers of bark beetle disturbances in previous studies (Seidl et al., 2015; Raffa et al., 2008). For the model we used beta-regression (Cribari-Neto and Zeileis, 2010) to account for the dependent data being

bounded between zero and one. We relied on an information-theoretic approach that depicts the likeliest models out of all possible model combinations based on the lowest small sample size adjusted Akaike's Information Criterion (AICc). We accounted for temporal autocorrelation in the residuals by using a robust sandwich estimator of the covariance matrix (Zeileis, 2006). All computations were performed in the R Language and Environment for Statistical Computing, using the *sandwich* (Zeileis, 2006), *betareg* (Cribari-Neto and Zeileis, 2010), and *MuMIn* (Barton, 2009) packages.

3.3 Results

3.3.1 Spatiotemporal patterns of western spruce budworm infestation in British Columbia

The Landsat analysis for the period 1995 to 2012 suggests that the western spruce budworm outbreak in our study area started to build in between 1999 and 2000 and increased until 2003, rapidly dropped in 2004, and then declined between 2005 and 2010 (Fig. 3.2). Even though very few infestation were initiated following 2010, defoliation caused by outbreaks in 2010 may persist after 2010.

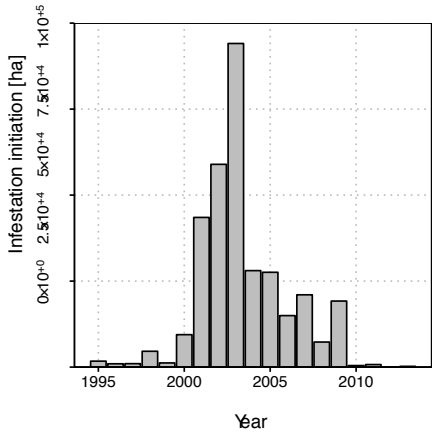

Figure 3.2: Temporal dynamics in western spruce budworm infestation during its most recent outbreak in British Columbia, Canada, according to our Landsat analysis.

The maps of annual infestation initiation (Fig. 3.3) indicated that between 1999 and 2001 the outbreak started to build-up in three epicenters in the northern, central, and southern part of the study area (Fig. 3.3 A, B, C). From those epicenters, infestation expanded into surrounding forests in 2002 and 2003, though most infestations during this time were observed in the north parts of the study area. Following the outbreak maximum in 2003, the outbreak expanded into higher elevation areas

in the western part of the study area (coastal mountains) and infested large parts of the southern and central Douglas-fir forests. From 2007 on, western spruce budworm infestations were detected in the eastern part of the study area (Okanagan valley) for the first time and expanded northwards in 2008 – 2009.

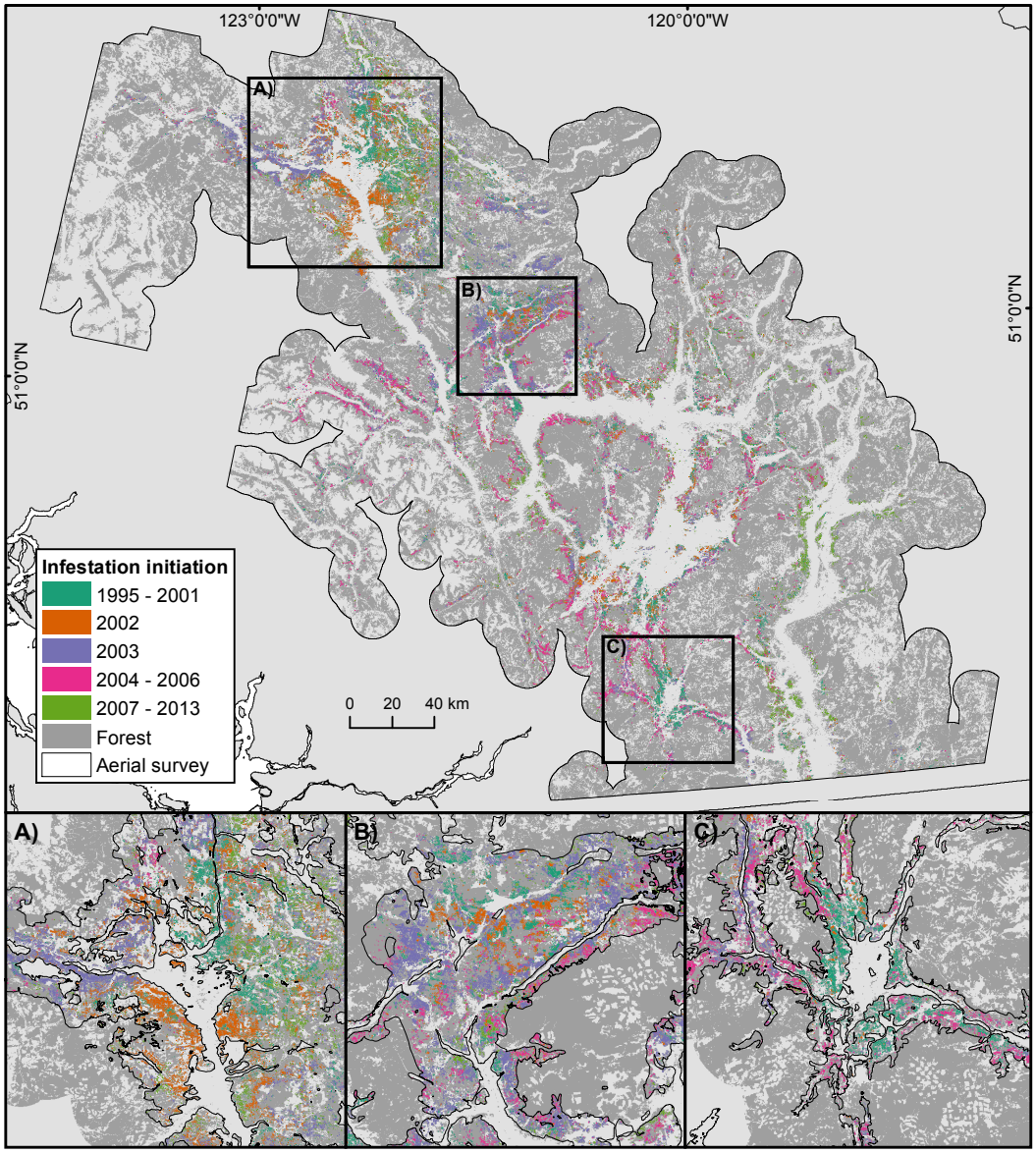

Figure 3.3: Western spruce budworm infestation mapped with Landsat time series during its most recent outbreak in British Columbia, Canada. For better interpretation we group years into quartiles. The zoom-in maps (A, B, and C) show examples of differences between the Landsat-based maps and the aerial overview survey polygons overlaid.

3.3.2 Seasonal weather anomalies related to infestation initiation

Superposed epoch analysis indicated western spruce budworm infestation initiation occurred during years with significantly lower than average summer precipitation and was preceded by significantly lower than average autumn precipitation (Fig. 3.4a; Table S3.1). Summer precipitation during and following infestation initiation was as much as to 26 mm (20%) lower than the long-term average and persisted for eight years following outbreak initiation. Summer precipitation shortly before the outbreak was not significantly different from the long-term normal, although significantly higher precipitation was found six to ten years prior to infestation initiation. Five consecutive years of low autumn precipitation preceded infestation initiation, with precipitation deficits of up to 17 mm (12%) below the average. No consistent relationships between spring and winter precipitation and infestation initiation were found.

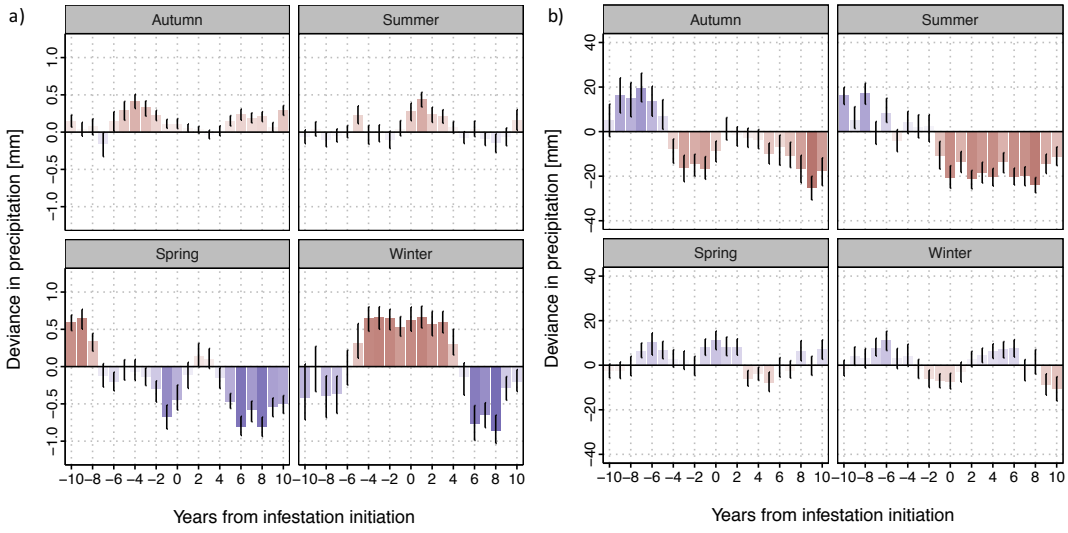

Figure 3.4: Superposed Epoch Analysis results, showing mean seasonal deviation in precipitation (a) and temperature (b) from the long-term mean for a 21-year window centered on western spruce budworm infestation initiation. Confidence intervals are at the 99% level (Bonferroni-corrected). Colors are scaled to the y-axis values. Details are provided in the Supplementary Materials.

We also found significant associations between temperature variability and western spruce budworm infestation initiation (Fig. 3.4b; Table S3.2). Mean spring temperatures in the year before infestation initiation were significantly colder than normal (0.7 °C). Four consecutive years preceding outbreak initiation and three consecutive years following infestation initiation, winter temperatures were significantly higher than the long-term average (0.3 – 0.6 °C). Autumn and summer temperatures showed only slightly significant deviation in association with outbreak patterns. Au-

tumn temperatures were higher before the infestation initiation (0.1 – 0.4 °C) and summer temperatures were higher following infestation initiation (0.2 – 0.3 °C), compared to the long-term averages. However, these effects were small compared to spring and winter temperature anomalies.

3.3.3 Regression analysis

The best ($\triangle AICc < 4$) regression models between annual western spruce budworm infestation rates and seasonal precipitation and temperature averages indicated that the most important predictors were autumn precipitation, winter temperature, summer temperature, and summer precipitation (Table 3.1). Autumn and summer precipitation were negatively correlated with infestation rates (Table 3.2). Winter temperatures were positively correlated with infestation rates and summer temperatures were negatively correlated with infestation rates (Table 3.2).

Table 3.1: The likeliest ($\triangle AICc < 4$) regression models of western spruce budworm infestation rate ($IR_t = x_t/\Sigma x_t$) obtained from all possible regression models.

Intercept	Precipitation				Temperature				DF	*LL*	AICc	$\triangle AICc$	w_i	Pseudo-R^2
	Autumn $\Sigma w_i = 0.76$	Summer $\Sigma w_i = 0.15$	Spring $\Sigma w_i = 0.1$	Winter $\Sigma w_i = 0.06$	Autumn $\Sigma w_i = 0$	Summer $\Sigma w_i = 0.21$	Spring $\Sigma w_i = 0.03$	Winter $\Sigma w_i = 0.26$						
-0.21	-0.02								3	35.81	-63.78	0	0.17	0.16
0.78	-0.02	-0.01							4	37.09	-62.84	0.94	0.1	0.24
0.87	-0.02							0.2	4	36.96	-62.58	1.2	0.09	0.25
6.53	-0.02					-0.41		0.27	5	38.93	-62.4	1.38	0.08	0.41
3.7	-0.01					-0.31			4	36.78	-62.23	1.55	0.08	0.26
-0.75	-0.02		0.01						4	36.6	-61.86	1.92	0.06	0.18
-0.75	-0.02			0.01					4	36.54	-61.74	2.03	0.06	0.24
3.21						-0.42			3	34.65	-61.45	2.33	0.05	0.25
1.71	-0.02	-0.01						0.2	5	38.45	-61.44	2.34	0.05	0.33
-2.77									2	33.03	-61.21	2.57	0.05	0
0.08	-0.02		0.01					0.24	5	38.22	-60.99	2.78	0.04	0.3
0.01	-0.02						-0.09		4	35.93	-60.53	3.25	0.03	0.17

Table 3.2: Average model coefficients obtained from the likeliest regression models ($\triangle AICc < 4$), estimated using robust sandwich estimator of the covariance matrix.

	Estimate	Standard error	Lower 95% confidence interval	Upper 95% confidence interval
Intercept	1.21	2.91	-4.5	6.92
Autumn precipitation	-0.02	0.01	-0.03	-0.01
Winter precipitation	0.01	0.01	0	0.02
Spring precipitation	0.01	0.01	0	0.02
Summer precipitation	-0.01	0.01	-0.02	0
Autumn temperature	-0.05	0.22	-0.48	0.37
Winter temperature	0.23	0.14	-0.04	0.49
Spring temperature	-0.14	0.19	-0.52	0.24
Summer temperature	-0.37	0.23	-0.83	0.08

3.3.4 Uncertainty analysis

The median difference between infestation initiation detected by Landsat and defoliation initiation detected in aerial surveys was minus one year (Fig. 3.5a), indicating that Landsat time series detected budworm infestation on average one year later

than aerial surveys detected defoliation. Variation around the median was relatively small, with 50% of the differences between Landsat and the aerial survey being in between zero and minus three years. The comparison of the temporal dynamics between the Landsat-based estimates and the aerial survey (Fig. 3.5b) showed that the temporal patterns generally matched, though the aerial survey indicated a greater area defoliated than Landsat, especially among aerial survey polygons assigned low and medium outbreak severity classes. Also, aerial surveys identified a second peak in defoliation initiation around 2007 that was not present in the Landsat-based estimates.

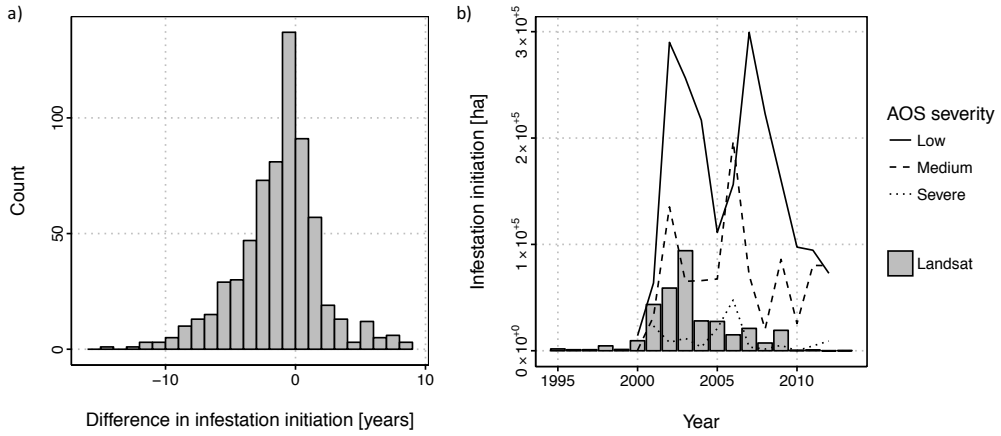

Figure 3.5: Differences in the initiation date (a) and temporal dynamics (b) between Landsat based estimates of western spruce budworm infestation and defoliation mapped by the aerial overview survey (AOS). For (a) the Landsat initiation date was subtracted from the aerial overview survey initiation date. For (b) we subdivided the aerial overview survey data by defoliation severity categories: low = Some branch tip and upper crown defoliation, barely visible from airborne view; medium = Thin foliage, top third of many trees severely defoliated, some completely stripped, easily visible from the air; severe = Bare branch tips and completely defoliated tops, most trees sustaining more than 50% total defoliation, many trees completely stripped.

3.4 Discussion

3.4.1 Using Landsat to estimate spatiotemporal patterns of western spruce budworm infestation

Our study utilized Landsat-based maps of western spruce budworm infestations to reconstruct the spatiotemporal patterns of the most recent outbreak in British Columbia. The method applied in this study allowed us to cover a spatial extent that would be impractical to cover with field data (i.e., dendrochronological time

series). Also, using Landsat enhanced the resolution for analysis and interpretation of ecological drivers of western spruce budworm disturbance dynamics. In particular, we captured spatial variation in infestation occurrence within aerial survey polygons, which greatly reduced the estimated extent of infestation at the regional-scale. While we focused on regional-scale weather variability in this study, the spatially explicit nature of the Landsat data also allows for the analysis of other stand- and landscape-scale drivers of disturbance occurrence and dynamics (Coops et al., 2006a), which would be impossible to assess with aerial survey data alone.

Our results confirm the usefulness of Landsat-based mapping of western spruce infestation, although key uncertainties remain. Some areas mapped by Landsat as western spruce budworm infestations could originate from other disturbance agents, including other insect agents, diseases, and drought stress. We endeavored to reduce such errors by intersecting the Landsat based maps and aerial survey maps, as suggested by Meigs et al. (2015). However, attribution errors also exist in the aerial survey polygons and they might be propagated into our maps. We assessed uncertainties in our Landsat-based maps of western spruce budworm infestations by comparing them directly to the aerial surveys. We found differences in the total area mapped and in the initiation date of infestation. Previous research has shown that aerial surveys tend to over-estimate the total area defoliated (Meigs et al., 2015; Bright et al., 2014), especially when mapping areas with low levels of defoliation. Aerial survey polygons represent broad areas with defoliation rather than fine-scale defoliation impacts.As such, a single polygon in the aerial survey might contain multiple small patches that experienced significant changes in foliage and vegetation structure adjacent to larger un-infested or mildly defoliated patches (see Fig. 3.3 for examples). The defoliation initiation date assigned in the aerial survey might therefore indicate defoliation in the surrounding forest landscape, but does not necessarily prove a notable change in foliage or vegetation structure at a particular location inside the polygon at this point in time. Moreover, observers conducting aerial surveys might record a change in foliage caused by western spruce budworm at the very early stages of an infestation (i.e., trace defoliation of single trees), earlier than Landsat can detect changes in the spectral response of one pixel. The lag that we found between the Landsat-based and aerial survey estimates of infestation initiation might result from these multiple uncertainties.

We found substantial differences in the area mapped as defoliated in the years 2006 and 2007 between Landsat and the aerial surveys. During this time, the study area underwent a significant outbreak of mountain pine beetle, which also attacked pine trees in Douglas-fir dominated forests (Meddens et al., 2012; Senf et al., 2015). Thus, the increase in western spruce budworm defoliation in the aerial survey after the initial peak in 2003 might be a result of confusion of insect agents in the aerial

survey. Alternatively, stands infested by both, western spruce budworm and mountain pine beetle, might have been attributed to mountain pine beetle in the Landsat time series analysis. This confusion appears to happen quite frequently in stands mixed of Douglas-fir and lodgepole pine (Senf et al., 2015). It is also possible that the aerial overview survey detected a resurgence of the western spruce budworm outbreak that could not be captured by Landsat; detecting multiple disturbances within one Landsat time series is challenging with current methods and we might have missed them in our analysis.

3.4.2 Weather variability associations with western spruce budworm infestations

Landsat-derived temporal patterns of western spruce budworm infestations in British Columbia varied significantly with seasonal weather and climate patterns.Infestations were associated with summer and autumn precipitation and winter and spring temperature anomalies. Most consistent were the prolonged autumn periods of lower than average precipitation from the beginning of the outbreak to its maximum (2000 – 2003) and significantly lower than average summer precipitation co-occurring with the outbreak maximum (2002/2003). Significantly lower than average autumn precipitation preceding an outbreak initiation is thought to promote budworm population growth (Campbell et al., 2005, 2006; Flower et al., 2014). In particular, the plant stress hypothesis (White, 1984) suggests that moderate drought stress leads to a concentration of sugars, nutrients, and other chemical components in the foliage, which enhances larvae survival, growth, and reproduction (Campbell, 1993; Mattson and Haack, 1987). The pronounced period of lower than average autumn precipitation might have caused such drought stress in the primary host of western spruce budworm – Douglas-fir – which is sensitive to autumn precipitation deficits (Chen et al., 2010; Campbell et al., 2006; Mildrexler et al., 2016). This interpretation was supported by our regression analysis, where autumn precipitation alone explained 16% of the variance in infestation rates during the current outbreak. The outbreak build-up phase (2000 – 2003), where infestation rates sharply increased, was associated with autumn precipitation around 100 mm (compared to a normal of 144 mm), which corresponds to precipitation patterns associated with historic western spruce budworm outbreaks in our study area (Campbell et al., 2006).

The significantly lower than average summer precipitation during and after infestation initiation may also be associated with drought stress in Douglas-fir (Watson and Luckman, 2002), thus benefiting larval development as discussed above.Although this finding is consistent with several previous studies reporting the coincidence western spruce budworm outbreaks with dry periods (Maclauchlan et al., 2006; Campbell, 1993; Murdock et al., 2013; Maclauchlan and Brooks, 2009), the pronounced

low summer precipitation during the maximum extent of the outbreak might also support an alternate interpretation. A recent dendrochronological study by Flower et al. (2014) found that wet periods followed by drought are beneficial for population growth, mainly due to improved foliage quantity and quality during high budworm population levels that prevent outbreak collapse due to starvation. Thus, while drought can trigger budworm population growth, extended drought periods can impair its further development. The extreme and extended summer drought present in our data may have caused the current outbreak to collapse (i.e., the sharp drop during 2004; Fig. 3.2) following the extreme dry summers of 2002 and 2003 (<80 mm compared to a normal of 133 mm). This interpretation lends support to the plant vigor hypothesis, which proposes that chronic host stress dampens herbivore population growth. Such dampening of western spruce budworm outbreaks in response to dry summers was also reported for outbreaks in the United States (Ryerson et al., 2003; Swetnam and Lynch, 1993).

We found significantly colder than average spring temperatures before outbreak initiation and significantly warmer than average winters during outbreaks. These weather anomalies might have influenced the phenology of Douglas-fir bud burst (Beedlow et al., 2013) and western spruce budworm development (Nealis and Regniere, 2014), and thus the degree of host-herbivore synchrony. Colder than average springs preceding infestation initiation might have delayed budworm emergence from hibernacula, improving insect-host synchrony and thus decreasing the risk of larvae starvation. The warmer winter temperatures could have resulting in an early Douglas-fir bud-burst. While our interpretations regarding temperature influences on the occurrence of budworm outbreaks are consistent with the conclusions of several other studies (Campbell et al., 2005; Swetnam and Lynch, 1993), the factors determining the synchrony between Douglas-fir and larvae phenology are highly complex and depend on many other factors not considered here (Nealis, 2012). An alternate explanation for outbreaks being associated with significantly warmer than average winters is increased over-wintering survival of budworm larvae. However, since budworms establish a hibernacula for overwintering, they are relatively tolerant to extreme cold winter temperatures (Fellin and Schmidt, 1973).

3.4.3 Limitations and uncertainties

Our interpretations about the spatiotemporal patterns of spruce budworm outbreaks come with three caveats. First, this study focuses on a single regional-scale outbreak of western spruce budworm rather than a temporal series of multiple outbreaks like those presented in dendrochronological studies, and to a lesser extent aerial survey data. The relationships we found between climate and western spruce budworm infestation patterns could be unique to the outbreak we studied. However, the ob-

served relationships conform to the results of several dendrochronological studies (Flower et al., 2014; Campbell et al., 2005, 2006), lending supporting to our conclusions about the influences of climate budworm outbreak dynamics . The second caveat is that our analyses only considers climate variation as potential explanatory factors of the budworm outbreak patterns we observed. However, it is well known that forest insect outbreaks are governed by multiple factors across several scales, including land-use, climate, and predator-prey systems (Raffa et al., 2008). Our study therefore largely focusses on one important factor out of multiple factors influencing budworm outbreak dynamics. Finally, the infestation initiation dates identified in our Landsat analysis mark a point where budworm populations have already grown sufficiently large to result in a level of defoliation visible using Landsat imagery. It is therefore difficult to make causal interferences about underlying population dynamics of western spruce budworm from our Landsat analysis. Considering these uncertainties, we suggest our results offer informative information about western spruce budworm disturbance dynamics and an additional line of evidence to support previous insights and expectations from studies based on field-based and simulation modeling. Further research should incorporate datasets across several scales, that is field data and remotely sensed data, to increase our understanding of the complex ecological processes driving insect outbreaks.

3.5 Conclusion

Using Landsat-based annual western spruce budworm maps and interpolated weather data, we have shown that western spruce budworm infestations during the most recent outbreak in British Columbia co-occurred with distinct weather patterns. Our Landsat-based approach allowed for a detailed characterization of those patterns, and while aerial surveys are a practical operational tool for rapidly assessing where defoliation occurs, ecological understanding of outbreak dynamics benefits from the spatially explicit view provided by medium spatial-resolution sensor such as Landsat.

In general, our results confirm the findings of previous dendrochronological studies that moisture stress is an important component in western spruce budworm population growth in British Columbia, though our results also show that there are seasonal variations in the precipitation and temperature patterns related to infestation initiation and that extended drought periods might hamper the development of large-scale outbreaks. Considering potential changes in climate for British Columbia (Hamann and Wang, 2006), we propose that western spruce budworm population dynamics likely will change in the future.

Acknowledgements

Dr. Brian Van Hezewijk, of the Canadian Forest Service, is thanked for providing insights and valuable recommendations on an earlier draft version of this manuscript.

Chapter 3

Supplementary materials

Table S3.1: Results of the Superimposed Epoch Analysis for precipitation measured in mm. The 99% confidence intervals are obtained from parametric bootstrap and are Bonferroni-corrected. Asterisks indicate significant deviation from zero at $p < 0.01$.

Lag	Autumn			Summer			Spring			Winter		
	Mean	99% confidence interval		Mean	99% confidence interval		Mean	99% confidence interval		Mean	99% confidence interval	
		Lower	Upper		Lower	Upper		Lower	Upper		Lower	Upper
-10	5.41	-3.96	15.24	16.16*	11.25	20.98	-2.59	-5.98	1.07	-1.65	-6.11	3.3
-9	16.40*	8.28	26.1	5.24*	0.05	10.4	-2.67	-6.4	1.64	4.23	-1.35	9.69
-8	14.79*	7.45	22.29	17.15*	11.29	22.87	-0.76	-5.22	4.12	3.13	-2.16	8.76
-7	19.69*	10.84	27.12	-0.44	-5.48	5.6	6.18*	1.83	10.53	7.81*	3.12	13.47
-6	13.69*	6.49	21.28	8.50*	2.79	15.07	10.17*	5.23	15.06	11.40*	6.54	16.84
-5	6.84	-0.58	14.45	-3.96	-10.26	1.88	6.97*	2.06	10.98	2.99	-2.66	8.55
-4	-7.81*	-14.82	-0.87	4.12	-1.24	10.45	2.78	-1.89	7.48	3.94	-1.87	9.13
-3	-16.29*	-23.6	-9.86	2.15	-4.27	7.87	2.02	-2.24	6.57	-1.56	-6.18	2.88
-2	-14.63*	-20.47	-8.16	2.36	-5.43	9.65	-0.6	-5.46	3.98	-5.91*	-10.89	-1.49
-1	-16.60*	-23.29	-11.21	-11.03*	-18.36	-3.49	8.08*	3.51	12.91	-6.93*	-12.06	-2.66
0	-8.79*	-14.08	-3.29	-20.56*	-25.94	-14.03	11.36*	6.04	15.78	-7.23*	-11.43	-2.97
1	0.55	-5.46	6.87	-13.54*	-19.33	-7.3	8.19*	3.07	13.09	-2.72	-7.31	2.09
2	-1.36	-6.41	3.84	-21.13*	-26.08	-15.92	7.85*	3.69	12.33	2.65	-1.61	6.64
3	-2.97	-8.29	2.2	-18.32*	-23.74	-12.33	-6.04*	-10.21	-2.36	4.34*	0.41	8.35
4	-3.62	-9.36	2.11	-20.43*	-24.14	-15.99	-4.01*	-7.31	-0.52	6.33*	3.1	9.87
5	-9.98*	-15.7	-5.04	-13.63*	-18.97	-8.4	-7.95*	-12.49	-3.66	7.14*	2.67	11.3
6	-6.69	-14.01	0.28	-20.48*	-25.31	-15.81	-0.93	-5.29	4.4	7.81*	2.74	12.58
7	-10.69*	-18.13	-4.27	-19.92*	-24.28	-15.36	-2.62	-7.34	2.06	-2.01	-8.51	3.59
8	-16.77*	-23.15	-10.33	-23.75*	-27.34	-19.66	6.48*	1.83	11.08	0.88	-5.57	6.62
9	-25.19*	-31.52	-18.63	-14.64*	-19.28	-9.2	-0.58	-5.83	4.7	-8.82*	-14.61	-3.2
10	-17.78*	-26.04	-10.17	-11.37*	-16.74	-6.81	7.16*	1.92	12.41	-10.56*	-16.88	-4.01

Table S3.2: Results of the Superimposed Epoch Analysis for temperature measured in °C. The 99% confidence intervals are obtained from parametric bootstrap and are Bonferroni-corrected. Asterisks indicate significant deviation from zero at $p < 0.01$.

Lag	Autumn			Summer			Spring			Winter		
	Mean	99% confidence interval		Mean	99% confidence interval		Mean	99% confidence interval		Mean	99% confidence interval	
		Lower	Upper		Lower	Upper		Lower	Upper		Lower	Upper
-10	0.14*	0.04	0.24	-0.06	-0.17	0.06	0.60*	0.47	0.73	-0.41*	-0.81	-0.03
-9	0.04	-0.09	0.16	0.04	-0.06	0.16	0.65*	0.5	0.79	-0.01	-0.35	0.35
-8	0.08	-0.04	0.19	-0.1	-0.21	0	0.34*	0.19	0.46	-0.39*	-0.67	-0.12
-7	-0.16	-0.34	0	-0.04	-0.14	0.06	-0.13	-0.28	0.04	-0.36*	-0.6	-0.13
-6	0.15	0	0.31	0.01	-0.08	0.11	-0.21*	-0.34	-0.09	-0.04	-0.29	0.19
-5	0.29*	0.12	0.44	0.23*	0.11	0.37	-0.05	-0.19	0.11	0.32*	0.08	0.57
-4	0.41*	0.3	0.53	-0.03	-0.15	0.09	-0.07	-0.22	0.06	0.65*	0.41	0.86
-3	0.33*	0.23	0.44	-0.02	-0.14	0.12	-0.14	-0.29	0	0.66*	0.5	0.83
-2	0.23*	0.14	0.32	-0.09	-0.21	0.03	-0.31*	-0.47	-0.15	0.65*	0.47	0.83
-1	0.10*	0.03	0.17	0.04	-0.07	0.16	-0.67*	-0.89	-0.49	0.54*	0.38	0.69
0	0.11*	0.03	0.19	0.28*	0.17	0.4	-0.44*	-0.64	-0.26	0.63*	0.44	0.8
1	0.05	-0.01	0.1	0.44*	0.33	0.56	-0.11	-0.29	0.06	0.67*	0.5	0.82
2	0.03	-0.03	0.08	0.24*	0.12	0.35	0.14	-0.04	0.33	0.57*	0.38	0.74
3	-0.04	-0.11	0.03	0.21*	0.1	0.33	0.1	-0.04	0.25	0.60*	0.4	0.79
4	0.02	-0.05	0.09	0.07	-0.03	0.18	-0.15*	-0.3	-0.01	0.31*	0.09	0.52
5	0.14*	0.07	0.22	-0.07	-0.17	0.04	-0.47*	-0.6	-0.35	-0.13	-0.38	0.1
6	0.23*	0.15	0.3	0.04	-0.06	0.15	-0.82*	-0.96	-0.68	-0.77*	-0.99	-0.5
7	0.19*	0.11	0.27	-0.09	-0.2	0	-0.58*	-0.73	-0.43	-0.65*	-0.85	-0.46
8	0.21*	0.14	0.28	-0.14	-0.28	0	-0.80*	-0.94	-0.63	-0.86*	-1.07	-0.68
9	0.06	-0.01	0.14	-0.06	-0.19	0.08	-0.54*	-0.67	-0.4	-0.29*	-0.48	-0.12
10	0.30*	0.22	0.39	0.16*	0.01	0.32	-0.50*	-0.66	-0.36	-0.20*	-0.39	-0.03

Chapter 4

A multi-scale analysis of western spruce budworm outbreak dynamics

Cornelius Senf, Elizabeth M. Campbell, Dirk Pflugmacher, Michael A. Wulder, and Patrick Hostert
Landscape Ecology, submitted

Submitted 16. June 2016

Abstract

Forest insect outbreaks are influenced by ecological processes operating at multiple spatial scales, including host-insect interactions within stands and across landscapes that are modified by regional-scale variations in climate. These drivers of outbreak dynamics are not well understood for the western spruce budworm (*Choristoneura freemani* Razowski = *Choristoneura occidentalis* Freeman), a defoliator that causes widespread damage in forests of western North America. Our aim was to assess how processes across multiple spatial scales drive western spruce budworm outbreak dynamics. Our objective was to assess the relative importance and influence of a set of factors covering the stand, landscape, and regional scales for explaining spatiotemporal western spruce budworm outbreak patterns in British Columbia, Canada. We used generalized linear mixed effect models within a multi-model interference framework to relate annual budworm outbreak initiation mapped from Landsat time series (1996 – 2012) to sets of stand-, landscape-, and regional-scale factors derived from forest inventory data, GIS analyses, and climate models. Spatiotemporal outbreak patterns of western spruce budworm were well explained by our model (R^2 = 92%). Most important predictors were the proximity to infestations in the previous year, landscape-scale host abundance, and dry autumn conditions. Stand characteristics were overall less important, though infestations were more likely in vertically complex, pure Douglas-fir stands with lower site index and higher crown closure. Our findings add to growing empirical evidence that insect outbreak dynamics are driven by multi-scaled processes. Managers should thus consider landscape and regional factors in addition to stand-scale management.

4.1 Introduction

Defoliation by insects is a natural phenomenon that occurs in forest ecosystems around the globe. Species from the genus *Choristoneura* ssp. are the most important native forest defoliators in North America (Nealis, 2008; Volney and Fleming, 2007). While native defoliators are an integral part of forest ecosystems and important for maintaining ecosystem functioning and heterogeneity (Turner, 2010), past outbreaks of the eastern spruce budworm (*C. fumiferana* Clemens), jack pine budworm (*C. pinus pinus* Freeman), western spruce budworm (*C. freemani* Razowski = *C. occidentalis* Freeman), and 2-year-cycle spruce budworm (*C. biennis* Free.) have caused widespread defoliation in coniferous forests of North America. Historic records indicate that outbreaks have increased in duration, intensity, and spatial extent (Flower et al., 2014; Swetnam and Lynch, 1993), raising concerns about the future role of susceptible forests for provision of important ecosystem services such as carbon sequestration (Dymond et al., 2010; Kurz et al., 2008a) and timber supply (Alfaro et al., 1982; Gray and MacKinnon, 2006). To better predict and manage the impact of future defoliator outbreaks, an improved understanding of their underlying ecological processes is required.

Several studies have identified common stand factors influencing the dynamics of western spruce budworm outbreaks: stand species composition, stand structure, and site quality, among others (Alfaro et al., 2001; Hadley and Veblen, 1993; Heppner and Turner, 2006; Nealis and Regniere, 2014; Nealis et al., 2009). Those studies, building on earlier recommendations (Carlson and Wulf, 1989), led to the development of management strategies to reduce stand susceptibility to future outbreaks, such as changing the species composition or structure by thinning or similar silvicultural actions (MacLean et al., 2001). However, as research on eastern spruce budworm (Campbell et al., 2008; Cappuccino et al., 1998) and other forest insect species (Bouchard and Auger, 2013; Foster et al., 2013b; Simard et al., 2012) indicates, stand characteristics alone cannot fully explain observed spatiotemporal patterns of budworm outbreaks. This suggests that dynamics of insect outbreaks are also driven by processes that extend well beyond the stand scale (Raffa et al., 2008). Not accounting for larger-scale processes hampers predictive models of budworm dynamics and management strategies to mitigate the impacts of future outbreaks.

Landscape- to regional-scale variations in climate and forest composition/structure are important drivers of insect outbreak dynamics. Regional weather variability, in particular moisture deficits, governs budworm population dynamics through synchronizing budworm and host phenology and through determining the quantity and quality of food (Nealis, 2012). Weather variability can thus trigger and synchronize the eruption of localized outbreaks (Flower et al., 2014). During outbreak build-up, higher budworm abundance leads to increased dispersal (Anderson and Sturtevant,

2011) and thus to the expansion of distinct and randomly distributed infestation patches to more continuous, landscape-scale patterns (Bouchard and Auger, 2013; Sturtevant et al., 2004; Turner and Gardner, 2015). However, even within regional-scale homogenous climate, not all susceptible forests experience the same level of defoliation, suggesting that some factors at the landscape scale facilitate or dampen the expansion of budworm outbreaks. Several studies provide empirical evidence that outbreak severity is not only affected by stand-scale characteristics but also by the composition and configuration of host populations in the surrounding landscape (Bouchard and Auger, 2013; Campbell et al., 2008; Radeloff et al., 2000). In particular, landscape-scale host abundance and configuration is thought to influence adult moth dispersal and predator-prey interactions. Thus, while stand-scale characteristics can explain variation in localized infestations patterns during periods of low budworm densities, it is the interaction of regional-scale weather variability and landscape structure that likely determines infestation patterns during outbreaks (Sturtevant et al., 2015). To improve our understanding – and capacity to predict – the spatiotemporal patterns of budworm outbreaks, we therefore need to consider processes and interactions across multiple scales, including the stand, landscape, and regional scale.

Understanding the multi-scaled processes underlying insect outbreaks requires an explicit view at the spatial and temporal outbreak patterns over large geographic extents, yet little data sources exist that track the dynamics of forest insects at a spatial and temporal resolution suitable for conducting landscape-scale analyses. Previous studies either used aerial overview survey maps (Bouchard and Auger, 2013), which have known limitations in terms of spatial accuracy (Wulder et al., 2006a); or maps created from aerial photo interpretation (Seidl et al., 2015), which often only cover small geographic extents (Wulder et al., 2004). Remote sensing, in particular the Landsat series of satellites, have the potential to fill this data gap (Kennedy et al., 2014). Recent advances in the Landsat time series based mapping of bark beetles and defoliator disturbances have allowed to map the spatiotemporal dynamics of insect infestation at am ecological valuable spatial (30 m) and temporal (annual) resolution (Meigs et al., 2015; Senf et al., 2015; Townsend et al., 2012), thus allowing for the development of spatially and temporally explicit models of outbreak dynamics (Foster et al., 2013b).

Our aim was to assess how ecological processes at multiple spatial scales drive budworm outbreak dynamics. We focused on the western spruce budworm, which is an important native defoliator of coniferous forests in western North American. Western spruce budworm primarily feeds on Douglas-fir (*Pseudotsuga menziesii* (Mirb.) Franco) and true fir (*Abies* spp.) and has recently been affecting large parts of the western United States and Canada (Hicke et al., 2012). Despite its eco-

nomic and ecological importance for forests of western North America, the drivers of western spruce budworm outbreak dynamics are yet largely unknown. Using annual (1996 – 2012) Landsat-based maps covering the recent outbreak of western spruce budworm in British Columbia, Canada, our objective was to assess the relative importance and functional relationship of a set of factors hypothesized to influence western spruce budworm outbreak dynamics at stand, landscape, and regional scales. We hypothesized that – in addition to stand factors – the probability of western spruce budworm outbreaks was driven by adult moth dispersal, spatiotemporal variability in the abundance and configuration of hosts in landscapes, by regional variability in climate, and by the interactions among these factors.

4.2 Data and methods

4.2.1 Study area

Our study area is located in British Columbia, Canada. It is delineated by the Interior Douglas-fir (IDF) biogeoclimatic zone (Hope et al., 1991) plus a 10 km buffer, which was added to mitigate possible edge effects in our analysis (Fig. 4.1). The study area, which is amongst the driest bioclimatic regions of Canada, is dominated by nearly homogeneous stands of Douglas-fir between 900 and 1,200 m, mixed stands of Douglas-fir and ponderosa pine (*Pinus ponderosa* Douglas ex C. Lawson) between 600 and 900 m, and mixed stands of Douglas-fir and lodgepole pine (*Pinus contorta* Douglas) between 1,200 and 1,450 m above sea-level. Forests at higher elevations and further north in the study area are dominated by lodgepole pine, which is not a budworm host. The study area has experienced widespread defoliation by western spruce budworm in recent decades (Maclauchlan et al., 2006) and infestation by mountain pine beetle (Wulder et al., 2009). British Columbia forest health reports indicate that western spruce budworm has defoliated more than one million hectares of forest since 1999[1].

4.2.2 Response variable and sampling design

In a previous study, Senf et al. (2015) identified and attributed annual changes in the spectral signal of Landsat pixels (30 by 30 m) to western spruce budworm infestation. Based on this information, the response variable used for subsequent analyses – annual spruce budworm outbreak initiation in a given Landsat pixel – was derived for the period 1996 – 2012. To minimize the number of data points

[1]Numbers obtained from:`http://www2.gov.bc.ca/gov/content/environment/research-monitoring-reporting/monitoring/aerial-overview-surveys/summary-reports/`

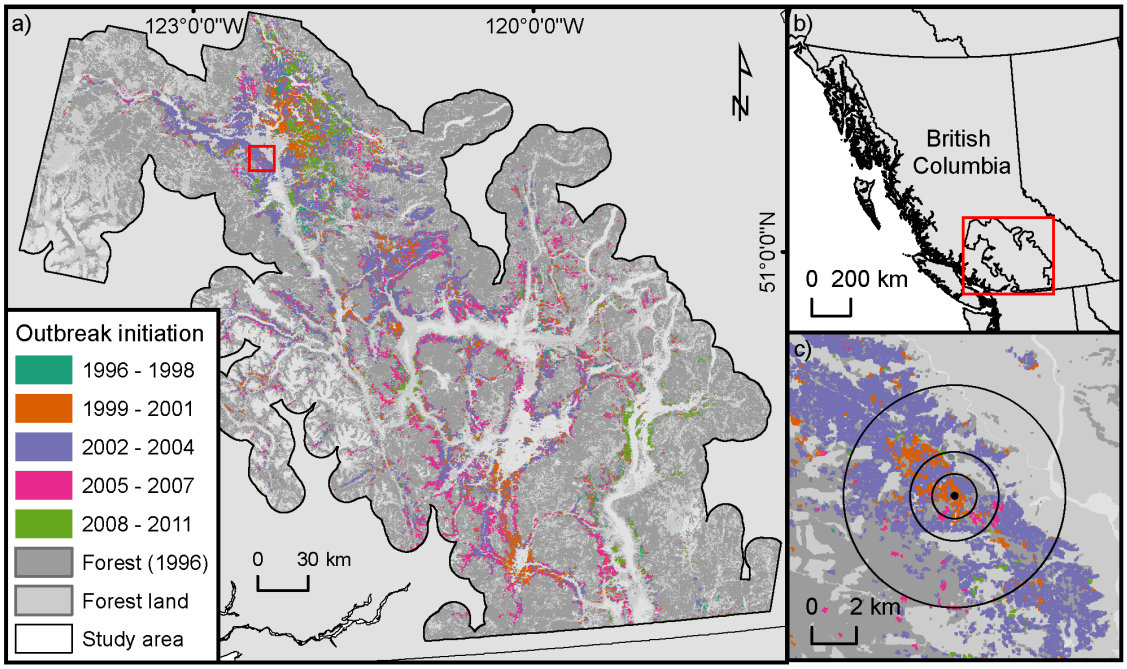

Figure 4.1: Map of infestation occurrences (a) for the study area location in British Columbia, Canada (b). For better interpretability years of outbreak initiation were grouped in quintiles. Forest land indicates all land potentially covered by forest according to the Vegetation Resource Inventory, whereas forest represents actual forest cover in 1996 as mapped from Landsat. The inset (c) shows sampling location example with the three radial buffer sizes (1,000, 2,000, 5,000 m) used for calculating landscape indices (host abundance and host edge density).

(i.e., Landsat pixels) used, and thus the computational resources needed for data analyses, we applied a case-cohort sampling design. A case-cohort sampling design is efficient for rare events (as in our case where outbreaks pixels only represented 0.4% of all pixels) that allows for un-biased parameter estimation with minimum prior correction (King and Zeng, 2001). We first randomly sampled 10,000 pixels from the whole study area and for each year and then, in a second step, randomly dropped absence samples in order to arrive at 1,000 samples per year. The total sample size thus consisted of 17,000 Landsat pixels (1,000 per year for 17 years, Table 4.1).

Table 4.1: Annual distribution of samples with western spruce budworm initiation.

Year	1996	1997	1998	1999	2000	2001	2002	2003	2004	2005	2006	2007	2008	2009	2010	2011	2012
No outbreak	999	997	993	998	976	909	871	808	943	943	972	951	975	968	999	997	1000
Outbreak	1	3	7	2	24	91	129	192	57	57	28	49	25	32	1	3	0

4.2.3 Potential predictors of western spruce budworm infestation

We assembled 13 predictor variables hypothesized to influence the initiation of spruce budworm outbreaks at the stand, landscape, and regional scale (Table 4.2).

Stand-scale predictors

Stand characteristics were obtained from British Columbia's Vegetation Resource Inventory (VRI) database, which is a polygon-based inventory database populated and updated by photo-interpretation and field measurements (Leckie and Gillis, 1995). We focused on six stand characteristics known to influence budworm habitat (Alfaro et al., 1985; Nealis et al., 2009; Shepherd, 1994): age (years), crown closure (percent of forest floor covered by forest canopy), host abundance (density of hosts as a percentage of total tree density), tree density (number of living stems per ha), site index (a metric of forest productivity measured as tree height at a given reference age) as measure of site productivity, and vertical complexity of the tree canopy (ordinal measure from 1 [very uniform] to 5 [very non-uniform]). The polygon-based inventory database was rasterized to a 30 by 30 m grid to match the spatial resolution of the Landsat-based map. Finally, we used a digital elevation model for estimating height and slope at each sampling location.

Landscape-scale predictors

We developed three predictors that describe the spatial distribution of host stands and budworm populations at landscape scale. First, we calculated the abundance and edge density of host tree patches within 1,000, 2,000, and 5,000 m radial buffers centered on each sampled Landsat pixel to characterize the spatial composition and configuration of host forests within the surrounding landscape (Fig. 4.1c). The buffer sizes were chosen based on a study of another *Choristoneura* species (Radeloff et al., 2000), because little is known about western spruce budworm dispersal distances (Flower et al., 2014). Second, we calculated the Euclidian distance between each sampled pixel and the nearest western spruce budworm outbreak in the previous year, assuming proximity to an infestation in the previous year increases the risk of outbreak occurrence from dispersing adult moths (Anderson and Sturtevant, 2011).

Regional-scale predictors

We acquired climate data from ClimateWNA (Wang et al., 2012), which generates climate time series for given locations using a down-scaled version of regional-scale PRISM climate model (Daly et al., 2002). We generated seasonal values of average temperature and total precipitation for our study region for each year of our

Table 4.2: Predictors used in the model. The predictors are grouped among observation scale (stand, landscape, and regional scale). A brief description of the hypothesized relationship with western spruce budworm outbreak initiation probability is given.

Scale	Variable	Hypothesized influence on outbreak initiation probability	
		Hypothesis	Source
Stand	Host abundance [%]	Higher availability of food and reduced losses during budworm dispersal	Swetnam and Lynch 2003; Nealis and Regniere 2009
	Age [years]	Older trees have higher crown exposure.	Alfaro2001
	Crown closure [%]	Higher crown closure decreases budworm dispersal losses.	Nealis and Regniere 2009
	Density [stems per ha]	Closer stand density decreases budworm dispersal losses.	Swetnam and Lynch 2003; Nealis and Regniere 2009
	Site index [m]	Higher site index indicates stands less susceptible to heavy defoliation.	Alfaro et al. 2001
	Vertical complexity	Higher vertical complexity indicates stands more susceptible to heavy defoliation.	Shepherd 1994
	Elevation [m]	Higher elevation areas might experience less moisture stress.	
	Slope [degree]	Steeper slopes might experience less moisture stress.	
Landscape	Host abundance [%] in 1,000, 2,000, and 5,000 m buffer (see Fig. 4.1c)	Higher landscape-scale host abundance eases insect dispersal.	Radeloff et al. 2000; Campbell et al. 2008
	Host edge density [%] in 1,000, 2,000, and 5,000 m buffer (see Fig. 4.1c)	Higher edge density eases insect dispersal. Higher edge density might increase risk of budworm predation and disease.	Radeloff et al. 2000
	Distance to infestation in the previous year [m]	Stands closer to infestation in the previous year are at higher risk of adult moth dispersal.	Anderson and Sturtevant 2011; Bouchard and Auger 2013
Regional	Autumn precipitation [mm]	Lower autumn precipitation increases host water stress and thus supports larvae development.	Flower et al. 2014; Mildrexler et al. 2016
	Spring temperature [°C]	Higher spring temperatures improve larvae survival through increased synchrony with host.	Swetnam and Lynch 1993

study period. From these data, we extracted two variables that have an important influence on western spruce budworm outbreak dynamics: autumn precipitation and spring temperature. Autumn precipitation affects Douglas-fir growth and vigor (Chen et al., 2010; Mildrexler et al., 2016) and thus western spruce budworm population development (Flower et al., 2014). Because prolonged periods of moisture stress are typically thought to trigger budworm outbreaks, we calculated a three-year running mean of total autumn precipitation preceding each year of our study period. Spring temperatures influence the phenological synchrony of western spruce budworm egg hatch and the annual flush of Douglas-fir foliage on which newly emerged larvae feed (Nealis, 2012).

4.2.4 Statistical analysis

We used hierarchical generalized linear mixed models (GLMM) with a logit link function to explain the annual probability of western spruce budworm outbreak initiation at the pixel level (Bolker et al., 2009). Using hierarchical GLMM allowed

us to integrate fixed effects measured at varying spatial scales while simultaneously accounting for annual differences in western spruce budworm infestation probability not explained by our model. A model that does not consider the multi-level structure of the data might not detect minor effects and bias inferences made based on the model. The model used in this study is defined as:

$$P(y_i = 1) = logit^{-1}(X_i * \beta + \alpha_j) \tag{4.1}$$

with $P(y_i = 1)$ indicating the probability of initiation at pixel i, X_i is a matrix containing the stand- and landscape-scale predictors at each pixel, the vector β contains the fixed effects at the stand-and landscape-scale, and α_j is the intercept varying among years j. The varying intercept is modeled by a normal distribution:

$$\alpha_j = N(\gamma_0 + U_j * \gamma, \sigma^2) \tag{4.2}$$

with γ_0 representing the baseline probability of occurrence, U_j is a matrix of regional-scale predictors available for each year j, the vector γ contains the regional-scale fixed effects, and σ^2 is the annual variability in infestation probability not explained by the regional predictors.

We first fit a full model with all predictors shown in Table 4.2 as fixed effects. However, host abundance and host edge density were highly correlated among the three nested buffer sizes (Pearson $r > 0.7$ and variance inflation factor > 5 for the 1,000 and 2,000 buffers), and host abundance within the 1,000 and 2,000 m buffer correlated moderately with host abundance at the stand scale (Pearson $r > 0.55$). To reduce multicollinearity in our model, we dropped host abundance and edge density measured within the 1,000 and 2,000 m buffers and only included both variables measured within the 5,000 m buffer. That way, we reduced the variance inflation factor to < 5, indicating low multicollinearity among predictors, while two variables characterizing host abundance and configuration in 5 km around each pixel and one variable characterizing host abundance at a smaller spatial scale (within a stand) were included in the model. We tested for intra-scale interactions between stand host abundance and other stand-scale predictors (controlling for structural differences among host and non-host stands); for intra-scale interactions between landscape scale host abundance and edge density and distance to infestation in the previous year; and for cross-scale interactions between the distance to infestation in the previous year and regional-scale weather variables. We finally centered and scaled all predictors to zero mean and a standard deviation of one to improve model convergence and interpretability of the estimated parameters and interactions.

To identify the models with the greatest likelihood from all possible predictor combinations, we followed a multi-model inference framework (Burnham et al., 2010). The performance of each model was assessed based on the marginal R^2 (R^2_m,

variance explained by the fixed effects; Nakagawa et al., 2013), the conditional R^2 (R^2_c, variance explained by both the fixed and random effects; Nakagawa et al., 2013), the Akaikes information criterion corrected for small sample sizes ($AICc$; Grueber et al., 2011), and the corresponding Akaike weights ($wAICc$), which assigns a relative strength of evidence to each competing model (Link and Barker, 2006). This information-theoretic framework is better suited to conducting statistical inference than classical methods, because it does not rely on arbitrary thresholds such as $P < 0.05$. Using the likeliest set of models ($\triangle AICc < 2$), we used model averaging to calculate average estimates and confidence intervals for each predictor. To address a potential bias in our estimates due to spatial and temporal auto-correlation in the residuals, we used robust sandwich estimators of the variance-covariance matrix (Zeileis, 2006). The relative influence of each predictor was assessed based on the summed Akaike weights ($\sum wAICc$). All statistical analyses were performed in the R Language and Environment for Statistical Computing using the *sandwich* (Zeileis, 2006), *lme4* (Bates et al., 2014), and *MuMIn* (Barton, 2009) packages.

4.3 Results

We identified nine models with similar $AICc$ ($\triangle AICc < 2$) and very good explanatory power of 92% for the marginal$R^2$and 94% for the conditional R^2 (Table 4.3). Thus, the random effect from annual variation in the intercept term explained only 2% of the observed variance in spatiotemporal outbreak patterns. The intercept of -7.91 indicated a very low baseline outbreak initiation probability of < 0.01 at mean values of all predictors (after correction for the sampling design), with small annual variation ($\sigma^2 = 1.13$).

We identified several important predictors of budworm outbreak dynamics (Table 4.3). Distance to infestation in the previous year, host abundance at the stand- and landscape-scale, crown closure, site index, vertical complexity, autumn precipitation, and slope were included in all candidate models with $\triangle AICc < 2$. Stand density and elevation had lower but still good support from the candidate models ($\sum wAICc \sim 0.8$). Spring temperature, age, and edge density had lowest support from the candidate models ($\sum wAICc < 0.2$). There was strong evidence for cross-scale interactions between autumn precipitation and distance to infestation in the previous year. Moreover, there was strong evidence for intra-scale interactions between landscape-scale host abundance and distance to infestation in the previous year, as well as for intra-scale interactions between stand-scale host abundance and crown closure, site index, and vertical complexity.

At the stand scale, host abundance was positively associated with outbreak initiation probability (Table 4.3; note that we here report changes in outbreak initiation

Table 4.3: Likeliest ($\triangle AICc < 2$) GLMM models explaining western spruce budworm outbreak initiation probability.

	Model										
Predictor	1	2	3	4	5	6	7	8	9	$\sum wAICc$	Average (95% CI)
Intercept	-7.91	-7.92	-7.92	-7.91	-7.91	-7.91	-7.91	-7.91	-7.92		-7.91 (-8.76 to -7.06)
Age			0.04						0.07	0.19	0.05 (-0.05 to 0.16)
Distance to infestation in previous year	-5.73	-5.76	-5.73	-5.69	-5.72	-5.72	-5.72	-5.74	-5.75	1	-5.73 (-6.65 to -4.81)
Crown closure	0.14	0.14	0.13	0.14	0.14	0.14	0.13	0.11	0.11	1	0.13 (0.02 to 0.25)
Density	-0.23	-0.25	-0.19	-0.24	-0.27	-0.23	-0.24			0.83	-0.24 (-0.54 to 0.06)
Elevation	-0.1		-0.11	-0.1	-0.1	-0.1	-0.1	-0.11	-0.12	0.87	-0.11 (-0.22 to 0.01)
Host abundance (5000 m)	1.44	1.46	1.45	1.44	1.44	1.44	1.44	1.45	1.46	1	1.45 (1.03 to 1.87)
Edge density (5000 m)				0.04						0.11	0.04 (-0.06 to 0.14)
Host abundance (stand)	0.55	0.56	0.54	0.55	0.55	0.55	0.55	0.56	0.54	1	0.55 (0.42 to 0.68)
Autumn precipitation	-0.04	-0.03	-0.04	-0.04	-0.04	-0.07	-0.04	-0.04	-0.04	1	-0.04 (-0.72 to 0.64)
Site index	0.09	0.11	0.09	0.08	0.09	0.09	0.09	0.08	0.08	1	0.09 (-0.05 to 0.23)
Slope	-0.15	-0.15	-0.15	-0.15	-0.15	-0.15	-0.15	-0.15	-0.15	1	-0.15 (-0.25 to -0.05)
Spring temperature						0.13				0.09	0.13 (-0.41 to 0.66)
Vertical complexity	-0.32	-0.32	-0.32	-0.32	-0.32	-0.32	-0.32	-0.31	-0.31	1	
Age × host abundance (stand)										0	
Distance to infestation in previous year × host abundance (5000 m)	1.65	1.66	1.65	1.63	1.64	1.65	1.64	1.66	1.66	1	1.65 (1.1 to 2.19)
Distance to infestation in previous year × edge density (5000 m)										0	
Distance to infestation in previous year × autumn precipitation	1.02	1.04	1.03	1.02	1.02	1.02	1.03	1.02	1.03	1	1.03 (0.37 to 1.68)
Distance to infestation in previous year × spring temperature										0	
Crown closure × host abundance (stand)							0.03			0.09	0.03 (-0.09 to 0.14)
Density × host abundance (stand)					0.1					0.1	0.1 (-0.19 to 0.39)
Site Index × host abundance (stand)	-0.25	-0.25	-0.25	-0.25	-0.26	-0.25	-0.26	-0.24	-0.24	1	-0.25 (-0.38 to -0.12)
Vertical complexity × host abundance (stand)	0.28	0.28	0.29	0.29	0.29	0.28	0.28	0.28	0.28	1	0.28 (0.15 to 0.42)
Random variation in the intercept (σ^2)	1.13	1.13	1.13	1.13	1.13	1.12	1.13	1.13	1.13		
Degrees of freedom	16	15	17	17	17	17	17	15	16		
Log-likelihood	-1866	-1867	-1865	-1865	-1866	-1866	-1866	-1868	-1867		
$AICc$	3764	3765	3765	3765	3765	3765	3765	3765	3766		
$\triangle AICc$	0	1	1.38	1.38	1.54	1.78	1.81	1.85	1.97		
$wAICc$	0.21	0.13	0.11	0.11	0.1	0.09	0.09	0.09	0.08		
R^2_m	0.92	0.92	0.92	0.92	0.92	0.92	0.92	0.92	0.92		
R^2_c	0.94	0.94	0.94	0.94	0.94	0.94	0.94	0.94	0.94		

probability obtained by: $P(initiation) = (exp(\beta) + 1) * 100$; where appropriate, we scaled the change in outbreak probability to reasonable values). In particular, with an increase in host abundance by 50%, the probability of outbreak initiation increased by 73% (52% to 97%). Moreover, outbreak initiation probability decreased for host stands as site index increased (Fig. 4.2a) but increased as host stands became vertically more complex (Fig.4.2b), and crown closure increased (Fig. 4.2c). However, those effects were largely dependent on stand-scale host abundance and showed weaker or even inverse relationships if Douglas-fir was not the dominant tree species within the stand. Finally, outbreak initiation probability decreased by -14% (-5% to -22%) with increasing slope and by -10% (1% to -22%) with increasing elevation.

At the landscape scale, we found strong evidence for the importance of proximity

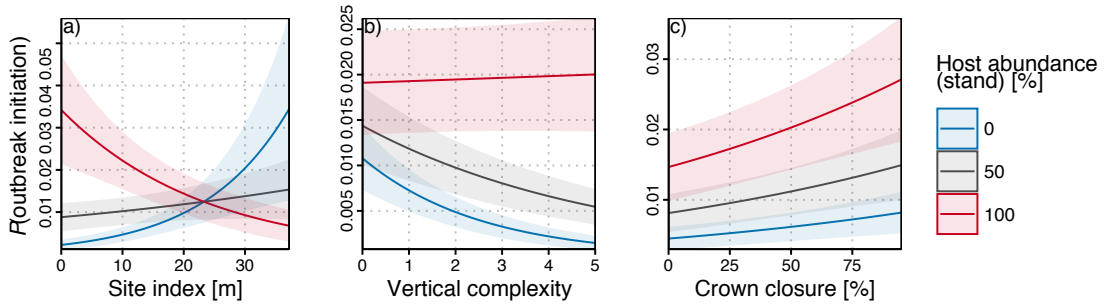

Figure 4.2: Varying effects of stand characteristics on outbreak initiation probability depending on host species abundance at the stand scale. Please note that the distance to infestation in the previous year was fixed at 5 km instead at its mean value for better interpretability.

to budworm infestation in the previous year and for landscape-scale host abundance (Table 4.3). Proximity to budworm infestation in the previous year was associated with a substantially higher probability of outbreak initiation. With one kilometer increase in distance, the probability of outbreak initiation dropped by 28% (24% to 32%). Interestingly, the distribution of distances to infestations in the previous year changed substantially throughout the outbreak cycle (Fig. 4.3). Before ($<$ 1999) and after ($>$ 2007) the outbreak, the distributions were nearly uniform. During the outbreak period (1999 to 2007), however, more than 90% of all newly initiated patches were within 5 km proximity to infestations in the previous year. Hence, while infestations seemed to occur independent from existing outbreak centers within the landscape before and after the outbreak, there was a clear pattern of spread observable during the outbreak (see also Fig. 4.1). According to our study, the average dispersal distance was 1.3km during the outbreak (1999 – 2007).

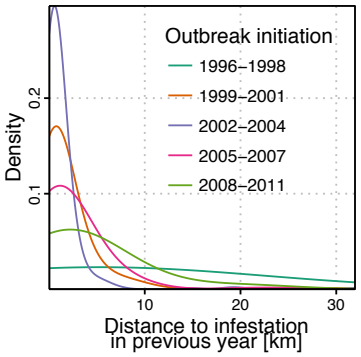

Figure 4.3: Distributions of distance to infestation in the previous year for varying periods of the study area. The periods are grouped into pre-outbreak (1996-1998), outbreak build-up (1999-2001), outbreak (2002-2004), outbreak decline (2005-2007), and post-outbreak (2008-2011) conditions.

A higher abundance of Douglas-fir patches in the surrounding landscape led

to higher probability of outbreak initiation, though the effect was dependent on the distance to infestations in the previous year (Fig. 4.4a). For example, while landscape-scale host abundance had little effect on outbreak initiation probability when the closest infestation was more than 15 km away, the effect increased with proximity to infestations in the previous year. However, at very close proximity to an infestation in the previous year (< 500 m), the effect of landscape-scale host abundance diminished and outbreak initiation probability was high, regardless of host abundance in the surrounding landscape.

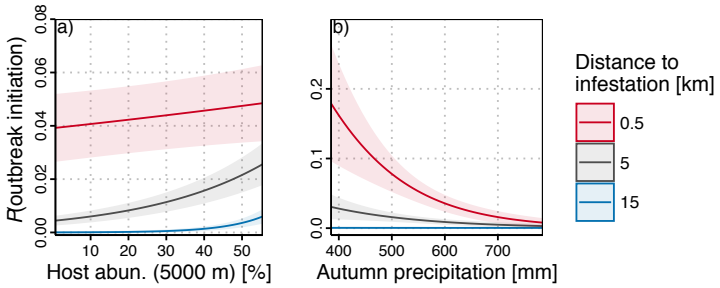

Figure 4.4: Varying effects of autumn precipitation and landscape scale host abundance on outbreak initiation probability depending on the distance to infestation in the previous year.

Considering the regional-scale predictors, outbreak initiation probability was decreased if preceded by years with higher than average autumn precipitation, but only if the distance to budworm infestations in the previous year was low (Fig. 4.4b). For pixels in close proximity to budworm infestations in the previous year (< 5 km), outbreak initiation probability increased significantly when average autumn precipitation was below 500 mm in preceding years.

4.4 Discussion

Using annual Landsat-based maps of the most recent outbreak in British Columbia, Canada, we tested the hypothesis that spatiotemporal patterns of western spruce budworm outbreaks are driven by multi-scale processes, that is, by ecological interactions among budworm, its host, their physical environment at stand, landscape, and regional scales. Our results support this hypothesis, adding to the growing empirical evidence that insect outbreak dynamics are driven by ecological processes occurring across multiple scales (Raffa et al., 2008; Seidl et al., 2015; Turner and Gardner, 2015). In particular, we showed that the probability of outbreak initiation was mainly driven by host abundance at the landscape scale, by stand structure and species composition, and by regional-scale precipitation patterns. In addition, we

found that those processes interacted within and across scales to determine probability of outbreak initiation.

Stand species composition had the most important influence on outbreak probability at the stand scale, with stands having a high percentage of Douglas-fir having a higher probability of outbreak initiation. This finding aligns well with previous studies of western spruce budworm (Maclauchlan et al., 2006; Swetnam and Lynch, 1993) and similar budworm species (Alfaro et al., 2001). Stands with high proportions of Douglas-fir can sustain larger populations of western spruce budworm due to higher availability of food, and dispersal losses are reduced with decreasing proportion of non-host species (Brookes et al., 1987, 1985). The effects of other stand characteristics (i.e., site index, tree density, crown closure) were not as strong; but higher outbreak probabilities tended to be associated with a lower site index, higher vertical complexity, and higher crown closure. Dense and vertically complex stands tend to have low losses during larvae and moth dispersal and can thus sustain larger budworm populations (Nealis et al., 2009; Swetnam and Lynch, 1993). Trees on high quality sites might accumulate high levels of secondary metabolites used for tree defense against budworm herbivore (Alfaro et al., 2001), resulting in lower probability of outbreak initiation. The reasons why stand-scale characteristics were generally weak predictors of outbreak probability compared to landscape- and regional-scale factors may be related to the geographic scale of the analysis (Sturtevant et al., 2015). For example, while stand characteristics might explain differences in outbreak probability among stands with similar environmental conditions, those effects are likely overridden by larger-scale processes. Similar effects were described for the mountain pine beetle, where once stand-scale thresholds are passed, outbreak dynamics are mostly governed by processes at the landscape and regional scale (Raffa et al., 2008).

We found that the distance to infestations in the previous year was the most important factor determining the initiation of western spruce budworm outbreak at a given location. Our model suggests that spatiotemporal outbreak patterns are mainly driven by adult moth dispersal, which leads to the colonization and infestation of new habitat and to the eruption and synchronization of local population dynamics. This finding well aligns with several studies of eastern spruce budworm and gypsy moth across North America (Bouchard and Auger, 2013; Foster et al., 2013b). By integrating two factors describing the composition and configuration of host patches within a 5 km radial buffer centered on each pixel location, and their interactions with budworm dispersal (i.e., distance to infestation in the previous year), we tested the hypothesis that dispersal of adult moth is only possible if habitat is available in the surrounding landscape, that is within average dispersal distance. We found that a higher abundance of Douglas-fir within the landscape increased

outbreak probability and thus of successful dispersal of adult moths from distant populations (> 500 m). Hence, it is the combined effect of adult moth dispersal and landscape-scale host availability that shaped the landscape-scale outbreak patterns observed in our study.

Regional weather variability, especially regional precipitation patterns, also had important effects on the probability of budworm outbreak initiation, but we found that the effect was strongly dependent on distance to infestation in the previous year. As shown by previous research, water stress in host trees is an important driver of regional-scale western spruce budworm outbreaks (Flower et al., 2014), supporting our findings of increased outbreak initiation probability following years of low autumn precipitation. Autumn precipitation was also shown to be a good indicator of water stress in Douglas-fir in other regions (Mildrexler et al., 2016), highlighting the importance of regional scale moisture variability for the eruption and spread of localized budworm populations throughout its native range. Contrary to our expectations, spring temperature was not an important predictor of budworm outbreak initiation probability. This might be explained by the fact that budworm and host phenology are highly variable across the landscape and depend on many factors not considered in this study (Nealis and Regniere, 2014). Finally, elevation and slope, which were both important stand scale predictors in our model, might further explain local variation in precipitation and moisture availability. Precipitation generally increases with increasing elevation and highest precipitation values are found on the steep slopes of the coastal mountain range at the western fringe of the study area. Lower elevation sites with more moderate slopes might thus have higher risk of local water deficits supporting budworm population development.

4.5 Implications and conclusion

Our findings have several implications for understanding, management, and modeling of budworm disturbances. First, our study highlights that there are important drivers beyond stand-scale characteristics that need to be evaluated when developing management strategies to mitigate the impacts of future budworm outbreaks. In particular, our study suggests that reducing western spruce budworm habitat quantity and quality within the landscape might prevent the development of regional-scale outbreaks. Reducing habitat quantity and quality could be achieved by developing management strategies that mimic natural disturbances (Long, 2009) and by increasing the landscape heterogeneity in terms of tree species composition, among other characteristics (Robert et al., 2012). Second, our study suggests that climate is an important driver of western spruce budworm outbreak development. Given this, climate change will likely alter the duration, intensity, and spatial extent of

future outbreaks (Murdock et al., 2013). While our study does not project how climate change might affect future budworm outbreaks, forest managers should be mindful of the uncertainties associated with climate change in long-term planning (Millar et al., 2007). Third, our study adds important information to a process-based understanding of budworm outbreaks, and could further enhance the development of mechanistic models (e.g., LANDIS; Sturtevant et al., 2004) simulating the landscape-scale progression of outbreaks. In particular, our study suggests that mechanistic models should incorporate processes across multiple scales to improve predictions of western spruce budworm outbreak dynamics under varying management and climate scenarios (Seidl et al., 2011; Sturtevant et al., 2015). Finally, our study demonstrates the usefulness of Landsat-based time series for assessing landscape- to regional-scale drivers of insect outbreaks. Many factors found important in our study would be difficult to tackle without the spatially and temporally explicit view offered by long-term landscape-scale observations based on globally available satellite data. Landsat allows for analyzing insect outbreaks over larger extents than would be possible with field data alone, and with higher ecological resolution than using aerial overview survey maps (Meigs et al., 2015).

Chapter 5

Synthesis

5.1 Summary and main conclusions

The overarching goal of this dissertation was to improve our understanding of the patterns and processes of insect disturbances in the coniferous forests of western North America. To achieve this goal, I employed a Landsat time series based approach that allowed for mapping and quantifying spatiotemporal patterns of defoliator outbreaks. In particular, I mapped the spatiotemporal patterns of western spruce budworm infestation in the Interior Douglas-fir Forest zone of British Columbia, Canada. Doing so required developing a novel approach that allowed for distinguishing between the disturbances caused by western spruce budworm and other disturbance agents, such as harvest, fire, and bark beetle infestation. This Landsat based approach was presented in Chapter II and Chapter III. Using the spatially and temporally explicit information on western spruce budworm disturbances obtained from Chapter II and III, I used a multi-level modeling approach to identify the key processes underlying budworm outbreaks across several magnitudes of scales. A regional modeling approach was outlined in Chapter III, whereas a landscape scale approach was presented in Chapter IV. Insights from the three core research chapters were used to answer the two research questions of this dissertation.

Research Question I: How can Landsat remote sensing be used to map and quantify insect defoliator outbreaks?

While mapping harvest and fire disturbances from Landsat is increasingly considered operational, mapping insect disturbances using Landsat time series is still challenging due to the often transient spectral changes caused by insect infestation (Coops et al., 2006a). This holds especially true for defoliators, which, in contrast to bark beetles, do not necessarily lead to tree mortality, but mainly change the foliage and upper canopy structure of a forest stand. It was hypothesized that those substantial biological differences between defoliator and bark beetle disturbances, as well as between insect and more severe disturbances, such as those caused by harvest and fire, would lead to distinct spectral-temporal signals. Indeed, the results of Chapter II showed that insect disturbances were not only distinguishable from more severe disturbances of harvest and fire, but also showed significant differences in the spectral-temporal characteristics between bark beetle and defoliator disturbances. The specific spectral and temporal features of each insect agent could be linked to biological characteristics of the individual agents, which greatly improved our understanding of disturbance characteristics related to bark beetles and defoliators in British Columbia. In particular, the results reinforced the ecological understanding that defoliators cause ephemeral disturbances from which trees can recovery, whereas bark beetles cause widespread tree mortality. I found that bark beetle disturbances

are of shorter duration, but higher magnitude. Those disturbance characteristics were explained by high tree mortality following bark beetle attack. Defoliator disturbances, in turn, are slightly longer in duration and less severe, which was explained by lower mortality rates, but ongoing chlorosis of tree crowns. Moreover, spectral recovery following bark beetle and defoliator disturbances showed distinct differences, which could be linked to processes described in past plot-based studies. Those results allowed for empirical and objective comparison to other regions with similar disturbance regime (Meigs et al., 2011), which can help understanding the role and importance of single insect agents for the whole disturbance regime (Hicke et al., 2012).

The technique employed in Chapter II not only allowed me to characterize disturbances of varying agents, but also provided more refined spatial and temporal information on disturbance outbreaks. In particular, the spectral-temporal differences between both insects allowed for discrimination between bark beetle and defoliator disturbances using classification models, and finally for the mapping of annual occurrences of each disturbance agent. I reduced the chance of false positives by intersecting those occurrence maps with official aerial overview survey maps. This approach is rather conservative, keeping in mind that even low false positive error rates can induce extreme bias in estimating underling process parameters (Royle and Link, 2006). In general, the mapped spatiotemporal outbreak patterns were found to be reasonable and well-aligned with prior knowledge obtained from other sources, such as the official aerial survey maps. Nonetheless, the Landsat-based analysis increased the spatial and temporal resolution for ecological analysis, meaning that the Landsat maps showed distinct spatial patterns of outbreak development that were not identifiable within the aerial survey maps, or spatially coarser satellite products (e.g., De Beurs and Townsend, 2008; Eklundh et al., 2009). In particular, using Landsat reduced the overall extent of infested areas and thus the amount of false positives, as reported from earlier research (De Beurs and Townsend, 2008; Meigs et al., 2015; Wulder et al., 2006a). As such, using Landsat time series allowed for conducting a landscape to regional scale analyses at a spatial (30 m) and temporal (annual) resolution that is of interest for many ecological and biological questions, such as the processes underlying insect outbreaks. Without the use of Landsat data, it would be unpractical or even impossible to collect historic information on insect disturbances over such large extents, and at such a fine spatial and temporal resolution (Cohen et al., 2016; McDowell et al., 2015).

Based on the results summarized above, two general conclusions can be drawn with respect to Research Question I: (1) Landsat time series allow for an agent-level assessment of insect disturbances that goes beyond grouping defoliator and bark beetle disturbances into one disturbance category. (2) Using Landsat (or spatially

and temporally similar sensor) time series allows for the assessment of landscape to regional scale patterns of defoliator disturbances that would be unidentifiable with alternative data sources, such as aerial survey maps, dendrochronological data, or MODIS.

Research Question II: What are the spatiotemporal patterns and processes of outbreaks of western spruce budworm in the coniferous forests of western North America?

We utilized the techniques and maps developed in Chapter II and III for estimating and mapping the spatiotemporal outbreak patterns of western spruce budworm infestation in the southern interior of British Columbia, Canada. Our analysis revealed that the outbreak started in three well-defined epicenters in 1999 and showed distinct patterns of eruption, spread, and collapse at the landscape and regional scale. Several predictors of those spatiotemporal dynamics could be identified that aligned with the hypothesized processes outlined in Section 4.2.3. The scheme presented in Fig. 5.1 was updated from Fig. 1.1 based on the results of Chapter III and IV in order to represent the drivers and processes underlying the current western spruce budworm outbreaks in British Columbia. The updated scheme shows that while precipitation and stand-scale availability/quality of hosts were the main driver of localized population eruptions, it was the landscape scale connectivity of hosts that allowed for the spread of localized eruptions to larger, continuous infestation patches. This process was thought to be driven by adult budworm dispersal, which was empirically quantified in this thesis to be about 1.3 km on average. The synchronized eruption of several localized populations resulted in a regional scale outbreak, with observable infestations occurring throughout the complete range of Douglas-fir in British Columbia. By testing the interactions between varying factors, this thesis also reinforced the theory that processes underlying insect outbreaks are interrelated within and across scales. This is the first study that empirically quantifies these processes and interactions for the western spruce budworm (to the Authors knowledge). As such, this dissertation adds to a growing body of literature highlighting the importance of multi-scale processes for understanding patterns of forest insect disturbances (Raffa et al., 2008; Seidl et al., 2011, 2015; Sturtevant et al., 2015).

While this dissertation made use of a case study located in the most northern habitat of western spruce budworm, the results also allow for some degree of generalization across the budworms native range. The importance of landscape scale host abundance and climate was also evident in earlier dendrochronological studies from more southern ecoregions (Flower et al., 2014; Ryerson et al., 2003; Swetnam

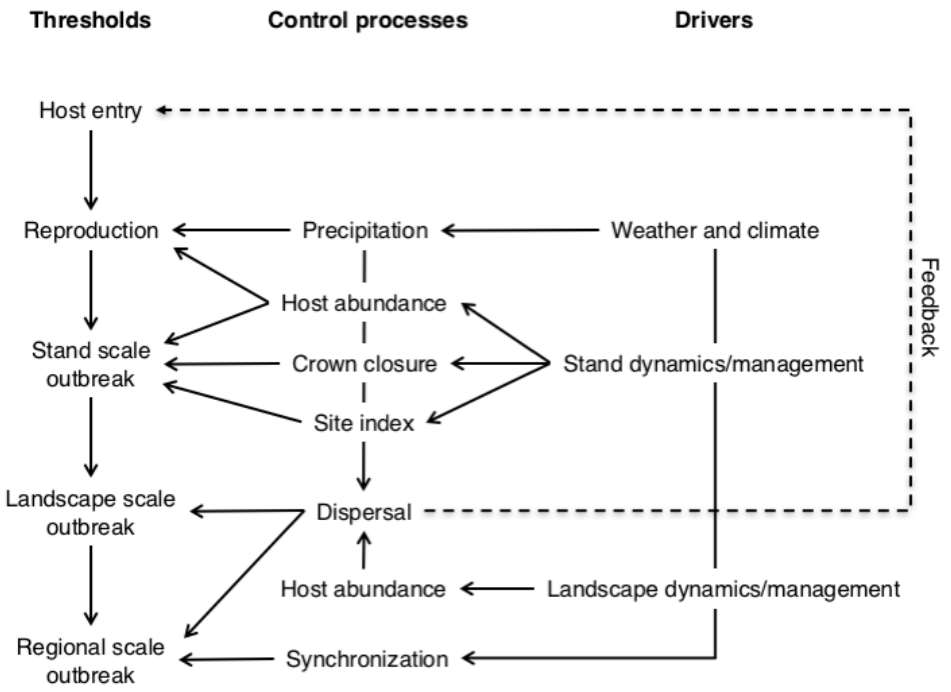

Figure 5.1: Updated scheme of the multi-scale drivers and processes controlling the dynamics of western spruce budworm outbreaks in British Columbia.

and Lynch, 1993). However, while the effects from landscape scale host abundance showed similar patterns among studies, the effects from climate varied among ecoregions. Hence, it is important to note that while climate is an important factor in the development of budworm outbreaks, the effects might vary depending on other more complex processes not considered in this dissertation (James et al., 2015).

Based on the results summarized above, three general conclusions can be drawn with respect to Research Question II: (1) Defoliator disturbances in coniferous forests of western North America are driven by multi-scale processes that go beyond the reach of stand scale management. (2) Those disturbance processes are interrelated within and across scales, adding significantly to their complexity. (3) For the western spruce budworm, landscape-scale host availability and weather variability seem to be particularly important.

5.2 Management implications

The conclusion that defoliator disturbances in the coniferous forests of western North America are driven by multi-scale processes has important implications for forest and landscape management. In particular, it underlines the need for developing adequate

management strategies depending on the stage of outbreak (Fig. 5.2). Management actions will be effectively only if they are applied congruent with the appropriate outbreak stage and thus affect factors that control the progression to the next outbreak stage (Raffa et al., 2008). For example, reproduction and aggregation of budworm populations is regularly monitored using egg-count samples, and spraying programs are initiated accordingly (Heppner and Turner, 2006). However, spraying might be ineffective once the landscape scale outbreak stage has been reached. Indeed, there is empirical evidence that spraying had little effect during landscape-scale outbreaks of gypsy moth, where the spatial dynamics of the outbreak were mainly driven by moth dispersal (Foster et al., 2013b). Equally, silvicultural actions such as thinning might be an efficient control of localized populations during low density phases, but might be overridden or even inverted by larger scale processes during landscape to regional scale outbreaks (Bauce and Fuentealba, 2013). Once outbreak levels have reached the landscape scale, there are, to date, no known management actions that can stop the eruptions. Outbreaks thus appear to continue until all available hosts are depleted or until weather conditions reduce population levels substantially (Flower et al., 2014).

To encounter future landscape to regional scale outbreaks, forest management must move towards developing strategies based on the biology of the insect, and the principals of the disturbance regime at hand. This includes a deeper understanding of the long-term adaptations of forest resources – from stand to landscape scale. Higher-level land-management policies in general, with particular attention paid to site selection and rotation, can reduce the risk of future landscape and regional scale outbreaks (Klapwijk et al., 2016; Long, 2009; Philip et al., 2015). As is evident in this dissertation, the current regional-scale outbreak of western spruce budworm might not have been possible without the widespread availability and connectivity of suitable habitat throughout the budworm's climatic range. More specifically, past land-management practices, namely fire suppression that promoted a high abundance of dense and mature Douglas-fir stands, likely have amplified the development of regional-scale outbreaks as observed in this dissertation (Parker et al., 2006). Allowing for a more 'natural' development of the forest resource, that is by mimicking or allowing for natural disturbances such as fire and insect outbreaks, could significantly reduce the risk of regional-scale disturbance events (James et al., 2010; Meigs et al., 2016). Hence, instead of suppressing natural disturbances, sustainable forest management should include disturbances as an important component in their short- and long-term management (Millar and Stephenson, 2015; O'Hara and Ramage, 2013).

Finally, there is emerging need for understanding future development of budworm outbreaks under climate change (Weed et al., 2013). Climate change will confront

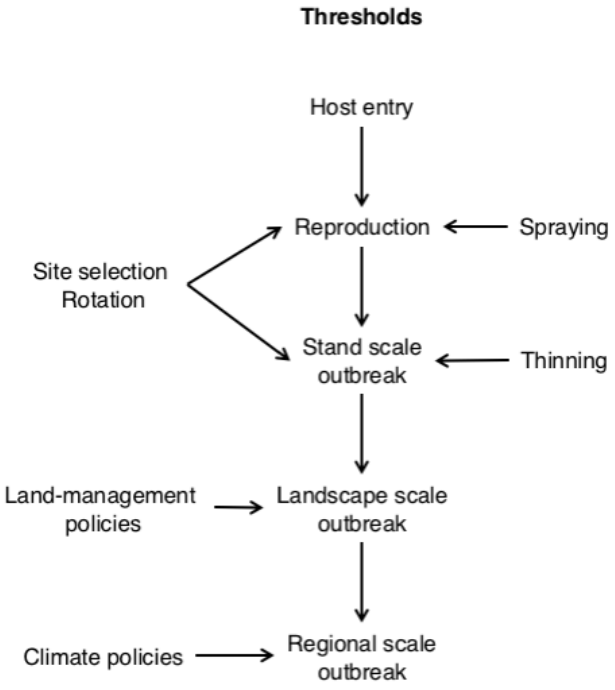

Figure 5.2: Management options for western spruce budworm outbreaks depending on the outbreak stage. Each management action is only effective if applied before the outbreak passes the next threshold.

managers with several problems in developing long-term management strategies. First, climate change might lead to an increase in extent, frequency, and magnitude of budworm disturbances (Murdock et al., 2013), which has substantial effects on long-term timber supply (MacLean et al., 2001). Second, management that aims at developing sustainable forest resources (i.e., balancing timber supply and habitat provision) are often based on historic information on 'natural' forests, such as before Euro-American settlement in North America (Radeloff et al., 1999). However, those historic baseline conditions might be unsuitable management goals under climate change (Millar et al., 2007). In particular, the results of this thesis reinforce that the effect of climate on budworm outbreak dynamics are highly variable across ecosystems, suggesting that with climate change the response of local insect populations might be unpredictable (Millar and Stephenson, 2015). Third, although there exists a variety of models that estimate potential changes in outbreak dynamics under climate change, those models can rarely predict the future with a level of accuracy and precision needed for developing management strategies (Boulanger et al., 2016). With these uncertainties in mind, managers must move towards developing strategies that increase the general ecosystems resilience to unpredictable changes under climate change (Millar and Stephenson, 2015; Millar et al., 2007).

5.3 Outlook

Several interesting aspects beyond the scope of this dissertation evolved during the course of the thesis. First, mapping of insect disturbances could be enhanced by translating the spectral-temporal changes caused by insects into units more applicable to forest management. For example, by building on earlier results from Pflugmacher et al. (2012), two recent studies by Bright et al. (2014) and Meigs et al. (2015) show that LandTrendr disturbance metrics can be translated into tree mortality, measured as dead tree basal area over very large, heterogeneous areas. However, my results show that while defoliation impacts tree growth and vigor, it might not result in substantial tree mortality. Therefore, dead tree basal area might not be the best measure of defoliation intensity. For broadleaved forests, defoliation intensity has been estimated as percent canopy loss (Townsend et al., 2012), which might be more complicated to estimate for coniferous trees. Nonetheless, a very recent study by Assal et al. (2016) explores the potential of Landsat time series for estimating canopy changes (as measured from hemispherical photographs) caused by defoliation and other trace disturbances in coniferous forests. Thus, a potential improvement of the methods applied in this dissertation would be to link Landsat spectral-temporal trajectories of insect defoliation to quantitative, field-based measures of foliage loss or similar measures of canopy changes to better quantify disturbance intensity. That way, models making use of Landsat as a response variable (as in the case of this dissertation) and models making use of Landsat as input (e.g., carbon models; Pflugmacher et al., 2014) would be substantially improved (Schroeder et al., 2014).

Second, further developing the methods applied in this dissertation might also enhance the development of predictors used in estimating the drivers underlying insect outbreaks. For example, studies of gypsy moth outbreak patterns have shown the potential for using MODIS-derived phenological measures as a proxy for habitat quality of early instar larvae (Foster et al., 2013b,a). While MODIS has several restrictions in terms of spatial resolution, a similar approach might be developed using dense time series of Landsat and similar sensors, in particular Sentinel-2, as it has similar spectral and spatial characteristics (Wulder et al., 2015). With a dense, intra-annual time series, it might be possible to estimate the difference in larvae development and host bud burst, which was discussed as a potential important factor for the development of regional-scale outbreaks in Chapter III and IV, though this was too challenging to tackle here, as exact phenological information was not available.

Third, this dissertation has given a better understanding of how to discriminate between insect agents. Building on this, the intra-annual processes related to insect disturbances might further help to better differentiate between insect agents (Olsson

et al., 2016a,b). This could be developed by making use of denser, intra-annual medium-resolution satellite time series, that is by combining Landsat with Sentinel-2 data. Those dense intra-annual time series will likely further enhance the mapping and analysis of insect outbreaks at the landscape to regional scale.

Finally, the increased understanding of budworm outbreak dynamics gained in this dissertation will also allow for the development of improved process-based, deterministic models of insect outbreaks. Process-based models – in contrast to purely statistical models as used in this dissertation – allow for predictions under novel environmental conditions, such as global climate change and/or varying management strategies (Seidl et al., 2011). Those process-based models could be substantially improved by including knowledge generated from quantitative studies such as this dissertation, on the one hand, and by remote sensing products that directly describe the structure and characteristics of insect and host populations, on the other. That way, process-based models that are developed and calibrated using remote sensing data could provide more refined and accurate long-term management recommendations in order to ensure more resilient forest systems.

Bibliography

Alfaro, R., Maclauchlan, L. E., 1992. A method to calculate the losses caused by western spruce budworm in uneven-aged douglas fir forests of british columbia. Forest Ecology and Management 55 (1–4), 295–313.

Alfaro, R. I., Berg, J., Axelson, J., 2014. Periodicity of western spruce budworm in southern british columbia, canada. Forest Ecology and Management 315, 72–79.

Alfaro, R. I., Sickle, G. A. V., Thomson, A. J., Wegwitz, E., 1982. Tree mortality and radial growth losses caused by the western spruce budworm in a douglas-fir stand in british columbia. Canadian Journal of Forest Research 12 (4), 780–787.

Alfaro, R. I., Taylor, S., Brown, R. G., Clowater, J. S., 2001. Susceptibility of northern british columbia forests to spruce budworm defoliation. Forest Ecology and Management 145, 181–190.

Alfaro, R. I., Thomson, A. J., Sickle, G. A. V., 1985. Quantification of douglas-fir growth losses caused by western spruce budworm defoliation using stem analysis. Canadian Journal of Forest Research 15 (1), 5–9.

Allen, C. D., Breshears, D. D., McDowell, N. G., 2015. On underestimation of global vulnerability to tree mortality and forest die-off from hotter drought in the anthropocene. Ecosphere 6 (8), art129.

Allen, C. D., Macalady, A. K., Chenchouni, H., Bachelet, D., McDowell, N., Vennetier, M., Kitzberger, T., Rigling, A., Breshears, D. D., Hogg, E. H., Gonzalez, P., Fensham, R., Zhang, Z., Castro, J., Demidova, N., Lim, J.-H., Allard, G., Running, S. W., Semerci, A., Cobb, N., 2010. A global overview of drought and heat-induced tree mortality reveals emerging climate change risks for forests. Forest Ecology and Management 259 (4), 660–684.

Anderson, D. P., Sturtevant, B. R., 2011. Pattern analysis of eastern spruce budworm choristoneura fumiferana dispersal. Ecography 34 (3), 488–497.

Arvidson, T., Goward, S. N., Gasch, J., Williams, D., 2006. Landsat-7 long-term acquisition plan: Development and validation. Photogrammetric Engineering & Remote Sensing 72 (10), 1137–1146.

Assal, T. J., Anderson, P. J., Sibold, J., 2016. Spatial and temporal trends of drought effects in a heterogeneous semi-arid forest ecosystem. Forest Ecology and Management 365, 137–151.

Assal, T. J., Sibold, J., Reich, R., 2014. Modeling a historical mountain pine beetle outbreak using Landsat MSS and multiple lines of evidence. Remote Sensing of Environment 155, 275–288.

Aukema, B. H., Carroll, A. L., Zhu, J., Raffa, K. F., Sickley, T. A., Taylor, S. W., 2006. Landscape level analysis of mountain pine beetle in british columbia, canada: spatiotemporal development and spatial synchrony within the present outbreak. Ecography 29 (3), 427–441.

Axelson, J. N., Alfaro, R. I., Hawkes, B. C., 2009. Influence of fire and mountain pine beetle on the dynamics of lodgepole pine stands in british columbia, canada. Forest Ecology and Management 257 (9), 1874–1882.

Axelson, J. N., Smith, D. J., Daniels, L. D., Alfaro, R. I., 2015. Multicentury reconstruction of western spruce budworm outbreaks in central british columbia, canada. Forest Ecology and Management 335, 235–248.

Banskota, A., Kayastha, N., Falkowski, M. J., Wulder, M. A., Froese, R. E., White, J. C., 2014. Forest monitoring using Landsat time series data: A review. Canadian Journal of Remote Sensing 40 (5), 362–384.

Barton, K., 2009. Mumin: multi-model inference. R package.

Bates, D., Maechler, M., Bolker, B., Walker, S., 2014. lme4: Linear mixed-effects models using eigen and s4. R package.

Bauce, É., Fuentealba, A., 2013. Interactions between stand thinning, site quality and host tree species on spruce budworm biological performance and host tree resistance over a 6 year period after thinning. Forest Ecology and Management 304, 212–223.

Bearup, L. A., Maxwell, R. M., Clow, D., McCray, J. E., 2014. Hydrological effects of forest transpiration loss in bark beetle-impacted watersheds. Nature Climate Change 4 (6), 481–486.

Beedlow, P. A., Lee, E. H., Tingey, D. T., Waschmann, R. S., Burdick, C. A., 2013. The importance of seasonal temperature and moisture patterns on growth of douglas-fir in western oregon, USA. Agricultural and Forest Meteorology 169, 174–185.

Belward, A. S., Skøien, J. O., 2015. Who launched what, when and why; trends in global land-cover observation capacity from civilian earth observation satellites. ISPRS Journal of Photogrammetry and Remote Sensing 103, 115–128.

Bentz, B. J., Régnière, J., Fettig, C. J., Hansen, E. M., Hayes, J. L., Hicke, J. A., Kelsey, R. G., Negrón, J. F., Seybold, S. J., 2010. Climate change and bark beetles of the western united states and canada: Direct and indirect effects. Bioscience 60 (8), 602–613.

Bigler, C., Kulakowski, D., Veblen, T. T., 2005. Multiple disturbance interactions and drought influence fire severity in rocky mountain subalpine forests. Ecology 86 (11), 3018–3029.

Bolker, B. M., Brooks, M. E., Clark, C. J., Geange, S. W., Poulsen, J. R., Stevens, M. H., White, J. S., 2009. Generalized linear mixed models: a practical guide for ecology and evolution. Trends in Ecology and Evolution 24 (3), 127–35.

Bolton, D. K., Coops, N. C., Wulder, M. A., 2013. Measuring forest structure along productivity gradients in the canadian boreal with small-footprint lidar. Environmental Monitoring and Assessment.

Bouchard, M., Auger, I., 2013. Influence of environmental factors and spatio-temporal covariates during the initial development of a spruce budworm outbreak. Landscape Ecology 29 (1), 111–126.

Boulanger, Y., Gray, D. R., Cooke, B. J., De Grandpre, L., 2016. Model-specification uncertainty in future forest pest outbreak. Global Change Biology 22 (4), 1595–1607.

Boyd, I. L., Freer-Smith, P. H., Gilligan, C. A., Godfray, H. C. J., 2013. The consequence of tree pests and diseases for ecosystem services. Science 342 (6160).

Breiman, L., 2001. Random forests. Machine Learning 45 (1), 5–32.

Bright, B. C., Hudak, A. T., Kennedy, R. E., Meddens, A. J. H., 2014. Landsat time series and lidar as predictors of live and dead basal area across five bark beetle-affected forests. IEEE Journal of Selected Topics in Applied Earth Observations and Remote Sensing 7 (8), 3440–3452.

Brookes, M. H., Campbell, R. W., Colbert, J. J., Mitchell, R. G., Stark, R. W., 1987. Western spruce budworm. Report, USDA Forest Service Cooperative State Research Service.

Brookes, M. H., Colbert, J. J., Mitchell, R. G., Stark, R. W., 1985. Managing trees and stands susceptible to western spruce budworm. Report, USDA Forest Service Cooperative State Research Service.

Burnham, K. P., Anderson, D. R., Huyvaert, K. P., 2010. Aic model selection and multimodel inference in behavioral ecology: some background, observations, and comparisons. Behavioral Ecology and Sociobiology 65 (1), 23–35.

Burton, P. J., 2010. Striving for sustainability and resilience in the face of unprecedented change: The case of the mountain pine beetle outbreak in british columbia. Sustainability 2, 2403–2423.

Campbell, E. M., MacLean, D. A., Bergeron, Y., 2008. The severity of budworm-caused growth reductions in balsam fir/spruce stands varies with the hardwood content of surrounding forest landscapes. Forest Science 54 (2), 195–205.

Campbell, J. B., Wynne, R. H., 2011. Introduction to remote sensing. Guilford Press.

Campbell, R., 1993. Population dynamics of the major north american needle-eating budworms. Report, United States Department of Agricultur.

Campbell, R., Smith, D. J., Arsenault, A., 2005. Dendroentomological and forest management implications in the interior douglas-fir zone of british columbia, canada. Dendrochronologia 22 (3), 135–140.

Campbell, R., Smith, D. J., Arsenault, A., 2006. Multicentury history of western spruce budworm outbreaks in interior douglas-fir forests near kamloops, british columbia. Canadian Journal of Forest Research 36 (7), 1758–1769.

Cappuccino, N., Lavertu, D., Bergeron, Y., Régnière, J., 1998. Spruce budworm impact, abundance and parasitism rate in a patchy landscape. Oecologia 114 (2), 236–242.

Cardinale, B. J., Duffy, J. E., Gonzalez, A., Hooper, D. U., Perrings, C., Venail, P., Narwani, A., Mace, G. M., Tilman, D., Wardle, D. A., Kinzig, A. P., Daily, G. C., Loreau, M., Grace, J. B., Larigauderie, A., Srivastava, D. S., Naeem, S., 2012. Biodiversity loss and its impact on humanity. Nature 486 (7401), 59–67.

Carlson, C. E., Wulf, n. W., 1989. Silvicultural strategies to reduce stand and forest susceptibility to the western spruce budworm. Report, United States Department of Agriculture.

Chen, P.-Y., Welsh, C., Hamann, A., 2010. Geographic variation in growth response of douglas-fir to interannual climate variability and projected climate change. Global Change Biology 16 (12), 3374–3385.

Claverie, M., Vermote, E. F., Franch, B., Masek, J. G., 2015. Evaluation of the Landsat-5 TM and Landsat-7 ETM+ surface reflectance products. Remote Sensing of Environment 169, 390–403.

Cohen, W. B., Goward, S. N., 2004. Landsat's role in ecological applications of remote sensing. Bioscience 54 (6), 535–545.

Cohen, W. B., Yang, Z., Kennedy, R., 2010. Detecting trends in forest disturbance and recovery using yearly Landsat time series: 2. timesync — tools for calibration and validation. Remote Sensing of Environment 114 (12), 2911–2924.

Cohen, W. B., Yang, Z., Stehman, S. V., Schroeder, T. A., Bell, D. M., Masek, J. G., Huang, C., Meigs, G. W., 2016. Forest disturbance across the conterminous united states from 1985–2012: The emerging dominance of forest decline. Forest Ecology and Management 360, 242–252.

Cooke, B., Nealis, V. G., Regniere, J., 2007. Insect Defoliators as Periodic Disturbances in Northern Forest Ecosystems. Elsevier, Burlington, Maine, pp. 487–525.

Coops, N. C., Gillanders, S. N., Wulder, M. A., Gergel, S. E., Nelson, T., Goodwin, N. R., 2010. Assessing changes in forest fragmentation following infestation using time series Landsat imagery. Forest Ecology and Management 259 (12), 2355–2365.

Coops, N. C., Waring, R. H., Schroeder, T. A., 2009. Combining a generic process-based productivity model and a statistical classification method to predict the presence and absence of tree species in the pacific northwest, u.s.a. Ecological Modelling 220 (15), 1787–1796.

Coops, N. C., Wulder, M. A., White, J. C., 2006a. Identifying and Describing Forest Disturbance and Spatial Pattern: Data Selection Issues and Methodological Implications. CRC Press, Boca Raton.

Coops, N. C., Wulder, M. A., White, J. C., 2006b. Integrating remotely sensed and ancillary data sources to characterize a mountain pine beetle infestation. Remote Sensing of Environment 105 (2), 83–97.

Cribari-Neto, F., Zeileis, A., 2010. Beta regression in R. Journal of Statistical Software 34 (2), 1–24.

Crist, E. P., 1985. A TM tasseled cap equivalent transformation for reflectance factor data. Remote Sensing of Environment 17, 301–306.

Dale, V. H., Joyce, L. A., McNulty, S., Neilson, R. P., Ayres, M. P., Flannigan, M. D., Hanson, P. J., Irland, L. C., Lugo, A. E., Peterson, C. J., Simberloff, D., Swanson, F. J., Stocks, B. J., Michael Wotton, B., 2001a. Climate change and forest disturbances. Bioscience 51 (9), 723–734.

Dale, V. H., Joyce, L. A., McNulty, S., Neilson, R. P., Ayres, M. P., Flannigan, M. D., Hanson, P. J., Irland, L. C., Lugo, A. E., Peterson, C. J., Simberloff, D., Swanson, F. J., Stocks, B. J., Wotton, B. M., 2001b. Climate change and forest disturbances. Bioscience 51 (9), 723–734.

Daly, C., Gibson, W. P., Taylor, G. H., Johnson, G. L., Pasteris, P., 2002. A knowledge-based approach to the statistical mapping of climate. Climate Research 22 (2), 99–113.

De Beurs, K., Townsend, P., 2008. Estimating the effect of gypsy moth defoliation using modis. Remote Sensing of Environment 112 (10), 3983–3990.

Dymond, C. C., Neilson, E. T., Stinson, G., Porter, K., MacLean, D. A., Gray, D. R., Campagna, M., Kurz, W. A., 2010. Future spruce budworm outbreak may create a carbon source in eastern canadian forests. Ecosystems 13 (6), 917–931.

Edburg, S. L., Hicke, J. A., Brooks, P. D., Pendall, E. G., Ewers, B. E., Norton, U., Gochis, D., Gutmann, E. D., Meddens, A. J. H., 2012. Cascading impacts of bark beetle-caused tree mortality on coupled biogeophysical and biogeochemical processes. Frontiers in Ecology and the Environment 10 (8), 416–424.

Eklundh, L., Johansson, T., Solberg, S., 2009. Mapping insect defoliation in scots pine with modis time-series data. Remote Sensing of Environment 113 (7), 1566–1573.

Falkowski, M. J., Wulder, M. A., White, J. C., Gillis, M. D., 2009. Supporting large-area, sample-based forest inventories with very high spatial resolution satellite imagery. Progress in Physical Geography 33 (3), 403–423.

Fellin, D. G., Schmidt, W. C., 1973. Frost reduces western spruce budworm populations and damage in montana. Agricultural Meteorology 11, 277–283.

Fleming, R. A., 2000. Climate change and insect disturbance regimes in canada's boreal forests. World Resource Review, Vol 12, Nos 2-4, 521–555.

Flower, A., Gavin, D. G., Heyerdahl, E. K., Parsons, R. A., Cohn, G. M., 2014. Drought-triggered western spruce budworm outbreaks in the interior pacific northwest: A multi-century dendrochronological record. Forest Ecology and Management 324, 16–27.

Food, of the United Nations, A. O., 2014. State of the world's forests - enhancing the socioeconomic benefits from forests. Report, Food and Agricultural Organization of the United Nations.

Foster, J. R., Townsend, P. A., Mladenoff, D. J., 2013a. Mapping asynchrony between gypsy moth egg-hatch and forest leaf-out: Putting the phenological window hypothesis in a spatial context. Forest Ecology and Management 287, 67–76.

Foster, J. R., Townsend, P. A., Mladenoff, D. J., 2013b. Spatial dynamics of a gypsy moth defoliation outbreak and dependence on habitat characteristics. Landscape Ecology 28 (7), 1307–1320.

Franklin, A., Waring, R. H., McGreight, R. W., Cohen, W. B., Fiorella, M., 1995. Aerial and satellite sensor detection and classification of western spruce budworm defoliation in a subalpine forest. Canadian Journal of Remote Sensing 21, 299–308.

Franklin, J. F., Denison, W., McKee, A., Maser, C., Sedell, J., Swanson, F., Juday, G., 1981. Ecological characteristics of old-growth douglas-fir forests. Report, U.S. Department of Agriculture, Forest Service, Pacific Northwest Research Station.

Franklin, J. F., Spies, T. A., Pelt, R. V., Carey, A. B., Thornburgh, D. A., Berg, D. R., Lindenmayer, D. B., Harmon, M. E., Keeton, W. S., Shaw, D. C., Bible, K., Chen, J., 2002. Disturbances and structural development of natural forest ecosystems with silvicultural implications, using douglas-fir forests as an example. Forest Ecology and Management 155 (1–3), 399–423.

Franklin, S. E., Fan, H., Guo, X., 2008. Relationship between Landsat TM and SPOT vegetation indices and cumulative spruce budworm defoliation. International Journal of Remote Sensing 29 (4), 1215–1220.

Franklin, S. E., Wulder, M. A., Skakun, R. S., Carroll, A. L., 2003. Mountain pine beetle red-attack forest damage classification using stratified Landsat ^{TM} data in british columbia, canada. Photogrammetric Engineering & Remote Sensing 69 (3), 283–288.

Frantz, D., A, R., x00F, der, Stellmes, M., Hill, J., 2016. An operational radiometric Landsat preprocessing framework for large-area time series applications. IEEE Transactions on Geoscience and Remote Sensing 54 (7), 3928–3943.

Frantz, D., A, R., x00F, der, Udelhoven, T., Schmidt, M., 2015. Enhancing the detectability of clouds and their shadows in multitemporal dryland Landsat imagery: Extending fmask. IEEE Geoscience and Remote Sensing Letters 12 (6), 1242–1246.

Garcia-Mora, T. J., Mas, J.-F., Hinkley, E. A., 2012. Land cover mapping applications with modis: a literature review. International Journal of Digital Earth 5 (1), 63–87.

Gauthier, S., Bernier, P., Kuuluvainen, T., Shvidenko, A. Z., Schepaschenko, D. G., 2015. Boreal froest health and global change. Science 349 (6250), 819–822.

Gennaretti, F., Arseneault, D., Nicault, A., Perreault, L., Begin, Y., 2014. Volcano-induced regime shifts in millennial tree-ring chronologies from northeastern north america. Proceedings of the National Academy of Sciences 111 (28), 10077–82.

Gillanders, S. N., Coops, N. C., Wulder, M. A., Gergel, S. E., Nelson, T., 2008. Multitemporal remote sensing of landscape dynamics and pattern change: describing natural and anthropogenic trends. Progress in Physical Geography 32 (5), 503–528.

Goodwin, N. R., Coops, N. C., Wulder, M. A., Gillanders, S., Schroeder, T. A., Nelson, T., 2008. Estimation of insect infestation dynamics using a temporal sequence of Landsat data. Remote Sensing of Environment 112 (9), 3680–3689.

Gray, D. R., MacKinnon, W. E., 2006. Outbreak patterns of the spruce budworm and their impacts in canada. The Forestry Chronicals 82 (4), 550–561.

Griffiths, P., Kuemmerle, T., Baumann, M., Radeloff, V. C., Abrudan, I. V., Lieskovsky, J., Munteanu, C., Ostapowicz, K., Hostert, P., 2014. Forest disturbances, forest recovery, and changes in forest types across the carpathian ecoregion from 1985 to 2010 based on Landsat image composites. Remote Sensing of Environment 151, 72–88.

Griffiths, P., Kuemmerle, T., Kennedy, R. E., Abrudan, I. V., Knorn, J., Hostert, P., 2012. Using annual time-series of Landsat images to assess the effects of forest restitution in post-socialist romania. Remote Sensing of Environment 118, 199–214.

Griffiths, P., Müller, D., Kuemmerle, T., Hostert, P., 2013. Agricultural land change in the carpathian ecoregion after the breakdown of socialism and expansion of the european union. Environmental Research Letters 8 (4), 045024.

Grueber, C. E., Nakagawa, S., Laws, R. J., Jamieson, I. G., 2011. Multimodel inference in ecology and evolution: challenges and solutions. Journal of Evolutional Biology 24 (4), 699–711.

Hadley, K. S., Veblen, T. T., 1993. Stand response to western spruce budworm and douglas-fir bark beetle outbreaks, colorado front range. Canadian Journal of Forest Research 23 (3), 479–491.

Hais, M., Jonášová, M., Langhammer, J., Kučera, T., 2009. Comparison of two types of forest disturbance using multitemporal Landsat TM/ETM+ imagery and field vegetation data. Remote Sensing of Environment 113 (4), 835–845.

Hamann, A., Wang, T., 2006. Potential effects of climate change on ecosystem and tree species distribution in british columbia. Ecology 87 (11), 2773–2786.

Hansen, M. C., Loveland, T. R., 2012. A review of large area monitoring of land cover change using Landsat data. Remote Sensing of Environment 122, 66–74.

Hansen, M. C., Potapov, P. V., Moore, R., Hancher, M., Turubanova, S. A., Tyukavina, A., Thau, D., Stehman, S. V., Goetz, S. J., Loveland, T. R., Kommareddy, A., Egorov, A., Chini, L., Justice, C. O., Townshend, J. R., 2013. High-resolution global maps of 21st-century forest cover change. Science 342 (6160), 850–3.

Haynes, K. J., Bjornstad, O. N., Allstadt, A. J., Liebhold, A. M., 2013. Geographical variation in the spatial synchrony of a forest-defoliating insect: isolation of environmental and spatial drivers. Proceedings of the Royal Society: Biological Sciences 280 (1753), 20122373.

Healey, S. P., Cohen, W. B., Spies, T. A., Moeur, M., Pflugmacher, D., Whitley, M. G., Lefsky, M., 2008. The relative impact of harvest and fire upon landscape-level dynamics of older forests: Lessons from the northwest forest plan. Ecosystems 11 (7), 1106–1119.

Heppner, D., Turner, J., 2006. Spruce weevil and western spruce budworm forest health stand establishment decision aids. BC Journal of Ecosystem and Management 7 (3), 45–49.

Hermosilla, T., Wulder, M. A., White, J. C., Coops, N. C., Hobart, G. W., 2015a. An integrated Landsat time series protocol for change detection and generation of annual gap-free surface reflectance composites. Remote Sensing of Environment 158, 220–234.

Hermosilla, T., Wulder, M. A., White, J. C., Coops, N. C., Hobart, G. W., 2015b. Regional detection, characterization, and attribution of annual forest change from

1984 to 2012 using Landsat-derived time-series metrics. Remote Sensing of Environment 170, 121–132.

Hicke, J. A., Allen, C. D., Desai, A. R., Dietze, M. C., Hall, R. J., Ted Hogg, E. H., Kashian, D. M., Moore, D., Raffa, K. F., Sturrock, R. N., Vogelmann, J., 2012. Effects of biotic disturbances on forest carbon cycling in the united states and canada. Global Change Biology 18 (1), 7–34.

Hope, G., Mitchell, W., Lloyd, D., Erickson, W., Harper, W., Wikeen, B., 1991. Interior Douglas-fir Zone. Special Report Series. British Columbia Ministry of Forests, Victory, British Columbia, Canada, book section 10, pp. 153–166.

Hostert, P., Griffiths, P., van der Linden, S., Pflugmacher, D., 2015. Time Series Analyses in a New Era of Optical Satellite Data. Vol. 22 of Remote Sensing and Digital Image Processin. Springer, pp. 25–41.

Huang, C. Q., Coward, S. N., Masek, J. G., Thomas, N., Zhu, Z. L., Vogelmann, J. E., 2010. An automated approach for reconstructing recent forest disturbance history using dense Landsat time series stacks. Remote Sensing of Environment 114 (1), 183–198.

Hummel, S., Agee, J. K., 2003. Western spruce budworm defoliation effects on forest structure and potential fire behavior. Northwest Science 77 (2), 159–169.

James, P. M., Cooke, B., Brunet, B. M., Lumley, L. M., Sperling, F. A., Fortin, M. J., Quinn, V. S., Sturtevant, B. R., 2015. Life-stage differences in spatial genetic structure in an irruptive forest insect: implications for dispersal and spatial synchrony. Molecular Ecology 24 (2), 296–309.

James, P. M. A., Fortin, M. J., Sturtevant, B. R., Fall, A., Kneeshaw, D., 2010. Modelling spatial interactions among fire, spruce budworm, and logging in the boreal forest. Ecosystems 14 (1), 60–75.

Jarvis, C., 1994. Modelling forest ecosystem dynamics using multitemporal multispectral scanner (MSS) data. Advances in Space Research 14 (3), 277–281.

Jin, S. M., Sader, S. A., 2005. Modis time-series imagery for forest disturbance detection and quantification of patch size effects. Remote Sensing of Environment 99 (4), 462–470.

Jonsson, P., Eklundh, L., 2002. Seasonality extraction by function fitting to time-series of satellite sensor data. IEEE Transactions on Geoscience and Remote Sensing 40 (8), 1824–1832.

Ju, J. C., Roy, D. P., 2008. The availability of cloud-free Landsat ETM plus data over the conterminous united states and globally. Remote Sensing of Environment 112 (3), 1196–1211.

Kaufman, Y. J., Wald, A. E., Remer, L. A., Gao, B. C., Li, R. R., Flynn, L., 1997. The modis 2.1-mu m channel - correlation with visible reflectance for use in remote sensing of aerosol. IEEE Transactions on Geoscience and Remote Sensing 35 (5), 1286–1298.

Kennedy, R. E., Andréfouët, S., Cohen, W. B., Gómez, C., Griffiths, P., Hais, M., Healey, S. P., Helmer, E. H., Hostert, P., Lyons, M. B., Meigs, G. W., Pflugmacher, D., Phinn, S. R., Powell, S. L., Scarth, P., Sen, S., Schroeder, T. A., Schneider, A., Sonnenschein, R., Vogelmann, J. E., Wulder, M. A., Zhu, Z., 2014. Bringing an ecological view of change to Landsat-based remote sensing. Frontiers in Ecology and the Environment 12 (6), 339–346.

Kennedy, R. E., Cohen, W. B., Schroeder, T. A., 2007. Trajectory-based change detection for automated characterization of forest disturbance dynamics. Remote Sensing of Environment 110 (3), 370–386.

Kennedy, R. E., Yang, Z., Braaten, J., Copass, C., Antonova, N., Jordan, C., Nelson, P., 2015. Attribution of disturbance change agent from Landsat time-series in support of habitat monitoring in the puget sound region, USA. Remote Sensing of Environment 166, 271–285.

Kennedy, R. E., Yang, Z., Cohen, W. B., Pfaff, E., Braaten, J., Nelson, P., 2012. Spatial and temporal patterns of forest disturbance and regrowth within the area of the northwest forest plan. Remote Sensing of Environment 122, 117–133.

Kennedy, R. E., Yang, Z. G., Cohen, W. B., 2010. Detecting trends in forest disturbance and recovery using yearly Landsat time series: 1. landtrendr - temporal segmentation algorithms. Remote Sensing of Environment 114 (12), 2897–2910.

Kimmins, J., 2004. Forest ecology, 3rd Edition. Prentice Hall, New York.

King, G., Zeng, L., 2001. Logistic regression in rare events data. Political analysis 9 (2), 137–163.

Klapwijk, M. J., Bylund, H., Schroeder, M., Björkman, C., 2016. Forest management and natural biocontrol of insect pests. Forestry 89 (3), 253–262.

Klutsch, J. G., Negron, J. F., Costello, S. L., Rhoades, C. C., West, D. R., Popp, J., Caissie, R., 2009. Stand characteristics and downed woody debris accumulations associated with a mountain pine beetle (dendroctonus ponderosae hopkins) outbreak in colorado. Forest Ecology and Management 258 (5), 641–649.

Kuemmerle, T., Chaskovskyy, O., Knorn, J., Radeloff, V. C., Kruhlov, I., Keeton, W. S., Hostert, P., 2009. Forest cover change and illegal logging in the ukrainian carpathians in the transition period from 1988 to 2007. Remote Sensing of Environment 113 (6), 1194–1207.

Kurz, W. A., Dymond, C. C., Stinson, G., Rampley, G. J., Neilson, E. T., Carroll, A. L., Ebata, T., Safranyik, L., 2008a. Mountain pine beetle and forest carbon feedback to climate change. Nature 452 (7190), 987–990.

Kurz, W. A., Stinson, G., Rampley, G. J., Dymond, C. C., Neilson, E. T., 2008b. Risk of natural disturbances makes future contribution of canada's forests to the global carbon cycle highly uncertain. Proceedings of the National Academy of Sciences 105 (5), 1551–5.

Leckie, D. G., Gillis, M. D., 1995. Forest inventory in canada with emphasis on map production. The Forestry Chronicle 71 (1), 74–88.

Liaw, A., Wiener, M., 2002. Classification and regression by randomforest. The R Journal 2 (3), 18–22.

Lindenmayer, D. B., Noss, R. F., 2006. Salvage logging, ecosystem processes, and biodiversity conservation. Conservation Biology 20 (4), 949–958.

Lindroth, A., Lagergren, F., Grelle, A., Klemedtsson, L., Langvall, O. L. A., Weslien, P. E. R., Tuulik, J., 2009. Storms can cause europe-wide reduction in forest carbon sink. Global Change Biology 15 (2), 346–355.

Link, W. A., Barker, R. J., 2006. Model weights and the foundations of multimodel inference. Ecology 87 (10), 2626–2635.

Logan, J. A., Régnière, J., Powell, J. A., 2003. Assessing the impacts of global warming on forest pest dynamics. Frontiers in Ecology and the Environment 1 (3), 130–137.

Long, J. N., 2009. Emulating natural disturbance regimes as a basis for forest management: A north american view. Forest Ecology and Management 257 (9), 1868–1873.

Lynch, H. J., Moorcroft, P. R., 2008. A spatiotemporal ripley'sk-function to analyze interactions between spruce budworm and fire in british columbia, canada. Canadian Journal of Forest Research 38 (12), 3112–3119.

Maclauchlan, L. E., Brooks, J. E., 2009. Influence of past forestry practices on western spruce budworm defoliation and associated impacts in southern british columbia. BC Journal of Ecosystems and Management 10 (2), 37–49.

Maclauchlan, L. E., Brooks, J. E., Hodge, J. C., 2006. Analysis of historic western spruce budworm defoliation in south central british columbia. Forest Ecology and Management 226 (1-3), 351–356.

MacLean, D. A., Erdle, T. A., MacKinnon, W. E., Porter, K. B., Beaton, K. P., Cormier, G., Morehouse, S., Budd, M., 2001. The spruce budworm decision support system: forest protection planning to sustain long-term wood supply. Canadian Journal of Forest Research 31 (10), 1742–1757.

Manel, S., Williams, H. C., Ormerod, S. J., 2001. Evaluating presence–absence models in ecology: the need to account for prevalence. Journal of Applied Ecology 38 (5), 921–931.

Masek, J. G., Goward, S. N., Kennedy, R. E., Cohen, W. B., Moisen, G. G., Schleeweis, K., Huang, C., 2013. United states forest disturbance trends observed using Landsat time series. Ecosystems 16 (6), 1087–1104.

Masek, J. G., Huang, C., Wolfe, R., Cohen, W., Hall, F., Kutler, J., Nelson, P., 2008. North american forest disturbance mapped from a decadal Landsat record. Remote Sensing of Environment 112 (6), 2914–2926.

Masek, J. G., Vermote, E. F., Saleous, N. E., Wolfe, R., Hall, F. G., Huemmrich, K. F., Feng, G., Kutler, J., Teng-Kui, L., 2006. A Landsat surface reflectance dataset for north america, 1990-2000. IEEE Geoscience and Remote Sensing Letters 3 (1), 68–72.

Mattson, W. J., Haack, R. A., 1987. Role of drought in outbreaks of plant-eating insencts. Bioscience 37 (2), 110–118.

McDowell, N. G., Coops, N. C., Beck, P. S., Chambers, J. Q., Gangodagamage, C., Hicke, J. A., Huang, C. Y., Kennedy, R., Krofcheck, D. J., Litvak, M., Meddens, A. J., Muss, J., Negron-Juarez, R., Peng, C., Schwantes, A. M., Swenson, J. J., Vernon, L. J., Williams, A. P., Xu, C., Zhao, M., Running, S. W., Allen, C. D., 2015. Global satellite monitoring of climate-induced vegetation disturbances. Trends in Plant Science 20 (2), 114–23.

Meddens, A. J., Hicke, J. A., Ferguson, C. A., 2012. Spatiotemporal patterns of observed bark beetle-caused tree mortality in british columbia and the western united states. Ecological Applications 22 (7), 1876–91.

Meddens, A. J. H., Hicke, J. A., 2014. Spatial and temporal patterns of Landsat-based detection of tree mortality caused by a mountain pine beetle outbreak in colorado, USA. Forest Ecology and Management 322, 78–88.

Meddens, A. J. H., Hicke, J. A., Vierling, L. A., 2011. Evaluating the potential of multispectral imagery to map multiple stages of tree mortality. Remote Sensing of Environment 115 (7), 1632–1642.

Meddens, A. J. H., Hicke, J. A., Vierling, L. A., Hudak, A. T., 2013. Evaluating methods to detect bark beetle-caused tree mortality using single-date and multi-date Landsat imagery. Remote Sensing of Environment 132 (0), 49–58.

Meigs, G. W., Campbell, J. L., Zald, H. S. J., Bailey, J. D., Shaw, D. C., Kennedy, R. E., 2015. Does wildfire likelihood increase following insect outbreaks in conifer forests? Ecosphere 6 (7), art118.

Meigs, G. W., Kennedy, R. E., Cohen, W. B., 2011. A Landsat time series approach to characterize bark beetle and defoliator impacts on tree mortality and surface fuels in conifer forests. Remote Sensing of Environment 115 (12), 3707–3718.

Meigs, G. W., Zald, H. S. J., Campbell, J. L., Keeton, W. S., Kennedy, R. E., 2016. Do insect outbreaks reduce the severity of subsequent forest fires? Environmental Research Letters 11 (4), 045008.

Meyer, W. B., BL Turner, I., 1994. Changes in land use and land cover: a global perspective. Vol. 4. Cambridge University Press.

Mildrexler, D., Yang, Z., Cohen, W. B., Bell, D. M., 2016. A forest vulnerability index based on drought and high temperatures. Remote Sensing of Environment 173, 314–325.

Millar, C. I., Stephenson, N. L., 2015. Temperate forest health in an era of emerging megadisturbances. Science 349 (6250), 823–826.

Millar, C. I., Stephenson, N. L., Stephens, S. L., 2007. Climate change and forests of the future: Managing in the face of uncertainty. Ecological Applications 17 (8), 2145–2151.

Mitchell, S. J., Hailemariam, T., Kulis, Y., 2001. Empirical modeling of cutblock edge windthrow risk on vancouver island, canada, using stand level information. Forest Ecology and Management 154 (1-2), 117–130.

Moisen, G. G., Meyer, M. C., Schroeder, T. A., Liao, X., Schleeweis, K. G., Freeman, E. A., Toney, J. C., [in press]. Shape selection in Landsat time series: A tool for monitoring forest dynamics. Global Change Biology.

Moran, P. A. P., 1953. The statistical analysis of the canadian lynx cycle. Australian Journal of Zoology 1 (3), 291.

Morehouse, K., Johns, T., Kaye, J., Kaye, A., 2008. Carbon and nitrogen cycling immediately following bark beetle outbreaks in southwestern ponderosa pine forests. Forest Ecology and Management 255 (7), 2698–2708.

Muller, J., Bussler, H., Gossner, M., Rettelbach, T., Duelli, P., 2008. The european spruce bark beetle ips typographus in a national park: from pest to keystone species. Biodiversity and Conservation 17 (12), 2979–3001.

Murdock, T. Q., Taylor, S. W., Flower, A., Mehlenbacher, A., Montenegro, A., Zwiers, F. W., Alfaro, R., Spittlehouse, D. L., 2013. Pest outbreak distribution and forest management impacts in a changing climate in british columbia. Environmental Science & Policy 26, 75–89.

Myers, N., Mittermeier, R. A., Mittermeier, C. G., da Fonseca, G. A. B., Kent, J., 2000. Biodiversity hotspots for conservation priorities. Nature 403 (6772), 853–858.

Nakagawa, S., Schielzeth, H., O'Hara, R. B., 2013. A general and simple method for obtainingr2from generalized linear mixed-effects models. Methods in Ecology and Evolution 4 (2), 133–142.

Nealis, V., 2008. Spruce Budworms, Choristoneura Lederer (Lepidoptera: Tortricidae). Springer Netherlands, book section 4352, pp. 3524–3531.

Nealis, V. G., 2012. The phenological window for western spruce budworm: seasonal decline in resource quality. Agricultural and Forest Entomology 14 (4), 340–347.

Nealis, V. G., Noseworthy, M. K., Turnquist, R., Waring, V. R., 2009. Balancing risks of disturbance from mountain pine beetle and western spruce budworm. Canadian Journal of Forest Research 39 (4), 839–848.

Nealis, V. G., Regniere, J., 2014. An individual-based phenology model for western spruce budworm (lepidoptera: Tortricidae). Canadian Entomologist 146 (3), 306–320.

Negron, J. F., Popp, J. B., 2004. Probability of ponderosa pine infestation by mountain pine beetle in the colorado front range. Forest Ecology and Management 191, 17–27.

Nelson, R., Case, D., Horning, N., Anderson, V., Pillai, S., 1987. Continental land cover assessment using Landsat MSS data. Remote Sensing of Environment 21 (1), 61–81.

Noble, I. R., Dirzo, R., 1997. Forests as human-dominated ecosystems. Science 277 (5325), 522–525.

O'Hara, K. L., Ramage, B. S., 2013. Silviculture in an uncertain world: utilizing multi-aged management systems to integrate disturbance. Forestry 86 (4), 401–410.

Olsson, P.-O., Kantola, T., Lyytikäinen-Saarenmaa, P., Jönsson, A., Eklundh, L., 2016a. Development of a method for monitoring of insect induced forest defoliation – limitation of modis data in fennoscandian forest landscapes. Silva Fennica 5 (2), 1495.

Olsson, P.-O., Lindström, J., Eklundh, L., 2016b. Near real-time monitoring of insect induced defoliation in subalpine birch forests with modis derived ndvi. Remote Sensing of Environment 181, 42–53.

Overpeck, J., Udall, B., 2010. Dry times ahead. Science 328 (5986), 1642–1643.

Ozdogan, M., 2010. The spatial distribution of crop types from modis data: Temporal unmixing using independent component analysis. Remote Sensing of Environment 114 (6), 1190–1204.

Pan, Y., Birdsey, R. A., Fang, J., Houghton, R., Kauppi, P. E., Kurz, W. A., Phillips, O. L., Shvidenko, A., Lewis, S. L., Canadell, J. G., Ciais, P., Jackson, R. B., Pacala, S. W., McGuire, A. D., Piao, S., Rautiainen, A., Sitch, S., Hayes, D., 2011. A large and persistent carbon sink in the world's forests. Science 333 (6045), 988–993.

Parker, T. J., Clancy, K. M., Mathiasen, R. L., 2006. Interactions among fire, insects and pathogens in coniferous forests of the interior western united states and canada. Agricultural and Forest Entomology 8 (3), 167–189.

Pecora, W. T., 1967. Surveying the earth's resources from space. Surveying and Mapping 27 (4), 639–643.

Pflugmacher, D., Cohen, W. B., E. Kennedy, R., 2012. Using Landsat-derived disturbance history (1972–2010) to predict current forest structure. Remote Sensing of Environment 122, 146–165.

Pflugmacher, D., Cohen, W. B., Kennedy, R. E., Yang, Z., 2014. Using Landsat-derived disturbance and recovery history and lidar to map forest biomass dynamics. Remote Sensing of Environment 151, 124–137.

Philip, J. B., Miroslav, S., Daniel, K., Kurt, W. G., 2015. Options for Promoting the Recovery and Rehabilitation of Forests Affected by Severe Insect Outbreaks. Integrative Studies in Water Management & Land Deve. CRC Press, pp. 495–518.

Pojar, J., Klinka, K., Meidinger, D. V., 1987. Biogeoclimatic ecosystem classification in british columbia. Forest Ecology and Management 22 (1–2), 119–154.

Potapov, P., Turubanova, S., Hansen, M. C., 2011. Regional-scale boreal forest cover and change mapping using Landsat data composites for european russia. Remote Sensing of Environment 115 (2), 548–561.

Potter, C., Klooster, S., Huete, A., Genovese, V., 2007. Terrestrial carbon sinks for the united states predicted from modis satellite data and ecosystem modeling. Earth Interactions 11 (13), 1–21.

Prestemon, J. P., Wear, D. N., Stewart, F. J., Holmes, T. P., 2006. Wildfire, timber salvage, and the economics of expediency. Forest Policy and Economics 8 (3), 312–322.

Progar, R. A., Gillette, N., Fettig, C. J., Hrinkevich, K., 2014. Applied chemical ecology of the mountain pine beetle. Forest Science 60 (3), 414–433.

Radeloff, V. C., Mladenoff, D. J., Boyce, M. S., 1999. Detecting jack pine budworm defoliation using spectral mixture analysis: Separating effects from determinants. Remote Sensing of Environment 69 (2), 156–169.

Radeloff, V. C., Mladenoff, D. J., Boyce, M. S., 2000. Effects of interacting disturbances on landscape patterns: Budworm defoliation and salvage logging. Ecological Applications 10 (1), 233–247.

Raffa, K. F., Aukema, B. H., Bentz, B. J., Carroll, A. L., Hicke, J. A., Turner, M. G., Romme, W. H., 2008. Cross-scale drivers of natural disturbances prone to anthropogenic amplification: The dynamics of bark beetle eruptions. Bioscience 58 (6), 501.

Robert, L.-E., Kneeshaw, D., Sturtevant, B. R., 2012. Effects of forest management legacies on spruce budworm (choristoneura fumiferana) outbreaks. Canadian Journal of Forest Research 42 (3), 463–475.

Robertson, C., Farmer, C. J. Q., Nelson, T. A., Mackenzie, I. K., Wulder, M. A., White, J. C., 2009. Determination of the compositional change (1999-2006) in the pine forests of british columbia due to mountain pine beetle infestation. Environmental Monitoring and Assessment 158 (1-4), 593–608.

Robertson, C., Nelson, T. A., Boots, B., 2007. Mountain pine beetle dispersal: The spatial-temporal interaction of infestations. Forest Science 53 (3), 395–405.

Roy, D. P., Kovalskyy, V., Zhang, H. K., Vermote, E. F., Yan, L., Kumar, S. S., Egorov, A., [in press]. Characterization of Landsat-7 to Landsat-8 reflective wavelength and normalized difference vegetation index continuity. Remote Sensing of Environment.

Royle, J. A., Link, W. A., 2006. Generalized site occupancy models allowing for false positive and false negative errors. Ecology 87 (4), 835–841.

Ryerson, D. E., Swetnam, T. W., Lynch, A. M., 2003. A tree-ring reconstruction of western spruce budworm outbreaks in the san juan mountains, colorado, u.s.a. Canadian Journal of Forest Research 33 (6), 1010–1028.

Saab, V. A., Latif, Q. S., Rowland, M. M., Johnson, T. N., Chalfoun, A. D., Buskirk, S. W., Heyward, J. E., Dresser, M. A., 2014. Ecological consequences of mountain pine beetle outbreaks for wildlife in western north american forests. Forest Science 60 (3), 539–559.

Sakamoto, T., Yokozawa, M., Toritani, H., Shibayama, M., Ishitsuka, N., Ohno, H., 2005. A crop phenology detection method using time-series modis data. Remote Sensing of Environment 96 (3–4), 366–374.

Schoennagel, T., Veblen, T. T., Romme, W. H., 2004. The interaction of fire, fuels and climate across rocky mountain forests. Bioscience 54 (7), 661–676.

Schroeder, T. A., Healey, S. P., Moisen, G. G., Frescino, T. S., Cohen, W. B., Huang, C., Kennedy, R. E., Yang, Z., 2014. Improving estimates of forest disturbance by combining observations from Landsat time series with u.s. forest service forest inventory and analysis data. Remote Sensing of Environment 154, 61–73.

Schroeder, T. A., Wulder, M. A., Healey, S. P., Moisen, G. G., 2011. Mapping wildfire and clearcut harvest disturbances in boreal forests with Landsat time series data. Remote Sensing of Environment 115 (6), 1421–1433.

Schulze, E. D., Bouriaud, L., Bussler, H., Gossner, M., Walentowski, H., Hessenmöller, D., Bouriaud, O., Gadow, K. v., 2014. Opinion paper: Forest management and biodiversity. Web Ecology 14 (1), 3–10.

Schwalm, C. R., Williams, C. A., Schaefer, K., Baldocchi, D., Black, T. A., Goldstein, A. H., Law, B. E., Oechel, W. C., Paw U, K. T., Scott, R. L., 2012. Reduction in carbon uptake during turn of the century drought in western north america. Nature Geosciences 5 (8), 551–556.

Seidl, R., Aggestam, F., Rammer, W., Blennow, K., Wolfslehner, B., 2015. The sensitivity of current and future forest managers to climate-induced changes in ecological processes. Ambio 45 (4), 430–441.

Seidl, R., Fernandes, P. M., Fonseca, T. F., Gillet, F., Jönsson, A. M., Merganičová, K., Netherer, S., Arpaci, A., Bontemps, J.-D., Bugmann, H., González-Olabarria, J. R., Lasch, P., Meredieu, C., Moreira, F., Schelhaas, M.-J., Mohren, F., 2011. Modelling natural disturbances in forest ecosystems: a review. Ecological Modelling 222 (4), 903–924.

Senf, C., Leitão, J. P., Pflugmacher, D., van der Linden, S., Hostert, P., 2015. Mapping land cover in complex mediterranean landscapes using Landsat: Improved classification accuracies from integrating multi-seasonal and synthetic imagery. Remote Sensing of Environment 156, 527–536.

Shepherd, R. F., 1994. Management strategies for forest insect defoliators in british columbia. Forest Ecology and Management 68 (2-3), 303–324.

Simard, M., Powell, E. N., Raffa, K. F., Turner, M. G., 2012. What explains landscape patterns of tree mortality caused by bark beetle outbreaks in greater yellowstone? Global Ecology and Biogeography 21 (5), 556–567.

Skakun, R. S., Wulder, M. A., Franklin, S. E., 2003. Sensitivity of the thematic mapper enhanced wetness difference index to detect mountain pine beetle red-attack damage. Remote Sensing of Environment 86 (4), 433–443.

Smith, M. L., Martin, M. E., Plourde, L., Ollinger, S. V., 2003. Analysis of hyperspectral data for estimation of temperate forest canopy nitrogen concentration: comparison between an airborne (aviris) and a spaceborne (hyperion) sensor. IEEE Transactions on Geoscience and Remote Sensing 41 (6), 1332–1337.

Stocker, T. F., 2014. Climate change 2013: the physical science basis: Working Group I contribution to the Fifth assessment report of the Intergovernmental Panel on Climate Change. Cambridge University Press.

Sturtevant, B., Cooke, B., Kneeshaw, D., MacLean, D., 2015. Modeling Insect Disturbance Across Forested Landscapes: Insights from the Spruce Budworm. Springer International Publishing, book section 5, pp. 93–134.

Sturtevant, B. R., Gustafson, E. J., Li, W., He, H. S., 2004. Modeling biological disturbances in landis: a module description and demonstration using spruce budworm. Ecological Modelling 180 (1), 153–174.

Swetnam, T. W., Lynch, A. M., 1993. Multicentury, regional-scale patterns of western spruce budworm outbreaks. Ecological Monographs 63 (4), 399–424.

Thayn, J. B., 2013. Using a remotely sensed optimized disturbance index to detect insect defoliation in the apostle islands, wisconsin, USA. Remote Sensing of Environment 136, 210–217.

Thomson, A. J., Shepherd, R. F., Harris, J. W. E., Silversides, R. H., 1984. Relating weather to outbreaks of western spruce budworm, choristoneura-occidentalis (lepidoptera, tortricidae), in british-columbia. Canadian Entomologist 116 (3), 375–381.

Townsend, P. A., Singh, A., Foster, J. R., Rehberg, N. J., Kingdon, C. C., Eshleman, K. N., Seagle, S. W., 2012. A general Landsat model to predict canopy defoliation in broadleaf deciduous forests. Remote Sensing of Environment 119, 255–265.

Trumbore, S., Brando, P., Hatmann, H., 2015. Forest health and global change. Science 349 (6250), 814–818.

Turner, M. G., 1989. Landscape ecology - the effect of pattern on process. Annual Review of Ecology and Systematics 20, 171–197.

Turner, M. G., 2005. Landscape ecology: What is the state of the science? Annual Review of Ecology, Evolution, and Systematics 36 (1), 319–344.

Turner, M. G., 2010. Disturbances and landscape dynamics in a changing world. Ecology 91 (10), 2833–2849.

Turner, M. G., Gardner, R. H., 2015. Landscape Ecology in Theory and Practice. Springer, New York.

Turner, M. G., Romme, W. H., Reed, R. A., Tuskan, G. A., 2003. Post-fire aspen seedling recruitment across the yellowstone (USA) landscape. Landscape Ecology 18 (2), 127–140.

Underwood, E., Ustin, S., DiPietro, D., 2003. Mapping nonnative plants using hyperspectral imagery. Remote Sensing of Environment 86 (2), 150–161.

Vermote, E., Justice, C., Claverie, M., Franch, B., [in press]. Preliminary analysis of the performance of the Landsat 8/oli land surface reflectance product. Remote Sensing of Environment.

Vermote, E. F., El Saleous, N., Justice, C. O., Kaufman, Y. J., Privette, J. L., Remer, L., Roger, J. C., Tanré, D., 1997. Atmospheric correction of visible to middle-infrared eos-modis data over land surfaces: Background, operational algorithm and validation. Journal of Geophysical Research: Atmospheres 102 (14), 17131–17141.

Vogelmann, J. E., Tolk, B., Zhu, Z., 2009. Monitoring forest changes in the southwestern united states using multitemporal Landsat data. Remote Sensing of Environment 113 (8), 1739–1748.

Vogelmann, J. E., Xian, G., Homer, C., Tolk, B., 2012. Monitoring gradual ecosystem change using Landsat time series analyses: Case studies in selected forest and rangeland ecosystems. Remote Sensing of Environment 122, 92–105.

Volney, W. J. A., Fleming, R. A., 2000. Climate change and impacts of boreal forest insects. Agriculture Ecosystems and Environment 82, 283–294.

Volney, W. J. A., Fleming, R. A., 2007. Spruce budworm (choristoneura spp.) biotype reactions to forest and climate characteristics. Global Change Biology 13 (8), 1630–1643.

Wang, T., Hamann, A., Spittlehouse, D. L., Murdock, T. Q., 2012. Climatewna—high-resolution spatial climate data for western north america. Journal of Applied Meteorology and Climatology 51 (1), 16–29.

Waring, R. H., Running, S. W., 2007. Forest ecosystems: analysis at multiple scales, 3rd Edition. Elsevier, Burlington, Maine.

Watson, E., Luckman, B. H., 2002. The dendroclimatic signal in douglas-fir and ponderosa pine tree-ring chronologies from the southern canadian cordillera. Canadian Journal of Forest Research-Revue Canadienne De Recherche Forestiere 32 (10), 1858–1874.

Weed, A. S., Ayres, M. P., Hicke, J. A., 2013. Consequences of climate change for biotic disturbances in north american forests. Ecological Monographs 83 (4), 441–470.

Westfall, J., Ebata, T., 2012. 2012 summary of forest health conditions in british columbia. Report, Ministry of Forests, Lands and Natural Resource Operations.

White, J. C., 2012. Digital high spatial resolution aerial imagery to support forest health monitoring: the mountain pine beetle context. Journal of Applied Remote Sensing 6 (1), 062527.

White, J. C., Wulder, M. A., 2014. The Landsat observation record of canada: 1972–2012. Canadian Journal of Remote Sensing, 1–13.

White, P. S., Pickett, S. T. A., 1985. Natural Disturbance and Patch Dynamics: An Introduction. Academic Press, San Diego, book section 1, pp. 3–13.

White, T. C. R., 1984. The abundance of invertebrate herbivores in relation to the availability of nitrogen in stressed food plants. Oecologia 63 (1), 90–105.

Woods, A. J., Heppner, D., Kope, H. H., Burleigh, J., Maclauchlan, L., 2010. Forest health and climate change: A british columbia perspective. The Forestry Chronicals 86 (4), 412–422.

Wu, J. G., Hobbs, R., 2002. Key issues and research priorities in landscape ecology: An idiosyncratic synthesis. Landscape Ecology 17 (4), 355–365.

Wulder, M. A., Dymond, C. C., White, J. C., Leckie, D. G., Carroll, A. L., 2006a. Surveying mountain pine beetle damage of forests: A review of remote sensing opportunities. Forest Ecology and Management 221 (1-3), 27–41.

Wulder, M. A., Hall, R. J., Coops, N. C., Franklin, S. E., 2004. High spatial resolution remotely sensed data for ecosystem characterization. Bioscience 54 (6), 511–521.

Wulder, M. A., Hilker, T., White, J. C., Coops, N. C., Masek, J. G., Pflugmacher, D., Crevier, Y., 2015. Virtual constellations for global terrestrial monitoring. Remote Sensing of Environment 170, 62–76.

Wulder, M. A., Masek, J. G., Cohen, W. B., Loveland, T. R., Woodcock, C. E., 2012. Opening the archive: How free data has enabled the science and monitoring promise of Landsat. Remote Sensing of Environment 122 (0), 2–10.

Wulder, M. A., Ortlepp, S. M., White, J. C., Coops, N. C., Coggins, S. B., 2009. Monitoring the impacts of mountain pine beetle mitigation. Forest Ecology and Management 258 (7), 1181–1187.

Wulder, M. A., White, J. C., Bentz, B., Alvarez, M. F., Coops, N. C., 2006b. Estimating the probability of mountain pine beetle red-attack damage. Remote Sensing of Environment 101 (2), 150–166.

Wulder, M. A., White, J. C., Goward, S. N., Masek, J. G., Irons, J. R., Herold, M., Cohen, W. B., Loveland, T. R., Woodcock, C. E., 2008. Landsat continuity: Issues and opportunities for land cover monitoring. Remote Sensing of Environment 112 (3), 955–969.

Wulder, M. A., White, J. C., Loveland, T. R., Woodcock, C. E., Belward, A. S., Cohen, W. B., Fosnight, E. A., Shaw, J., Masek, J. G., Roy, D. P., [in press]. The global Landsat archive: Status, consolidation, and direction. Remote Sensing of Environment.

Zeileis, A., 2006. Object-oriented computation of sandwich estimators. Journal of Statistical Software 16 (9), 1–16.

Zhang, X. Y., Friedl, M. A., Schaaf, C. B., Strahler, A. H., Hodges, J. C. F., Gao, F., Reed, B. C., Huete, A., 2003. Monitoring vegetation phenology using modis. Remote Sensing of Environment 84 (3), 471–475.

Zhu, Z., Woodcock, C. E., 2012. Object-based cloud and cloud shadow detection in Landsat imagery. Remote Sensing of Environment 118 (0), 83–94.

Eidesstattliche Erklärung

Ich erkläre, dass ich die Dissertation selbständig und nur unter Verwendung der von mir gemäß §7 Abs. 3 der Promotionsordnung der Mathematisch-Naturwissenschaftlichen Fakultät, veröffentlicht im Amtlichen Mitteilungsblatt der Humboldt-Universität zu Berlin Nr. 126/2014 am 18.11.2014 angegebenen Hilfsmittel angefertigt habe. Ich habe mich nicht anderwärts um einem Doktorgrad im Promotionsfach Geographie beworben und besitze keinen Doktorgrad im Promotionsfach Geographie. Die Promotionsordnung der Mathematisch-Naturwissenschaftlichen Fakultät, veröffentlicht im Amtlichen Mitteilungsblatt der Humboldt-Universität zu Berlin Nr. 126/2014 am 18.11.2014 habe ich zur Kenntnis genommen.

Cornelius Senf

Berlin, den 08.07.2016